Behavior of wood under transverse compression

by

Bohumil Kasal

Thesis submitted to the Faculty of the

Virginia Polytechnic Institute and State University

in partial fulfillment of the requirements for the degree of

Master of Science

in

Wood Science and Forest Products

APPROVED:

Frederick A. Kamke, Co-chairman

David A. Dillard, Co-chairman

Christen Skaar

January, 1989

Blacksburg, Virginia

Behavior of wood under transverse compression

by

Bohumil Kasal

Frederick A. Kamke, Co-chairman David A. Dillard, Co-chairman

Wood Science and Forest Products

(ABSTRACT)

The increasing demand on wood and wood products, and the simultaneously decreasing quality of wood as a raw material leads to the increasing significance of wood-based composites such as particleboard or flakeboard. The resulting mechanical and physical properties are to the large extend dictated by the densification of the wood component. To be able to predict the density of the material, the behavior of structural elements must be known. A theory developed for rigid plastic foams was modified and applied to the deformation of wood in transverse compression. A testing procedure for high strain compression over a range of temperatures was developed. In addition, a stochastic model for prediction of high strain behavior was developed. Wood of yellow poplar (*Liriodendron tulipifera*) was used as the experimental material.

Acknowledgements

I express my sincere appreciation to my advisors Dr. F.A. Kamke and Dr. D.A. Dillard for their support throughout the course of this investigation and the critical review of the presented work. I wish to thank Dr. C. Skaar for his careful review of this text. My thank is due to Dr. G. Ifju for his support and personal understanding which helped me to solve many problems.

My colleagues, , and assisted me in numerous ways. I owe them and many others my thanks and appreciation.

Finally, my love and gratitude are due to my wife, , for her support and patience which made this study easier and helped me to overcome all the critical stages of this research.

Table of Contents

Introduction 1

Objectives 3

Literature review 4

Compression properties of wood 4

Theories developed for foams applicable to transverse compression of wood 5

Effect of temperature and moisture content on mechanical properties of wood 10

Material and Methods 13

Test specimens 13

Compression apparatus 15

Test procedure 18

Results and discussion 23

Effect of specimen height 23

Effect of surface quality and load eccentricity 30

Effect of density 30

Effect of the load direction 33

Temperature and moisture content effect 45

Lateral expansion during the compression. 45

Testing of flakes 55

Foam model applied to thin specimens 59

Sensitivity study 59

Quality of the model 66

Stochastic Model **73**

Theoretical basis 75

Monte Carlo simulation 77

Conclusions **87**

Literature cited **89**

Appendix A. Two dimensional model of cellular material **94**

Appendix B. Geometrical approach to the derivation of the expansion ratio for cellular material 104

Appendix C. Computer program for Monte Carlo simulation **110**

Vita **120**

List of Illustrations

Figure 1. Schematic model of the regular hexagon. 6

Figure 2. Theoretical transverse compression stress-strain curve. 9

Figure 3. Schematic diagram of compression testing apparatus. 16

Figure 4. Compression testing apparatus. 17

Figure 5. Clip gage for measuring of the expansion ratio. 19

Figure 6. Calibration curve for the clip gage. 20

Figure 7. Normalized Young's modulus in compression as a function of specimen height for yellow poplar and poly(methyl methacrylate) 24

Figure 8. Yield stress and strain as a function of specimen height for yellow poplar 25

Figure 9. Crack development in 3 mm specimen of yellow poplar in radial direction. 27

Figure 10. Electron micrograph of the specimen surface before and after compression . . 28

Figure 11. Electron micrograph of the flake compressed to 60% strain. 29

Figure 12. Model of compression specimen with (a) surface roughness and (b) non-parallel mating platen-surfaces. 31

Figure 13. Predicted ratio of apparent modulus (Eapp) to actual modulus (E) 32

Figure 14. Density cubed - yield stress relationship for transverse compression of yellow poplar in radial direction. 34

Figure 15. Densities for 20 mm yellow poplar cubes in radial and tangential direction for the treatments listed in Table 2. 40

Figure 16. Modulus for 20 mm yellow poplar cubes in radial direction for the treatments listed in Table 2. 41

Figure 17. Modulus for 20 mm yellow poplar cubes in tangential direction for the treatments listed in Table 2. 42

Figure 18. Yield stress for 20 mm yellow poplar cubes in radial direction for the treatments listed in Table 2. 43

Figure 19. Yield stress for 20 mm yellow poplar cubes in tangential direction for the treatments listed in Table 2. 44

Figure 20. Normalized yield stress for 20 mm yellow poplar cubes in radial and tangential direction for the treatments listed in Table 46

Figure 21. Normalized modulus for 20 mm yellow poplar cubes in radial and tangential direction for the treatments listed in Table 2 47

Figure 22. Strain-expansion ratio relationship for yellow poplar in radial direction for specimen measuring 20x20x20 mm. 49

Figure 23. Strain-expansion ratio relationship for yellow poplar in radial direction for specimen measuring 20x20x5 mm. 50

Figure 24. Strain-expansion ratio relationship for yellow poplar in radial direction for specimen measuring 20x20x3 mm. 51

Figure 25. Strain-expansion ratio relationship for yellow poplar in radial direction for specimen measuring 20x20x1 mm. 52

Figure 26. Influence of the non-zero expansion coefficient on the density without surface restraint 54

Figure 27. Influence of the non-zero expansion coefficient on the density with surface restraint 56

Figure 28. Relative density as a function of strain and expansion ratio. 57

Figure 29. Prediction of compression behavior for yellow poplar for treatments listed in Table 2 58

Figure 30. Influence of the modulus on the proposed model 63

Figure 31. Influence of relative density on the proposed model 64

Figure 32. Influence of the yield stress on the proposed model 65

Figure 33. Influence of the expansion ratio on the proposed model 67

Figure 34. Calculation of the error of prediction. 69

Figure 35. Density-yield stress relationship from the Monte Carlo simulation. 78

Figure 36. Density-E relationship from the Monte Carlo simulation. 79

Figure 37. Modulus-yield stress relationship from the Monte Carlo simulation. 80

Figure 38. Histogram and probability density function for density 81

Figure 39. Histogram and probability density function for yield stress 82

Figure 40. Histogram and probability density function for modulus 83

Figure 41. Expected stress-strain relationship for yellow poplar as a result of Monte Carlo simulation 84

Figure 42. Schematic model of a regular hexagon. 95

Figure 43. Elastic bending 97

Figure 44. Elastic buckling 99

Figure 45. Plastic collapse 101

Figure 46. Schematic model of lateral expansion of the hexagon. 105

Figure 47. Model of cylindrical cell 107

Figure 48. Expansion ratio as a function of the axial strain for different cell models 109

List of Tables

Table 1. LSD test on differences between ρ for radial and tangential direction for yellow poplar 20 mm cubes ($\alpha = 0.05$). 35

Table 2. Modulus and yield stress at different moisture content and temperatures for yellow poplar 20mm cubes. 36

Table 3. LSD test on differences between moduli for radial and tangential direction for yellow poplar 20 mm cubes ($\alpha = 0.05$). 37

Table 4. LSD test on differences between normalized moduli for radial and tangential direction for yellow poplar 20 mm cubes 38

Table 5. LSD test on differences between normalized yield stress for radial and tangential direction for yellow poplar 20 mm cubes. 39

Table 6. Yield stress and density for yellow poplar flakes. 60

Table 7. LSD test on differences between normalized yield stress in radial compression of yellow poplar flakes ($\alpha = 0.05$). 61

Table 8. Modulus of the cell wall and c_2 coefficient. 71

Table 9. LSD test on differences between c_2 for radial and tangential direction ($\alpha = 0.05$). . . 72

Table 10. Results from Monte Carlo simulation. 86

Introduction

The increasing demand on wood and wood products, and simultaneously decreasing quality of wood as a raw material, leads to the application of wood composite materials, such as particleboard or flakeboard. The mechanical properties of wood composites are to a large extent determined by the density (Geimer et. al 1985). Density can be controlled during the manufacturing process. Thus knowing the mechanisms which are responsible for density formation provides the necessary tool to significantly control the resulting properties of the materials. This approach of tailoring composite materials based on the known properties of its components has been used for the design of synthetic fiber reinforced composites (Jones 1975, Askhenazi and Ganov 1980, Malmeister et al 1980).

Wood, being a natural material, possesses a rather high variability of properties; as a result, the situation here is even more difficult than in the case of more uniform synthetic materials (e.g. carbon fibers and epoxy matrix). During the production of composite materials, wood is subjected to high pressure under extreme temperature and moisture content conditions. When the resulting thickness of the board is achieved, the wood is compressed far beyond the proportional limit and is highly densified. Thus the process of pressing changes the structure and mechanical properties of the wood components. The mechanism of flake deformation during the pressing process is basic information which can be used for the prediction of material properties.

Wood can be qualitatively compared with the man-made cellular foams, which have similar structure. Rather intensive research efforts have been dedicated to the development of theories describing foam deformation characteristics (Meinecke, Clark 1973, Gibson el al.1981, Menges and Knipschild 1982 etc.). Those foam theories gave rather promising results for wood (Easterling et al.1982), mainly for lower density species, such as balsa (*Ochroma lagopus*). Ashby et al. (1985) modelled wood as a system of hexagonal cells. A number of different materials including wood species of different densities were tested. Although, no analysis of the results was presented, a good qualitative agreement between theory and data was found.

Objectives

The objectives of the research are:

1. Apply an existing theory developed for foams to explain behavior of wood in transverse compression.

2. Examine the effect of a non-zero expansion coefficient on the performance of the foam theory.

3. Develop an experimental technique to measure wood behavior under high strain in transverse compression.

4. Measure the qualitative effect of temperature and moisture content on transverse compression.

5. To use Monte Carlo simulation to predict the transverse compression behavior.

Literature review

Compression properties of wood

There are not many works dedicated to the study of transverse compression. Most of the research has been conducted to study the properties up to the proportional limit, whereas little has been done in high strain regions. Schneeweiss (1961) studied the influence of specimen dimensions on yield stress. He found a non-linear relationship between the yield stress and volume of the specimen. Since the specimens were large (cubes from 45 mm to 150 mm) it was difficult to retain the same angle of annual rings. Also, the moisture content was different for each compared dimension (from 16% to 29.5%). Bodig (1963) studied the influence of the specimen height on modulus of elasticity (E) and yield stress (σ_y). Whereas there was no difference between the values of σ_y, E increased with increased height (heights 1, 1.5, 2.0, and 3.0 inches were tested). He explained this phenomena by the structure of wood assuming non-uniform strain distribution. According to this theory, weak earlywood layers take up most of the deformation and an additional height does not totally control the overall deformation. Thus the strain decreases with the height of the specimen. If this assumption is valid, then this phenomena should not occur in homogeneous materials. Bodig (1965) also studied the failure modes in transverse compression by defining progressive failure

of cell wall rows as a controlling phenomena. He indicated a buckling type of failure. Kunesh (1966) studied properties of Douglas Fir (*Pseudotsuga menziensii*) and Western Hemlock (*Tsuga heterophylla*) on 0.5, 1.0, and 2.0 inch thick specimens and different cross-sectional areas (1, 4, and 36 square inch). An increase of E and slight decrease of the proportional limit with increasing thickness was reported. Easterling et al. (1982) studied the behavior of balsa under high strains. A foam theory, developed by Gibson et al. (1982) was used to explain high strain behavior. Ashby et al. (1985) did similar tests as Easterling, but studied several different species. Quite good agreement between theory and experiments was found. Wingate-Hill and Cunningham (1986) and Wingate-Hill and Crowes (1987) studied the moisture content change of several species during compression up to 40% strain. However, no stress-strain relationship was presented.

Theories developed for foams applicable to transverse compression of wood

Wood can be considered a cellular material composed of a system of cells of different sizes. Dimensions of those structural elements are random variables; however, if one is interested in overall response of the material to the applied load or strain, the whole system can be modeled in terms of an average cell. This approach was applied by Gibson et al. (1981) who modelled cellular foam as hexagons. Easterling (1982) and Ashby (1983,1984) have shown the applicability of this theory to wood. A brief description follows:

A regular hexagon of wall thickness t and side length l is used to model an individual cell. Then, relative density of a cellular material can be expressed as a ratio of the wall area and the total area of the hexagon (see Figure 1). The linear elastic behavior is assumed to be controlled by the bending of the cell wall.

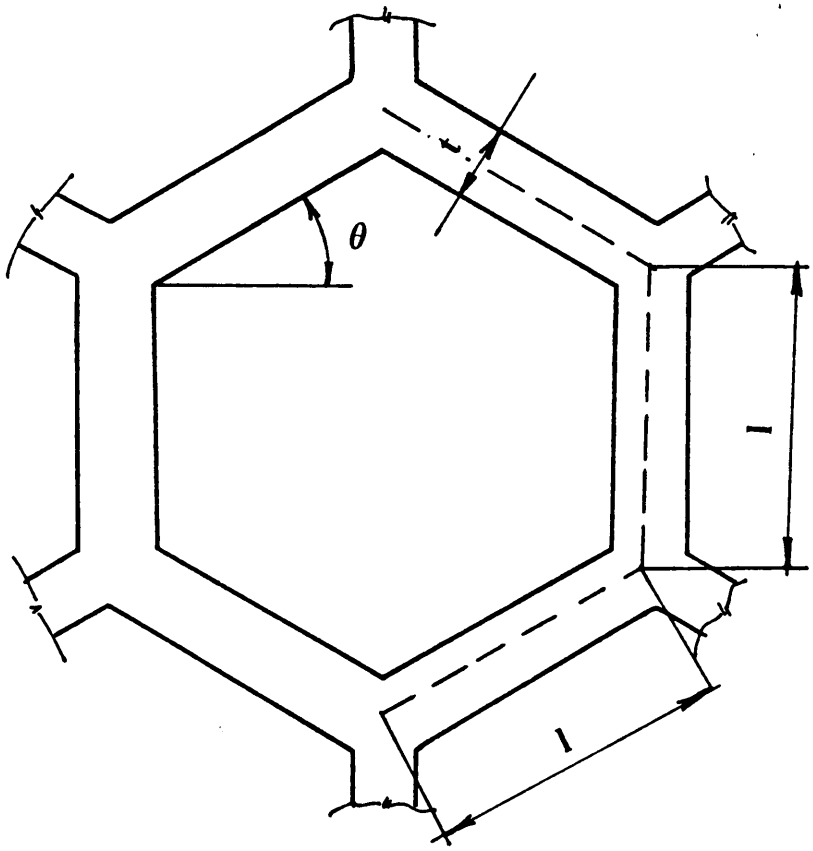

Figure 1. Schematic model of the regular hexagon.

Under linear elastic behavior a linear stress-strain relationship is understood and terms such as E can be defined; then, from the simple geometrical calculation and the elastic beam theory, the modulus of elasticity can be expressed in terms of the cell wall E_s and a relative density.

$$E = c_1 E_s \rho_{rel}^3 \qquad [1]$$

where

$$\rho_{rel} = \frac{\rho}{\rho_s} \qquad [2]$$

where:

$\rho =$ density of the foam

$\rho_s =$ density of the cell wall

Note: Easterling et al (1982) suggested $c_1 = 1.0$, because $E = E_s$ if $\rho_{rel} = 1.0$.

The onset of non-linear elastic behavior is derived from the assumption of the elastic buckling of the cell wall:

$$\sigma_y = c_2 E_s \rho_{rel}^3 \qquad [3]$$

Where:

$c_2 =$ constant

The non-linear elastic behavior is based on the elastic buckling theory, where the first buckling mode is assumed. This equation is derived in the original work by Gibson et al (1981), where the elastic buckling of the regular hexagon was used as a model (see Timoshenko, Gere 1961). If elastic buckling occurs first, and is immediately followed by plastic deformations, the value of the yield

stress σ_y is very close to critical stress resulting from the critical buckling load. Thus, σ_y can be determined from Eq. [3]. The non-linear elastic behavior starts at point 1 in Figure 2.

If yielding of the cell wall occurs, then the foam yield stress is a function of a cell wall yield stress and relative density:

$$\sigma_y = c_3 \ \sigma_{y,s} \rho_{rel}^{3/2} \qquad [4]$$

where c_3 is a constant.

If non-linear elastic behavior is assumed to be responsible for further plastic collapse of the cell wall Eq. [5] can be derived (Ashby et al 1985).

$$\sigma = E_s \rho_{rel}^3 [\frac{1 - \rho_{rel}^{1/3}}{1 - (\rho_{rel} \frac{1}{1-\varepsilon})^{1/3}}]^3 \qquad [5]$$

The existing theory assumes that there is no Poisson's effect on the stress-strain relationship. However, Papirno, Mescall and Hower (1983) show, that the cross-sectional area change is an important factor in calculating stress for metallic materials subjected to high strains. Guess and Ericksen (1983) considered the Poisson's ratio effect not to be negligible for Kevlar-Epoxy composites with porosity up to 20 %. They also found, that the Poisson's ratio changes as a function of the strain. However, no theoretical explanation was given in their work. Casey (1987) measured the thickness and width change of yellow poplar flakes isolated from compressed flakeboard. A 38 % change in thickness and only 0.48 % change in width (measured after recovery) was reported.

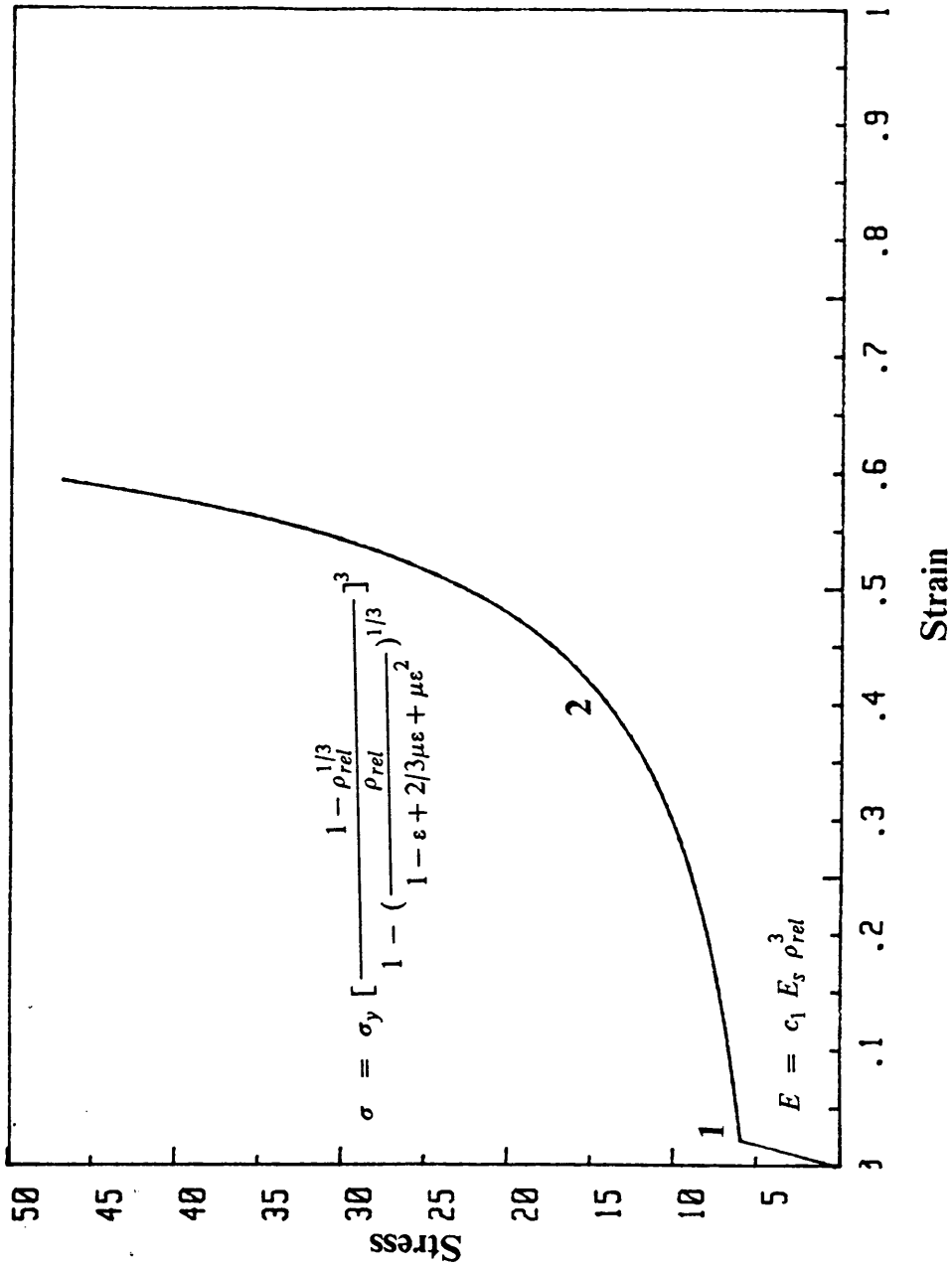

Figure 2. Theoretical transverse compression stress-strain curve.

Effect of temperature and moisture content on mechanical properties of wood

Temperature and moisture content have a significant influence on wood properties. The relationships are discussed in many citations in classical wood literature (Kollmann 1952, Skaar 1972, Panshin and de Zeeuw 1980 , Bodig and Jayne 1982 etc.). Generally, the modulus and strength of wood decrease with increasing moisture content up to the fiber saturation point, where curves describing this relationship became flat. A temperature increase causes a decrease of both elastic and strength properties. Zadorina and Tschernova (1965) studied the properties of Sibirian larch (*Larix spp.*) at 8, 15, 20, and 30% moisture content and 20, 50, 80 and 100°C. A 78% decrease in bending strength from conditions 20°C and 10% moisture content to 100°C and 10% moisture content was found. A similar relation was found for shearing strength. A linear relationship between temperature and those properties was proposed. Schneider (1971) studied properties of pine sapwood (*Pinus spp.*) and beechwood (*Fagus silvatica*) after temperature treatment up to 200°C. Modulus of elasticity of both species was considerably reduced after heating above 150°C. Similar results were obtained for crushing strength parallel to the fibers. A thermal degradation expressed as a loss of wood substance was reported to be higher for small specimens. Erinsch and Kulkevitsa (1981) studied the properties of birch (*Betula spp.*) and pine (*Pinus spp.*) after plasticization in boiling water and subsequent compression to 50% strain and drying at 20, 105 and 160 °C. No significant influence of post-compression drying temperature on the amount of 'spring-back' was found for birch. Skhirando et al (1983) conducted a chemical analysis of fiberboards pressed at 9.0, 30.2, and 68.1% moisture content of fibers and 190°C. The best mechanical characteristics were obtained for boards manufactured at 30.2% moisture content of fibers. At this moisture content, lignin contained the fewest number of hydroxylic groups. As a result, this lignin kept its thermosetting character and was involved in fiber bonding. The change of the mechanical properties can be irreversible depending upon environment conditions and time (Sumi 1978). Östman

(1985) tested spruce (*Picea spp.*) in tension parallel to the grain up to 250°C. Moisture content varied from 0 to 30% when temperature was below 100°C and 0% for higher temperatures. Both modulus and strength decreased with increasing temperature for any given moisture content. From the rate of the decrease of E and strength Östman estimated the glass transition temperature to be between 200 and 250°C for dry wood. Ganowicz et al. (1980) studied the elastic properties of pine (*Pinus spp.*) up to 60°C under different moisture content conditions (0, 15 and 30%). A linear relationship between the E in bending and temperature with the correlation coefficients about R = -0.90 was found. Melcer (1985) assumed lignin and hemicellulose to be responsible for the change of the wood properties as a result of imposed temperature and moisture. The glass transition temperature of cellulose was assumed to be above 230°C and thus its contribution to wood softening was low. According to this theory the lignin-hemicellulosis matrix can become a viscous fluid independently of the celluloses behavior. Hillis and Rosza (1985) applied torsion to relate the torsional stiffness to changing temperature up to 80°C and moisture content 30%. For *Pinus radiata* three regions of accelerated rates of change in twist angle under a constant torque were found. The first softening point was defined at the temperature T = 60-70°C and was attributed to the hemicelluloses; the second point was at T = 90-110°C and was attributed to lignin. They also defined a third point between 70-90°C where the rate of the change of the twist angle decreased. Differences in glass-transition temperature for wood chemical components were found responsible for those points. Babicki et al. (1977) found that temperatures up to 50°C did not produce any significant changes in mechanical properties of beech (*Fagus spp.*) wood heated in water. Scharr (1986) applied torsion to spruce (*Picea spp.*) and oak (*Quercus spp.*) at a temperature range from 20 - 70 ° C and moisture content 6 - 9 %. Temperature had a significant influence on creep compliance in torsion. Khmelidze (1986) tested pine (*Pinus spp.*) and larch (*Larix spp.*) in tension and compression parallel to the fibers at temperatures up to 230°C. It was found that wood behaved as an elastic material independently of applied temperature.

Ladomersky and Pajtik (1987) considered the slope of the plateau of the stress-strain relationship (see Figure 2, point 1-2) as a quantitative measure of the degree of plasticization. The influence of temperature and different chemicals (including water) on transverse compression characteristics

was studied. However, slope of the plateau region had a high variability (7-33%), possibly because no density corrections were taken.

Material and Methods

Test specimens

To study the effect of specimen height on transverse compression, yellow poplar specimens, conditioned to 12% moisture content, were cut with a cross-section of 20x20 mm and heights of 3, 6, 10, 20, 30 and 40 mm. Commercially obtained poly(methyl methacrylate) (PMMA) samples were cut 20x20 mm in cross-section and 6, 10 and 18 mm high. These two materials represent a non-isotropic cellular material and a homogeneous, isotropic solid for comparison purposes.

To investigate the influence of temperature and moisture on E and σ_y , specimens 20x20x20 mm were used. Samples were cut from the mature wood region of a quarter-sawn board. This enabled the suppression of the variability across the diameter. To eliminate the influence of the density, pairs of radial (RD) and tangential (TG) specimens were randomly assigned to groups. The number of specimens required was calculated using the following formula (Walpole and Myers 1985):

$$n = \left(\frac{s}{\Delta}\right)^2 (z_{\alpha/2} + z_{\beta})^2 \qquad [6]$$

Where:

n = number of observations

s = estimated standard deviation

Δ = error of the observed parameter

α = probability of type I error

β = probability of type II error

z = value from the standard normal distribution

α means the probability that the zero hypothesis will be rejected, although it is true. β represents the probability that zero hypothesis will be accepted, although it is false (see Walpole and Myers 1985).

Based on the results in the literature (Kollman 1952, Bodig and Jayne 1982) the following values were assumed:

- s = 8
- Δ = 12
- α = 0.05
- β = 0.05

From the standard normal distribution tables and Eq. [6] we obtain $z_{\alpha/2} = 1.96$, $z_\beta = 1.65$ and n = 6. Thus 6 replications were used for each group. This implies that for a property having a mean value of 50 units and 16% variability, the prediction of the population mean based on 6 observations will be accurate within ± 12 units (assuming α and β errors are 5%). A goal of this study is a qualitative assessment rather than quantitative, therefore, we assume that n = 6 gives sufficient information.

To test the high strain behavior of thin specimens, flakes of approximately 1 mm in thickness and 20x20 mm in cross-section were cut and conditioned to the required moisture content. To suppress the density influence on the properties, flakes from different locations within a growth increment were randomly assigned to groups.

For estimating the density effect on yield stress, specimens of different thickness were cut along a bar of 20x20 mm cross-section in such a way that there was always different amounts of early and latewood present. This yielded a wide variation of densities from the same tree. This technique eliminated the influence of variability in wood structure, but allowed a variation in specimen thickness.

Note: In this work the density is expressed as a ratio of the dry weight and the wet volume. This ratio is equivalent to specific gravity using the SI systems of units (Siau 1971). We will use the term density with units g/cm^3.

Compression apparatus

The compression testing apparatus is shown in Figures 3 and 4. A universal hydraulic testing machine (MTS) was used for compression tests. Heated platens (4) were firmly attached to the load cell (1) and machine table (7). The loading block consisted of heated aluminum (4) which was directly in contact with the specimen. The surface of this plate was ground smooth to within 0.025 mm. A thermocouple was placed beneath the surface of the heated block to monitor the temper-

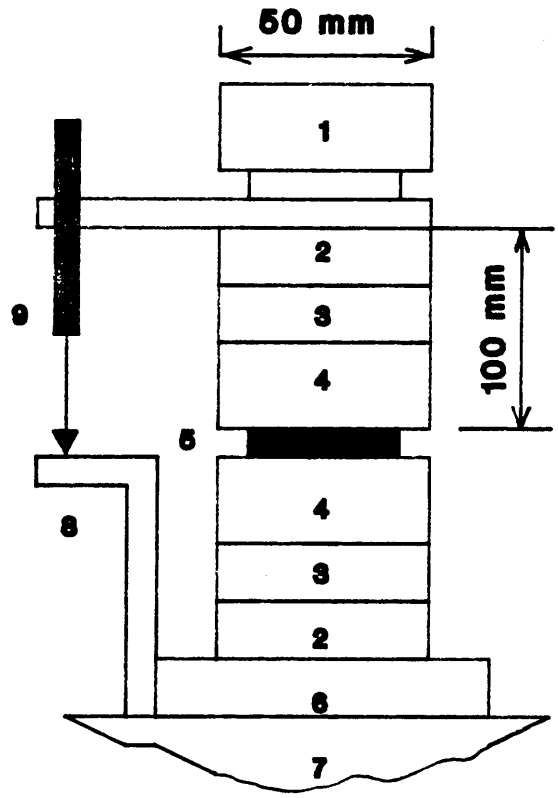

1 - load cell
2 - cooling manifold
3 - steel block
4 - heated platen
5 - specimen
6 - steel block
7 - machine table
8 - strain measurement reference
9 - LVDT

Figure 3. Schematic diagram of compression testing apparatus.

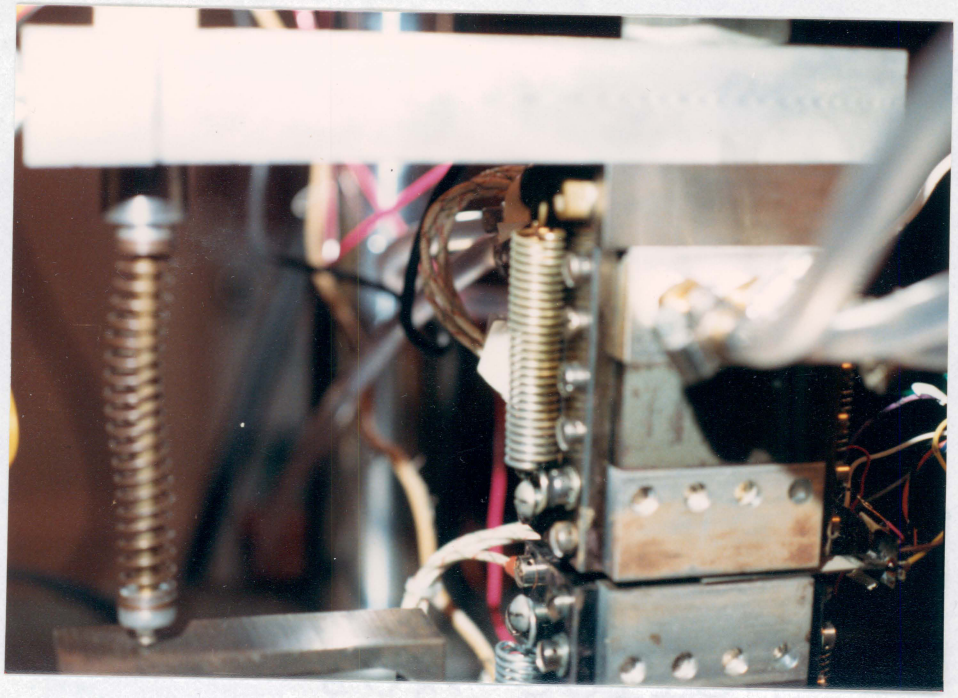

Figure 4. Compression testing apparatus.

ature. To get a uniform heat distribution, three heating cartridges were located at the upper surface of the aluminum block. A steel block (3) was placed between the heated and cooled zone (2). An aluminum cooling manifold (2) enabled the load cell to remain within the calibrated temperature range. A stiff aluminum arm was placed between the cooling manifold and the load cell. A linear variable differential transformer (LVDT) was attached to the arm and placed against the strain measurement reference (8). Thus, the deformation of the load frame was excluded from the measurement. The horizontal and parallel position of the platens was adjusted with an accuracy of 0.05 mm.

A clip gage (see Figure 5) was designed to monitor the transverse deformation of the samples. Two steel arms (3) were soldered to the elastic bronze ribbon (2). A strain gage (1) was bonded to the tension and compression side. Sharp tips (4) on the arm ends prevented gage slippage on the specimen.

An HP 2000 Data Acquisition System was used to collect data. Time intervals between the readings were automatically adjusted with respect to the stress rate. The calibration curve for the clip gage is in Figure 6.

Temperature of the platens was electronically controlled with an accuracy $\pm 1°$ C and time step 1 second. Two independent temperature control units, one for each plate, were used.

Test procedure

The strain rate was 6% per minute. This rate has been used by many researchers for tests on foams as well as wood (Easterling et al 1982, Ashby et al 1985). For the height effect study, samples were tested between 25x25x6 mm steel plates that were ground flat and parallel to within 0.025 mm. To eliminate the error introduced by the inherent flexure in the testing apparatus, a compression test was conducted on the steel plates with no specimen present. The load-deflection relationship of the testing apparatus was found to be linear. Thus, the deflection attributable to the apparatus

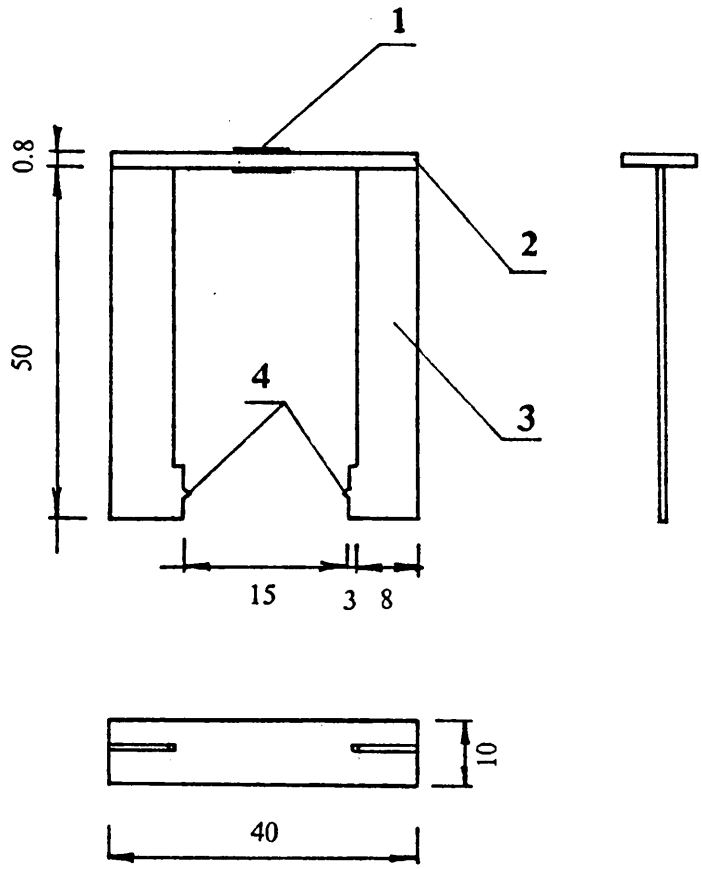

Figure 5. Clip gage for measuring of the expansion ratio.

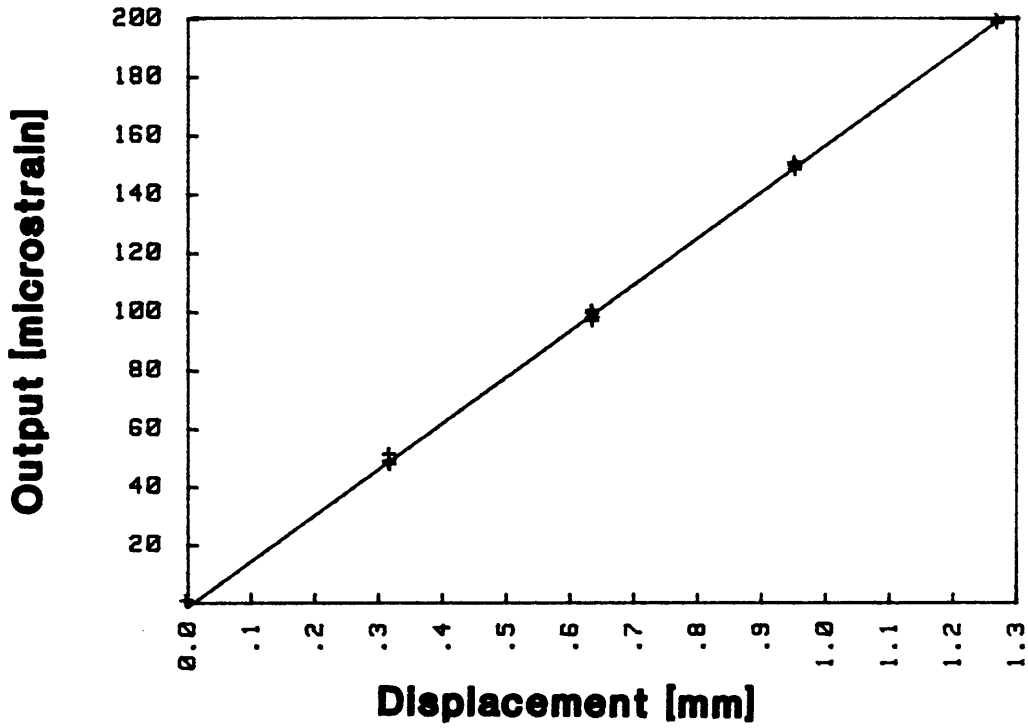

Figure 6. Calibration curve for the clip gage.

could be easily subtracted from the overall deflection. This error is not significant for high strains beyond the proportional limit. However, it introduces a significant error in the measured deflection within the elastic region of thin specimens (Wolcott et al 1988).

For tests on yellow poplar 20 mm, cubes at different temperature and MC conditions, no steel plates were used and specimens were in direct contact with the heated surfaces. As the test time was approximately 10 minutes, there was a possibility of a moisture content change, especially at higher temperatures. In order to maintain a non-zero equilibrium moisture content above 100°C the environment surrounding the specimen must be pressurized. To retard the moisture escape, specimens were sealed into poly (vinylidene chloride) foil (SARAN Wrap 560) 0.15 mm thick. Using this procedure a moisture content of 8% at 115°C can be maintained. As higher temperatures and moisture content levels require higher pressures, they cannot be reached using this technique. Before the tests, specimens were equilibriated to the desired temperature and moisture content, when possible. For the temperature and moisture content of 225°C and 0% MC, dry specimens were preheated in an oven for 15 minutes at 225°C. A thermocouple was placed in the center of several specimens to verify that 15 minutes was sufficient time for the center of a 20 mm specimen to reach 225°C. To prevent heat conduction through the thermocouple wire, silicon rubber was used to insulate the part of the wire exposed to the heat.

The temperature and moisture combinations studied are shown in Table 2. As no quantitative relationship was sought, combinations where a glass transition temperature region could be expected were investigated.

The expansion ratio (which is equivalent to the Poisson's ratio in the densification region) was measured at 30°C and 12% moisture content on 3, 5, and 20 mm specimens (loaded in the radial direction). Flakes were placed between two 20x20 mm aluminum plates to avoid the contact of the gage arms with the surface of the heated platens.

Flake behavior at high strains was tested using the same procedure as the 20 mm specimens. As the polymer foil deformation can represent a significant error for the thin specimens, an aluminum foil was used to retard moisture escape. Specimens were wrapped in three layers of 0.05 mm thick foil. The deformation of the foil was neglected. This procedure was sufficient for temperatures

below 100°C as no pressurization was necessary. Most of the flake tests were conducted at 30°C or 0% MC.

Results and discussion

Effect of specimen height

The effect of specimen height was determined using an analysis of variance. A least significance difference test (LSD) was employed to determine the differences between treatment means at the 99% confidence level.

Despite corrections made for machine flexure, the apparent modulus (*Eapp*) increased with specimen height for both yellow poplar and PMMA (Figure 8). For PMMA samples, *Eapp* increased for each specimen height tested. The *Eapp* of yellow poplar increased with heights less than 6 mm. No significant difference was noted for *Eapp* of specimens 12 mm and higher.

In addition to *Eapp*, the yield stress (σ_y) and yield strain (ε_y) were studied for yellow poplar. The effect of specimen height on σ_y was statistically significant as determined through analysis of variance. However, no significant differences were noted among treatment means with the LSD test. In addition, no trend between the two variables was apparent (Figure 8). Whereas the effect of height on σ_y may be statistically significant, the effect may, in reality, be small enough to ignore. The percent difference between the extreme treatment means was approximately 15%.

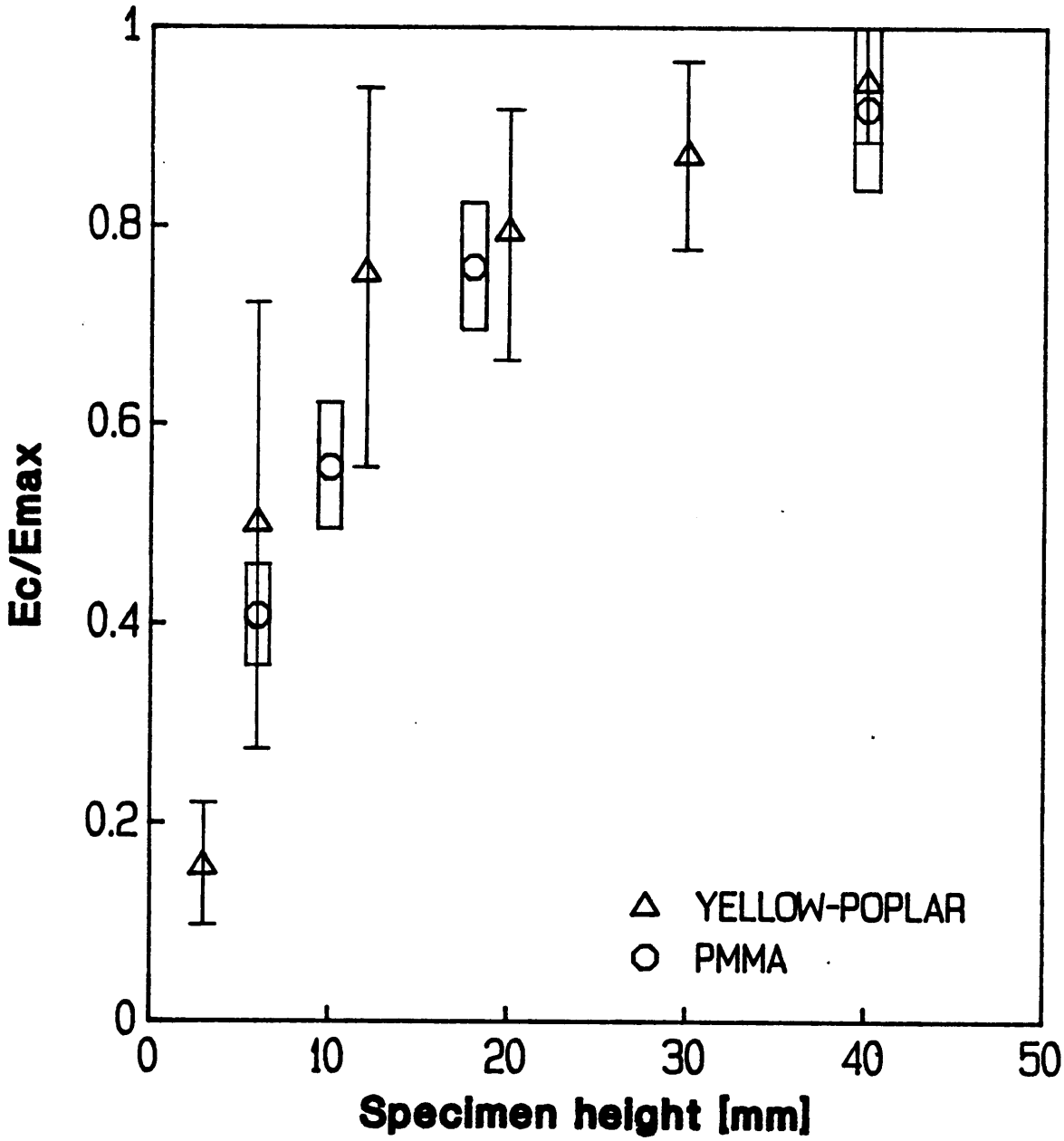

Figure 7. Normalized Young's modulus in compression as a function of specimen height for yellow poplar and poly(methyl methacrylate): Error bars denote 99% confidence interval.

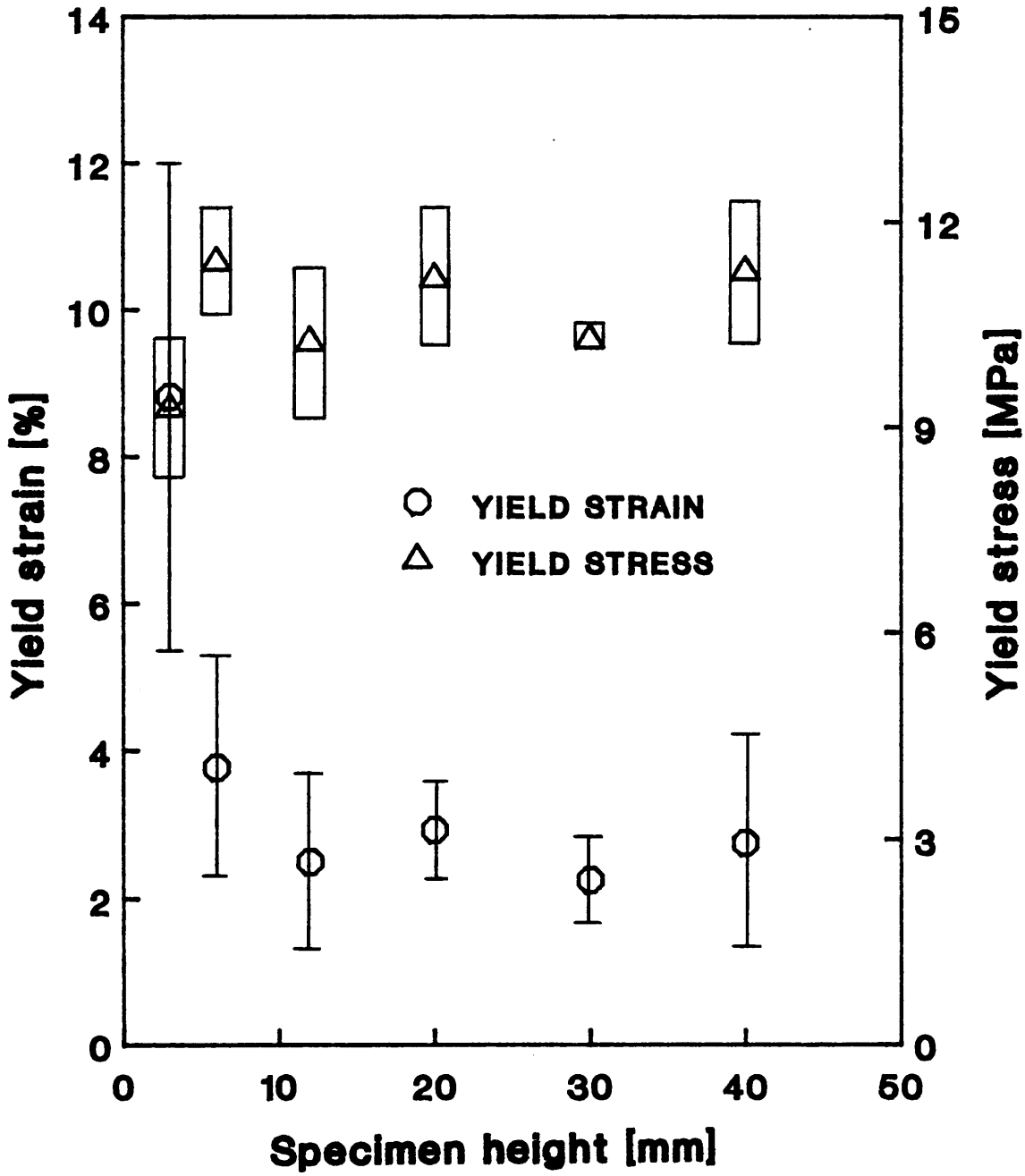

Figure 8. Yield stress and strain as a function of specimen height for yellow poplar: Error bars denote 99% confidence interval.

Similar relationships of E with specimen height have been shown for wood, PMMA, and foams (Menges and Knipschild 1982). These corroborative findings suggest that this relationship is an anomaly of the testing technique and not a true material property unique to wood. However, from the findings above, no statement can be made on the origin of the phenomenon.

Under the higher strains (more than 20%), the tall specimens tend to buckle because of the non-uniform structure. The growth rings have a finite curvature which results in shear stress and moment development. As a result, no pure compression stress-state can be achieved and thus there is a non-uniform deformation. When high strain is imposed the specimen center tends to expand, whereas the restrained surface remains fixed. This leads to the additional shear and tensile stress development in the edge zone and consequently cracks occur. The tendency for crack development was observed even in 3 mm thick specimens (see Figure 9). The collapse of the cell wall can probably contribute to crack initiation. Electron micrographs were taken from the transverse surfaces of 20mm cubes and 1mm thick flakes. No change was observed on the cube before and after compression to σ_y (see Figure 10). This coincides with the assumption of Gibson (1982) that the elastic buckling of the cell wall controls yielding of the specimen. Thus Eq. [1] can be used to express the σ_y. In Figure 11 a cross-section of the flake compressed to 60% strain at 0% moisture content and 125 °C is shown. One can recognize that fracturing of the cell wall occurs. This may not be the case at higher moisture contents or temperatures, when the cell wall may be highly plasticized.

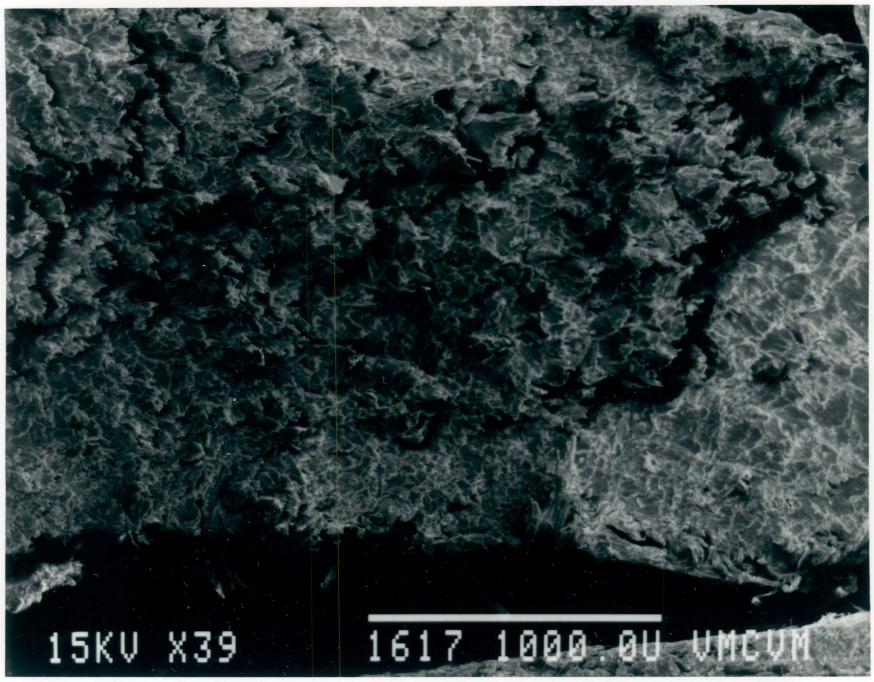

Figure 9. Crack development in 3 mm specimen of Yellow poplar in radial direction.

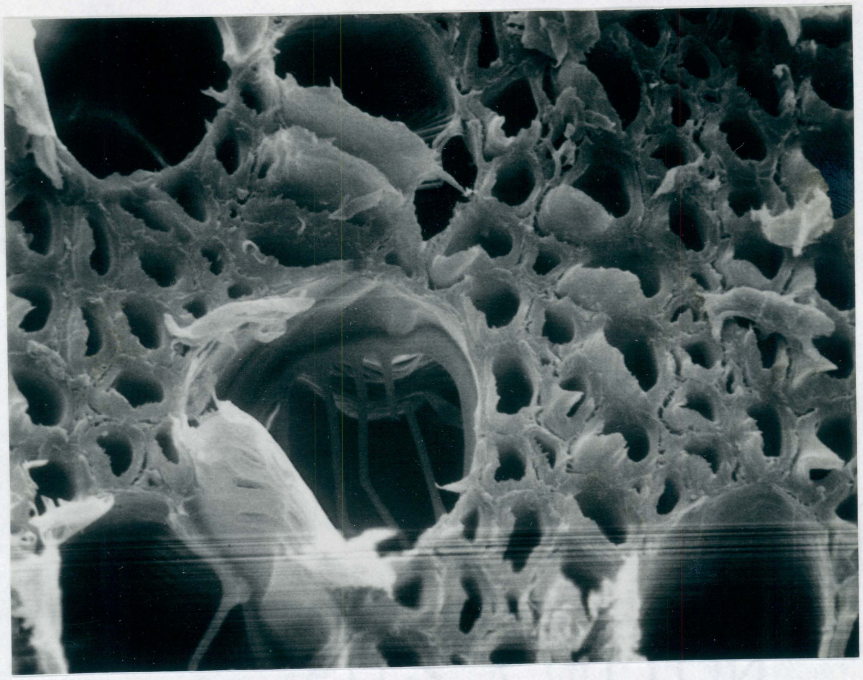

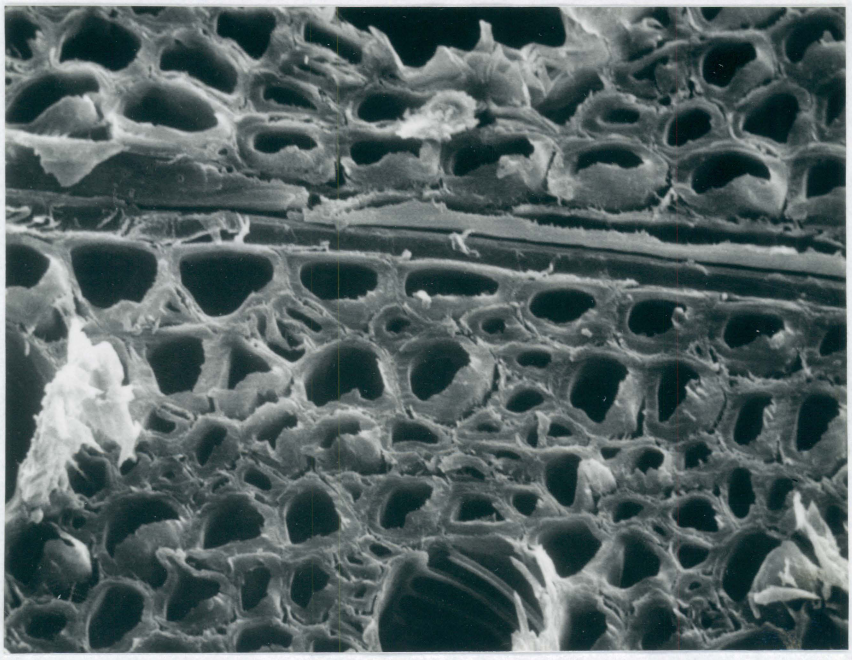

Load direction

Figure 10. Electron micrograph of the specimen surface before and after compression to σ_y: yellow poplar 20mm cube in radial direction.

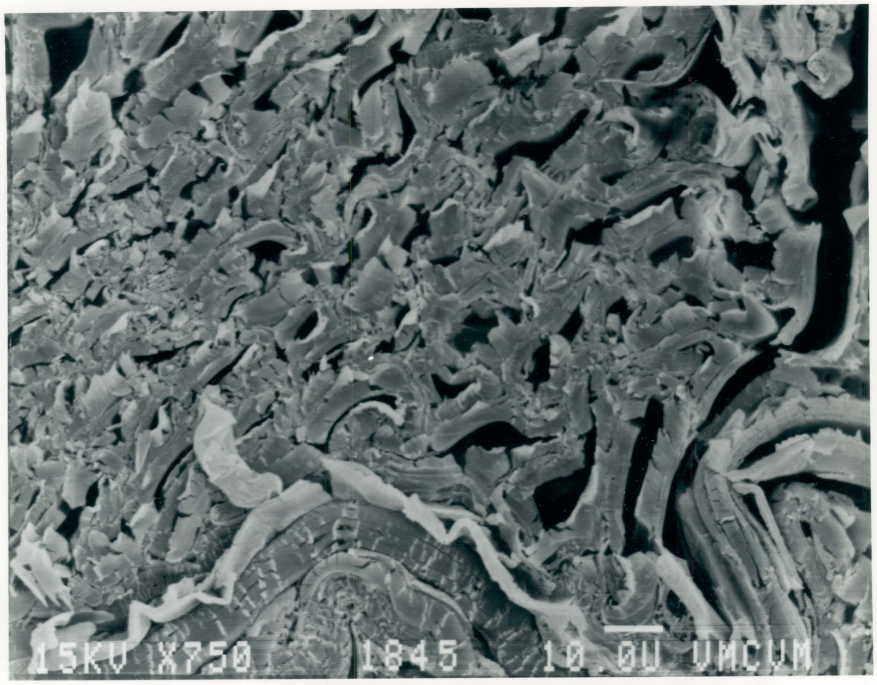

Figure 11. Electron micrograph of the flake compressed to 60% strain.

Effect of surface quality and load eccentricity

This effect was discussed in the paper of Wolcott et al (1988). A simple model was proposed, where surface roughness or non-parallelism are modelled as triangular (Figure 12). Surface quality may have a significant influence on E. For example, for a specimen with a height of 5 mm, a roughness of only 0.05 mm gives a 45% drop in E. Due to the natural structure of wood it is apparent that the influence of the surface quality cannot be eliminated. In Figure 13 the effect of surface roughness on E for different thicknesses is shown. One can recognize that the trends are similar to the experimental results presented in Figure 7. The asperities are totally collapsed when the stress is equal to σ_y. Therefore, the σ_y exhibited by the specimen is independent of the specimen height as is seen in the experimental results. This also implies that ε_y will vary with the inverse of the E. Thus, if thin specimens or flakes are tested in compression, the values of E and ε_y do not reflect the real material property, however σ_y is not affected by the specimen height.

Effect of density

Density has a significant influence on transverse compression properties. In Figure 14, σ_y is plotted against ρ^3 in the radial direction for yellow poplar. This result was obtained from the test described above, where samples were cut along the bar. When influences such as moisture content or structural differences are suppressed, there is a high correlation ($R^2 = 0.99$) between those two properties. This shows a very good agreement with the proposed theory. As E does not have a significant

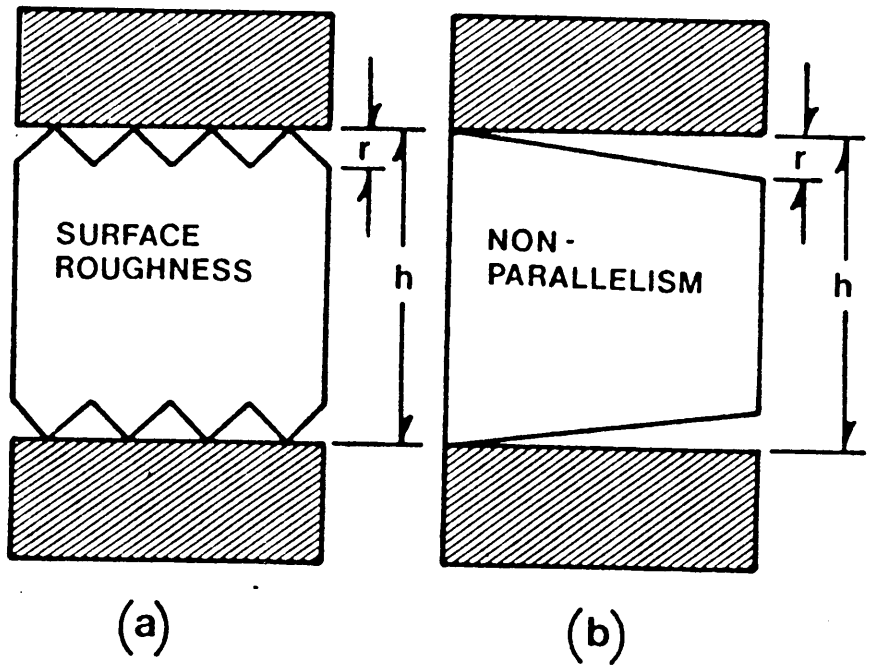

Figure 12. Model of compression specimen with (a) surface roughness and (b) non-parallel mating platen-surfaces.

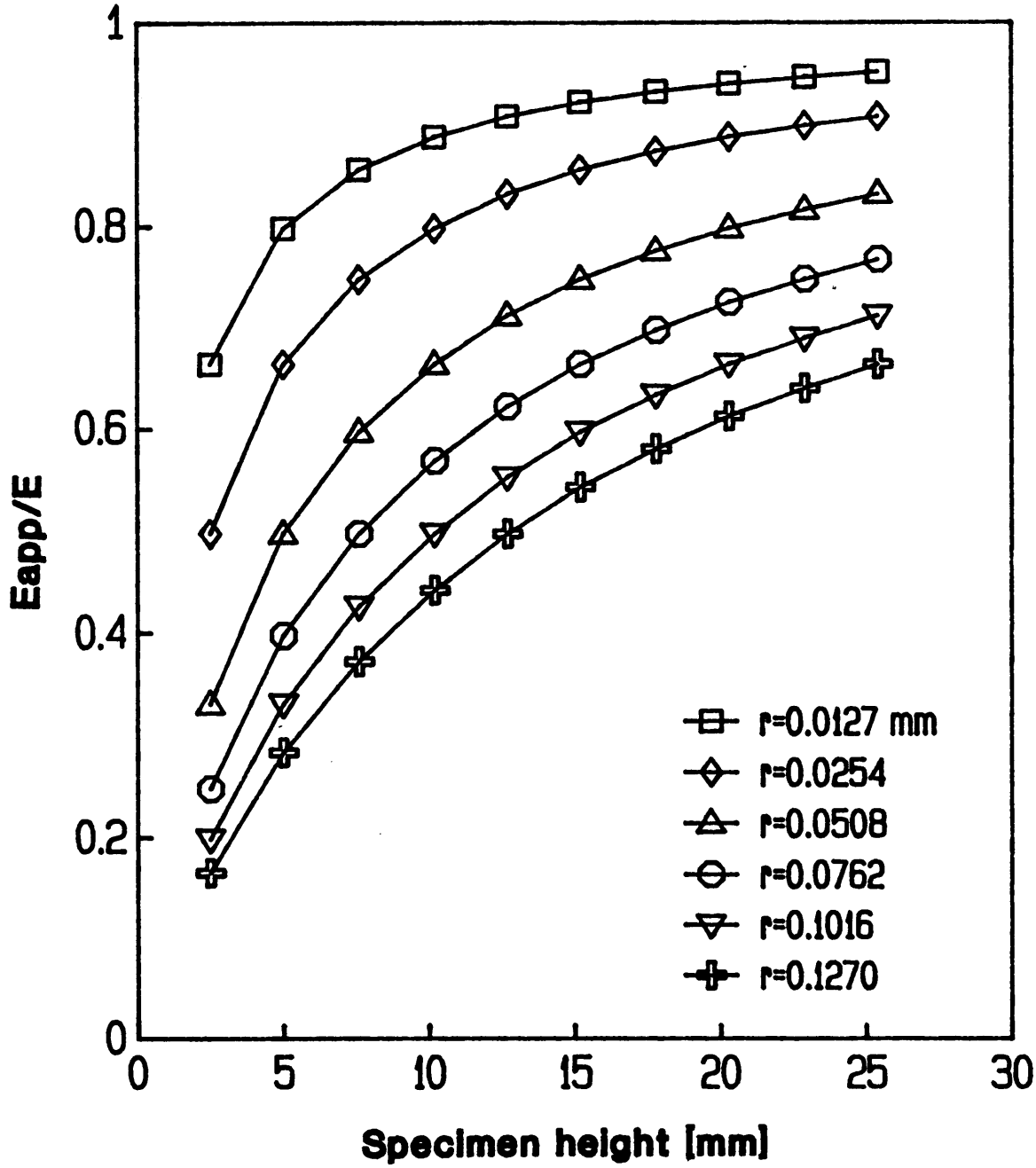

Figure 13. Predicted ratio of apparent modulus (Eapp) to actual modulus (E): expressed as a function of specimen height (h) for different surface roughnesses (r).

influence on the foam model at high strain (this will be discussed further), the relationship between ρ and E was not studied and results from the literature were employed (Bodig and Jayne 1982). The analysis of variance was used to detect the statistical differences between the densities for individual treatments means. Results are summarized in Tables 1 to 5 and Figures 15-19.

The asterisk under the values in Tables 1, 3-5 means, that there in no statistical difference between the treatments. As the radial and tangential specimens were paired, the rank of the values has the same order for both directions except treatments 2 and 3. There is, however, no significant difference between the radial and tangential densities.

The total average for all treatments and directions was $\rho_{tot} = 0.456$ g/cm^3 with the COV = 6 % which coincides with values reported in the literature for mature wood (Core et al 1978) and is somewhat higher than the average values taken for the whole tree (Bodig and Jayne 1982, Haygreen and Bowyer 1982).

Effect of the load direction

The influence of the load direction on E and σ_y for all treatments was studied. A significant difference between the radial and tangential directions was found for all treatments tested (see Table 2). A t-test on an $\alpha = 0.01$ level was employed. Mean values of E and σ_y for the tangential direction were significantly lower. This is possibly caused by the difference in the wood structure. Rays running in the radial direction represent longitudinal elements which cause higher stiffness in this direction (Bodig and Jayne 1982). The influence of the rays probably offsets the fact that in the radial direction the weaker earlywood zones deform more (earlywood and latewood are in series) which would imply less stiffness in the radial direction.

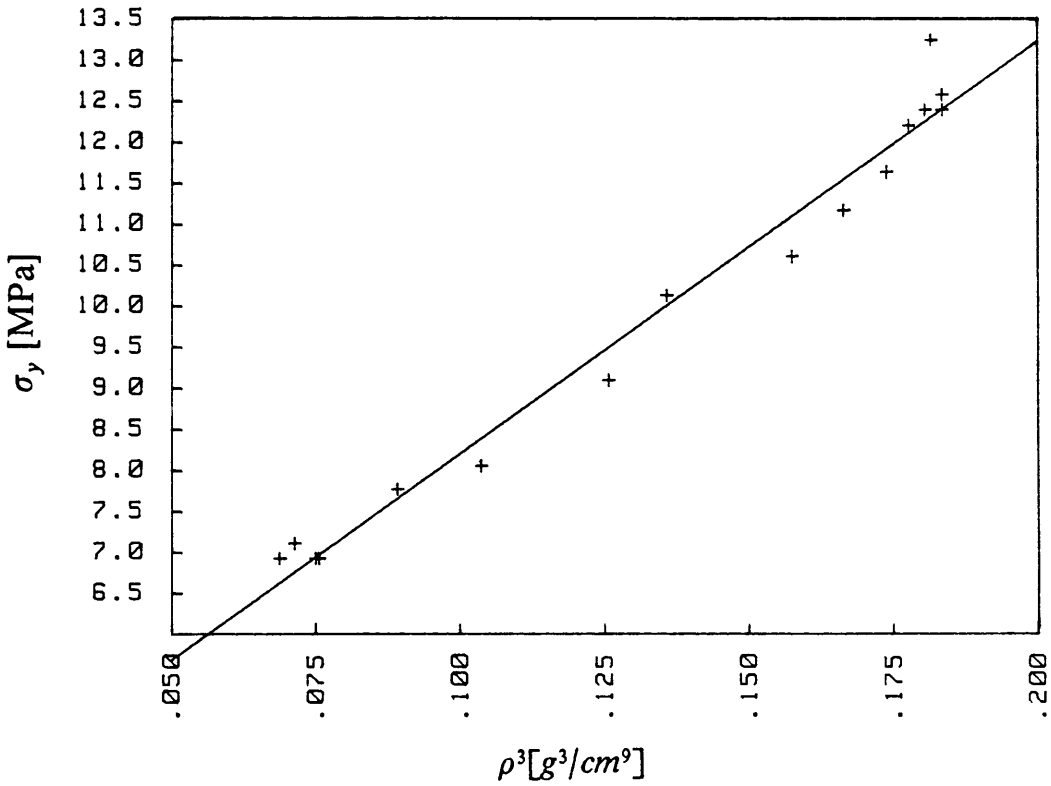

Figure 14. Density cubed - yield stress relationship for transverse compression of yellow poplar in radial direction.

Table 1. LSD test on differences between ρ for radial and tangential direction for yellow poplar 20 mm cubes ($\alpha = 0.05$).

Radial direction								
Treatment	2	8	5	1	3	6	4	7
ρ [g/cm^3]	0.479	0.475	0.468	0.468	0.460	0.437	0.437	0.425
	*	*	*	*	*			
					*	*	*	
						*	*	*
Tangential direction								
Treatment	2	3	5	1	8	6	4	7
ρ [g/cm^3]	0.480	0.473	0.470	0.468	0.467	0.430	0.429	0.428
	*	*	*	*	*			
						*	*	*

Asterisks in the line mean that there is no statistical difference between treatments.

Table 2. Modulus and yield stress at different moisture content and temperatures for yellow poplar 20mm cubes.

Trt.	n	MC	T	Dir	σ_y	s	E	s	ρ	s
-	-	%	°C	-	MPa	MPa	MPa	MPa	g/cm^3	g/cm^3
1	6	8	30	rd	8.99	1.20	680	91.3	0.468	0.022
1	6	8	30	tg	4.81	0.51	377	37.7	0.468	0.026
2	6	8	60	rd	8.70	1.15	550	96.0	0.479	0.028
2	6	8	60	tg	4.87	0.61	250	34.5	0.480	0.025
3	6	8	100	rd	6.11	0.50	404	50.7	0.460	0.018
3	6	8	100	tg	3.54	0.37	274	30.7	0.473	0.020
4	6	12	30	rd	6.42	0.51	478	43.8	0.437	0.020
4	6	12	30	tg	3.55	0.28	227	27.3	0.429	0.012
5	6	12	60	rd	7.27	0.54	537	72.0	0.468	0.013
5	6	12	60	tg	4.02	0.31	225	44.7	0.470	0.011
6	6	20	30	rd	4.79	0.39	376	63.9	0.438	0.021
6	6	20	30	tg	2.54	0.21	143	27.8	0.430	0.019
7	6	20	60	rd	3.04	0.25	240	10.6	0.425	0.017
7	6	20	60	tg	1.68	0.29	98	22.8	0.428	0.020
8	6	0	225	rd	2.36	0.50	254	28.9	0.475	0.019
8	6	0	225	tg	1.47	0.24	131	16.3	0.467	0.020

Table 3. LSD test on differences between E for radial and tangential direction for yellow poplar 20 mm cubes ($\alpha = 0.05$).

Radial direction								
Treatment	1	2	5	4	3	6	8	7
E [MPa]	680	550	537	478	404	376	254	240
		*	*	*				
					*	*		
							*	*
Tangential direction								
Treatment	1	3	2	4	5	6	8	7
E [MPa]	377	274	250	227	226	143	131	98
		*	*					
		*	*	*				
						*	*	

Asterisks in the line mean that there is no statistical difference between treatments.

Table 4. LSD test on differences between normalized moduli for radial and tangential direction for yellow poplar 20 mm cubes ($\alpha =$

Radial direction								
Treatment	1	4	5	2	6	3	7	8
E/ρ^3	6659	5755	5242	5108	4506	3951	3133	2380
	*	*						
		*	*	*				
			*	*	*			
					*	*		
						*	*	
							*	*
Tangential direction								
Treatment	1	4	3	2	5	6	8	7
E/ρ^3	3777	2872	2621	2297	2174	1812	1311	1265
		*	*					
			*	*	*			
						*	*	
				*	*	*		
							*	*

Asterisks in the line means that there is no statistical difference between treatments.

Table 5. LSD test on differences between normalized yield stress for radial and tangential direction for yellow poplar 20 mm cubes.

Radial direction								
Treatment	1	2	4	5	3	6	7	8
σ_y/ρ^3	87.4	79.4	77.5	71.2	64.8	57.3	39.7	22.0
				*	*			
		*	*					
					*	*		
Tangential direction								
Treatment	1	4	2	5	3	6	7	8
σ_y/ρ^3	48.8	44.7	44.1	38.8	33.6	32.4	21.7	14.4
	*	*	*					
					*	*		
				*	*			

Asterisks in the line mean that there is no statistical difference between treatments.

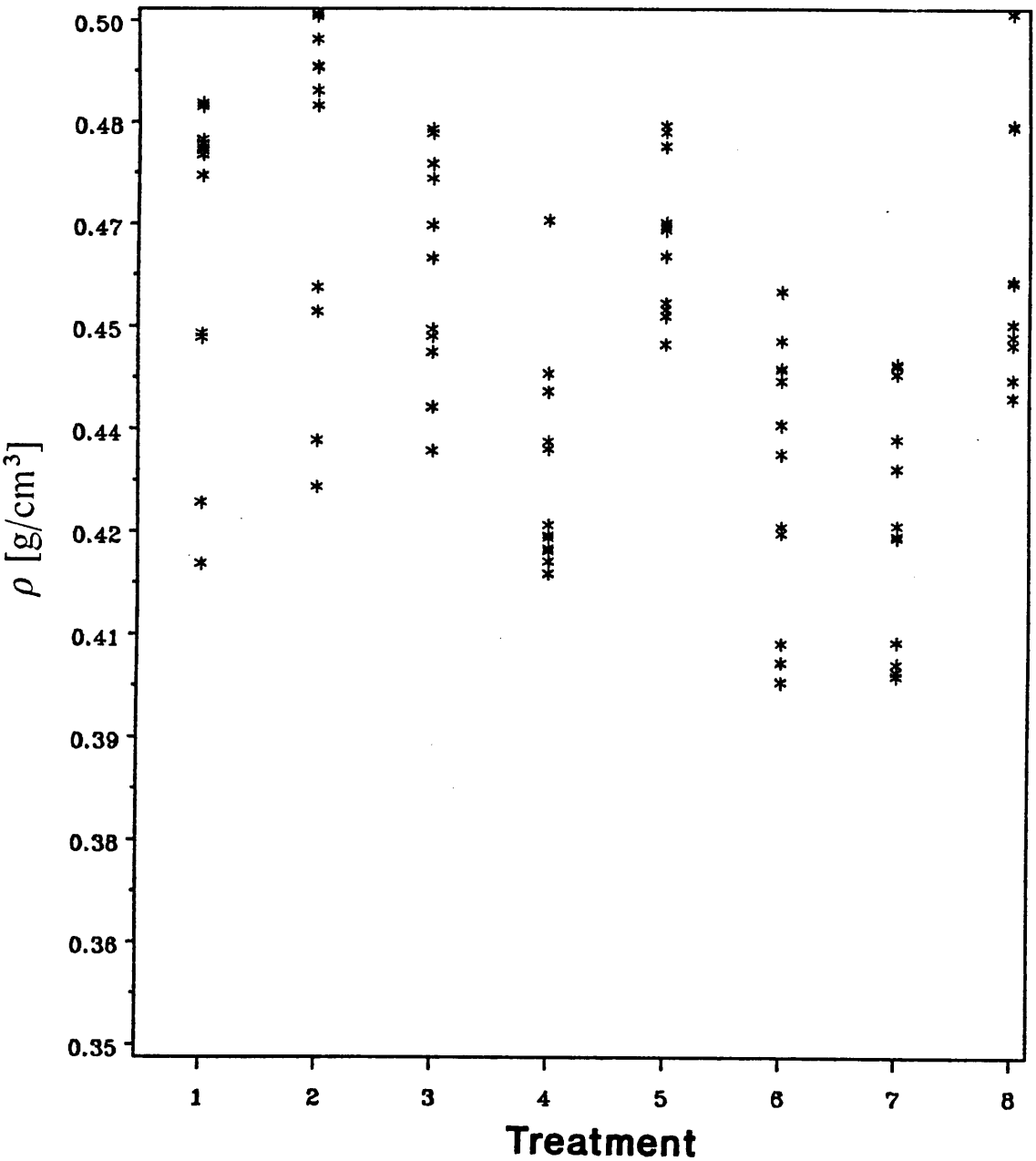

Figure 15. Densities for 20 mm yellow poplar cubes in radial and tangential direction for the treatments listed in Table 2.

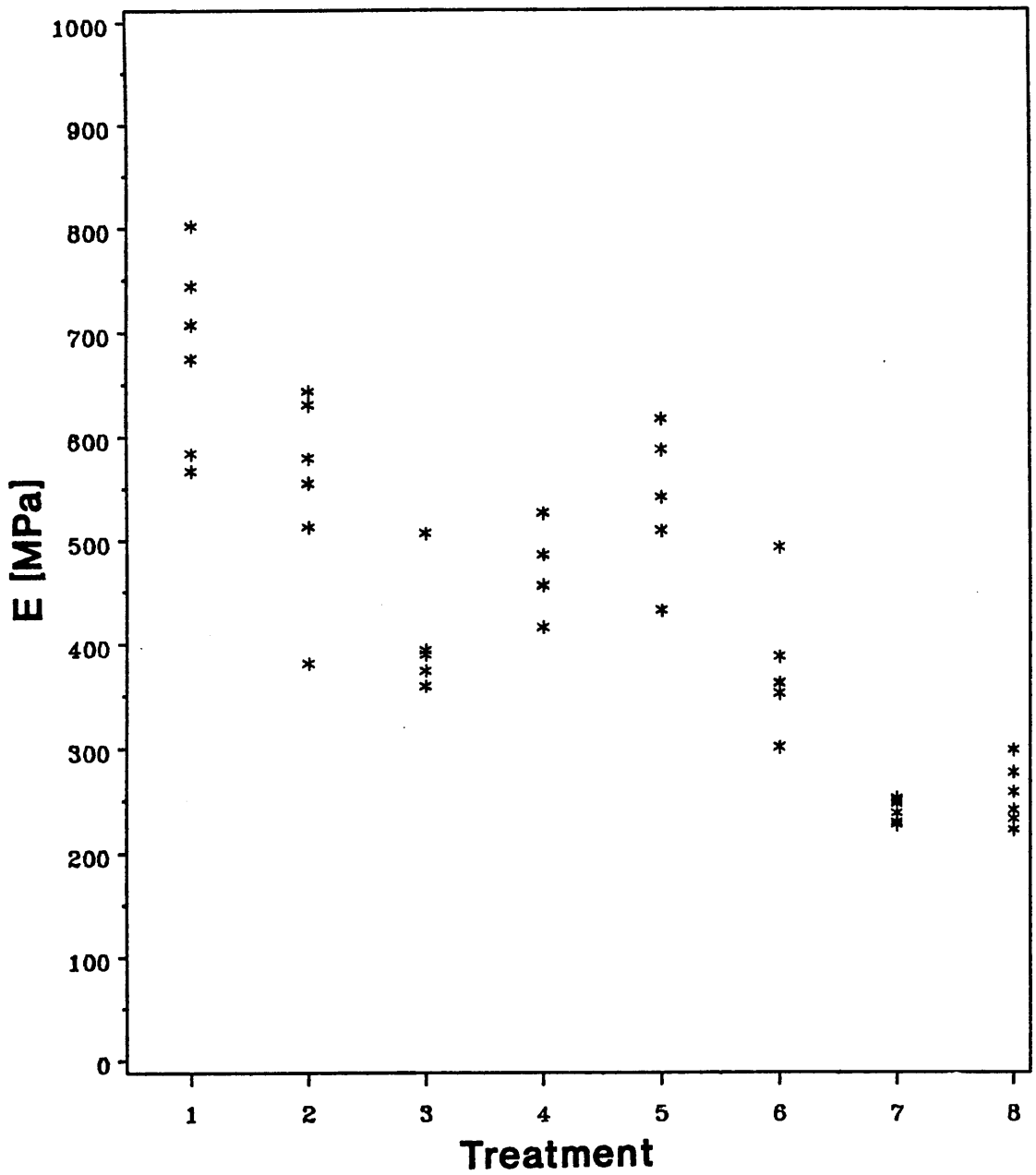

Figure 16. Modulus for 20 mm yellow poplar cubes in radial direction for the treatments listed in Table 2.

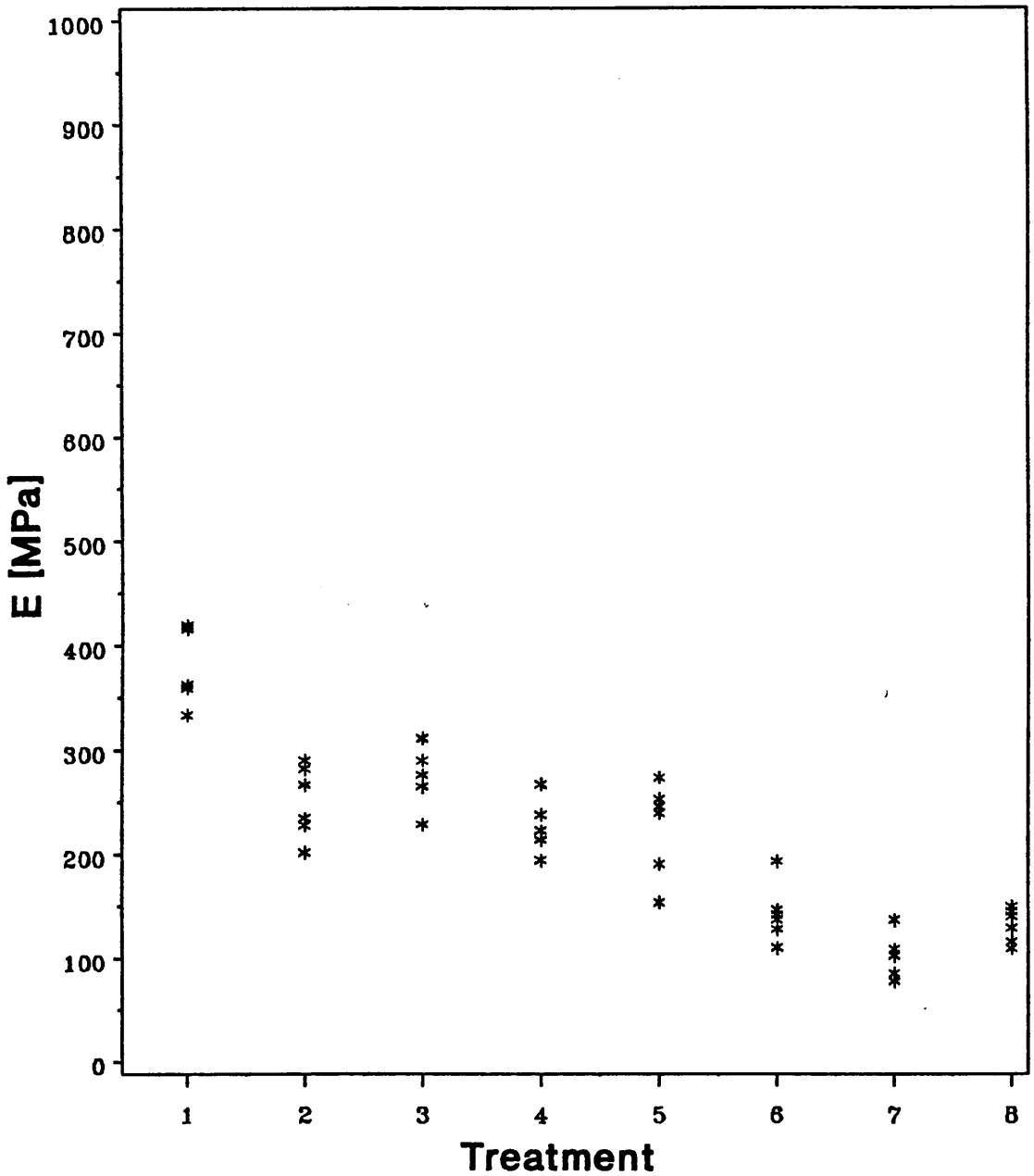

Figure 17. Modulus for 20 mm yellow poplar cubes in tangential direction for the treatments listed in Table 2.

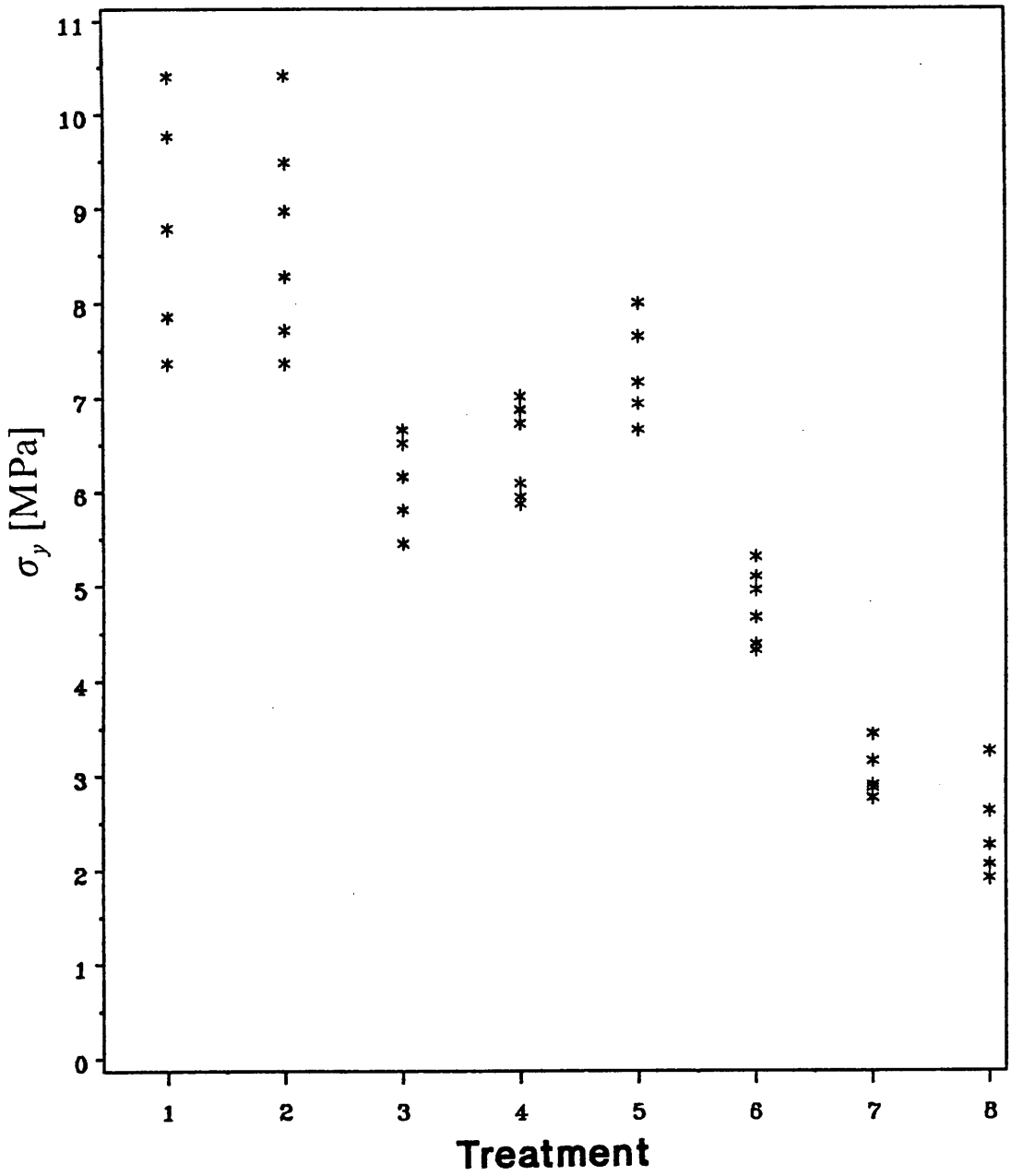

Figure 18. Yield stress for 20 mm yellow poplar cubes in radial direction for the treatments listed in Table 2.

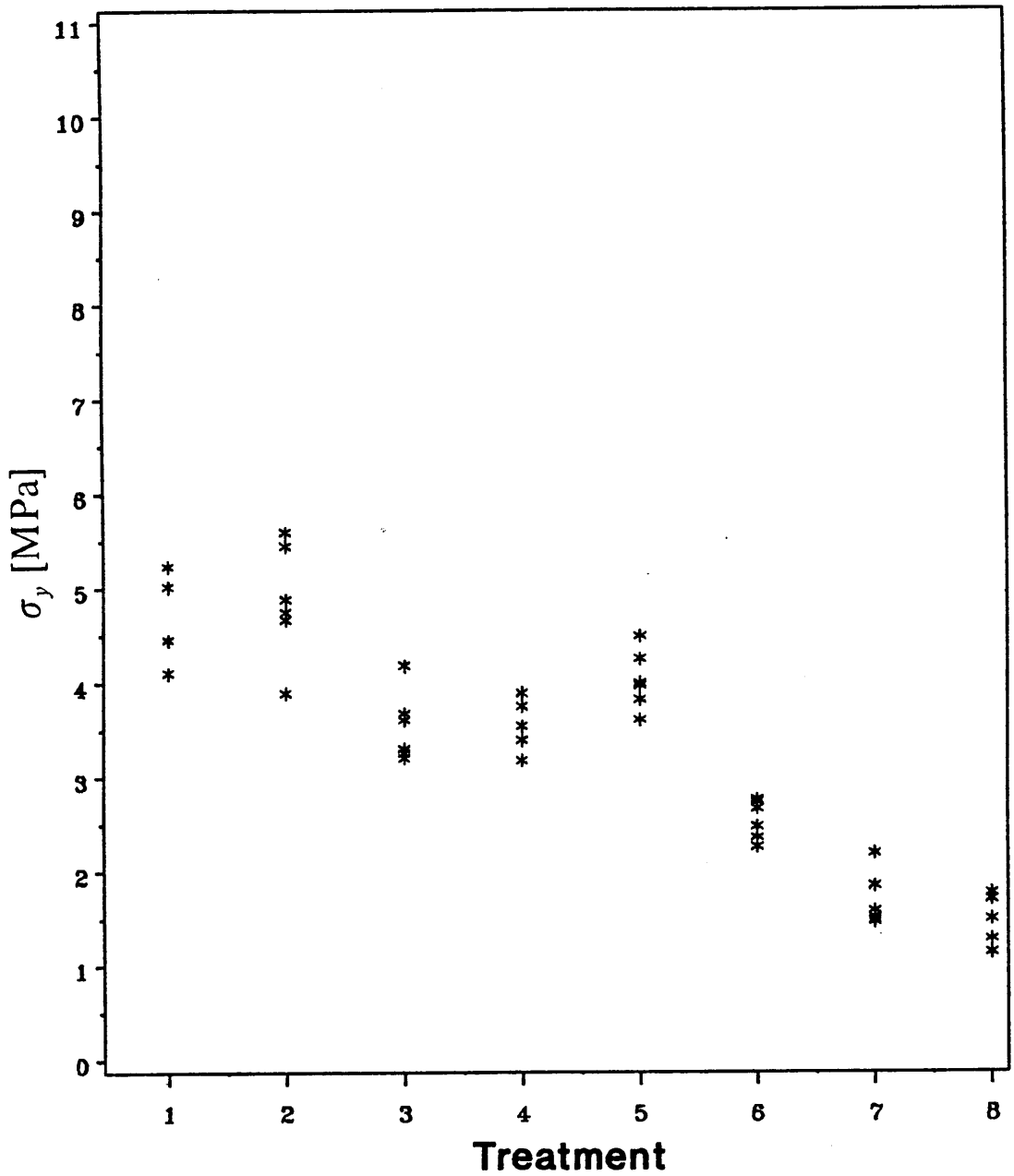

Figure 19. Yield stress for 20 mm yellow poplar cubes in tangential direction for the treatments listed in Table 2.

Temperature and moisture content effect

The effect of moisture content and temperature was studied separately for both directions. Results are summarized in Table 2. A least square difference test on means was employed and results are given in Tables 3-5 and Figures 18 and 19. Again, an asterisk under the mean value means that there is no statistical difference for the tested level. One can recognize that there is an identical trend in the moisture and temperature effect for both directions. It can be also noticed that some treatments have the same effect. In general, a high moisture content has a similar effect as a high temperature (e.g. for E/ρ^3 MC = 20% and T = 60°C gave statistically not different results from the treatment with MC = 0% and T = 225°C). This can be explained by the effect of bound water which causes the plasticization of the cell wall. Bound water interacts with the secondary linkage between adjacent polymer molecules and as a result, the wood becomes softer. High temperature causes greater molecular motion of chemical components in wood which causes further softenning. The moisture and temperature influence is generally known and has been studied mostly for properties along the fibers (Kollmann 1969, Bodig and Jayne 1982). Results presented coincide with findings of other researchers for directions parallel to the fibers.

The influence of different treatments on σ_y and modulus is shown in Figures 20 and 21.

Lateral expansion during the compression.

As mentioned in the literature review, there are rather contradictory opinions on the expansion of materials subjected to high strains. To clarify this problem, several tests on different specimen thicknesses were conducted and expansion was measured. Typical relationships are shown in Figures 22-25. The solid line represents the stress-strain relationship, whereas the dashed line shows

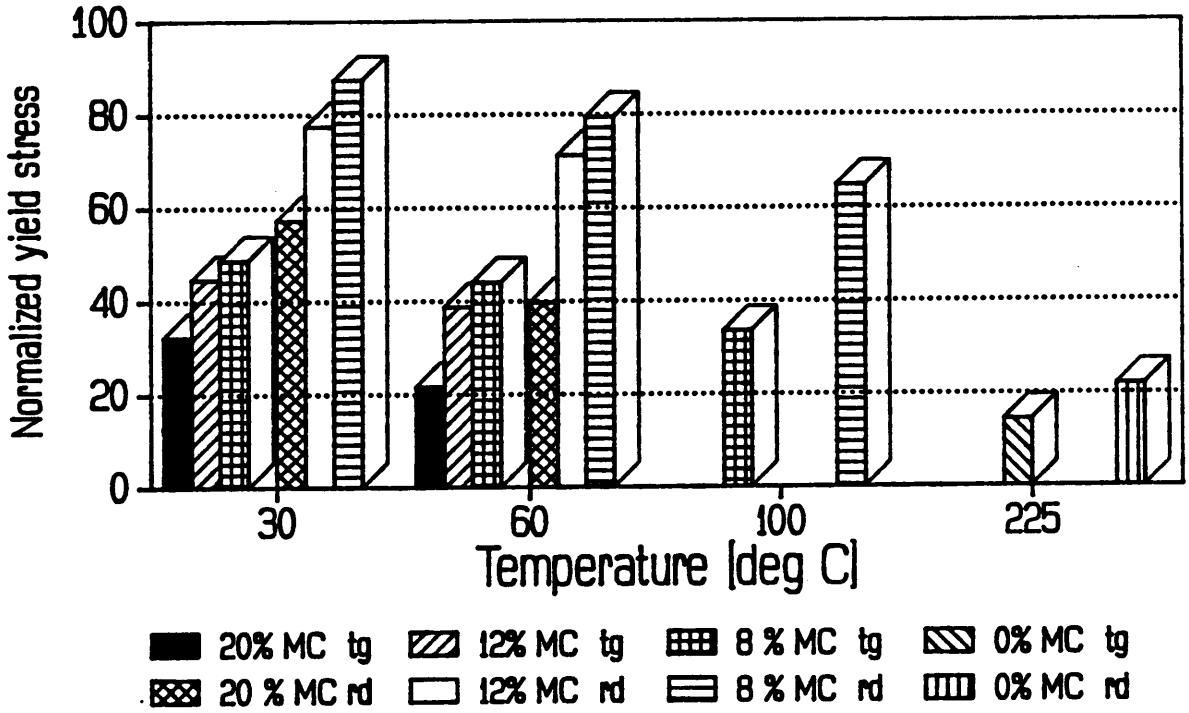

Figure 20. Normalized yield stress for 20 mm yellow poplar cubes in radial and tangential direction for the treatments listed in Table: Yield stress divided by the density cubed

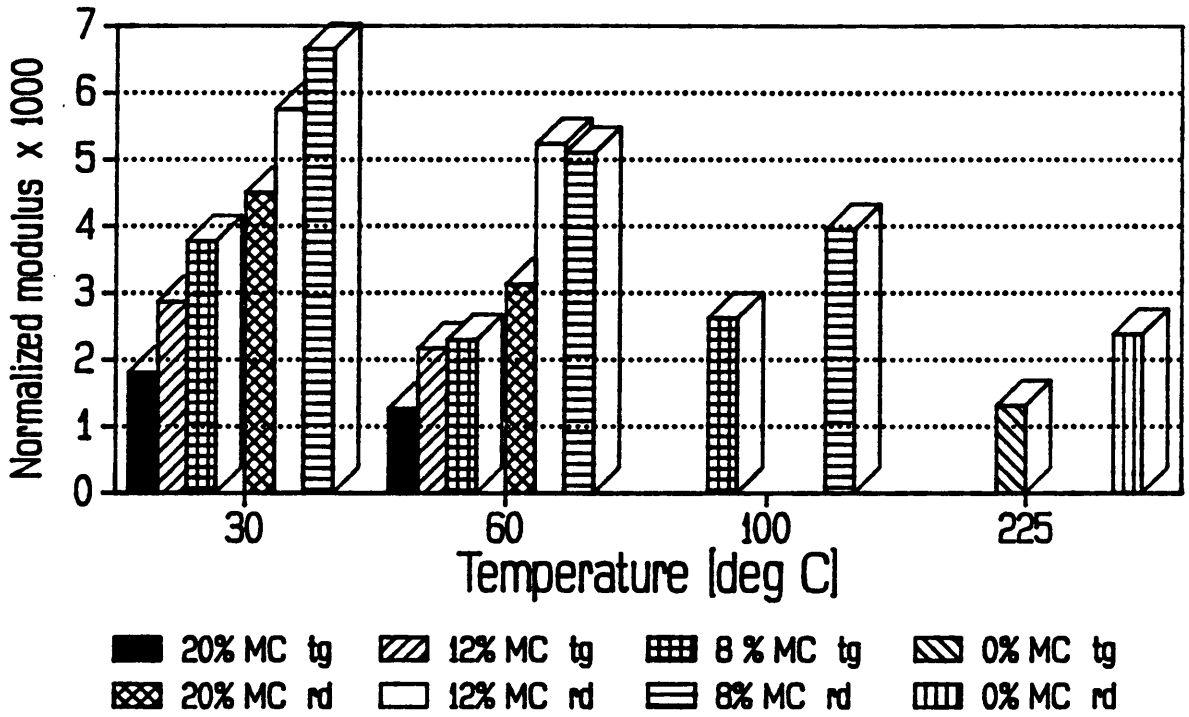

Figure 21. Normalized modulus for 20 mm yellow poplar cubes in radial and tangential direction for the treatments listed in Table 2: Modulus divided by the density cubed

the expansion coefficient as a function of strain. In Figure 22 a typical test result for a 20 mm cube is shown. One can recognize that the expansion ratio is approximately 0.4-0.45 in the linear region, which is the value that is usually reported for the Poisson's ratio. However, after σ_y was reached, the rate of the strain in the load direction was much higher than in the lateral direction, which caused a rapid decrease of the expansion coefficient. Tests on 20mm specimens could not be conducted beyond the strains of 0.2, because of the cracks mentioned earlier.

In Figures 23 and 24 typical curves for 5 mm and 3 mm specimen are shown. A similar shape as for the 20 mm specimen can be observed. However, the surface restraint caused a faster decrease and a lower value of the expansion ratio in the elastic region. For high strains, the value of the expansion ratio levels off and becomes approximately constant. The initial decrease of the expansion ratio was most likely caused by the surface roughness of the specimen as well as nonparallel surfaces. Thus the initial measured deformation in the load direction was too high as a result of the surface effects. As load increased, the specimen started to deform in the lateral direction. This can be observed as an increase of the Poisson's ratio in the linear region. This increase, however could not take place in thin specimens, because of the strong influence of the surface restraint. The constant value of the expansion ratio means that there is a proportional relationship between axial and transverse strain. A curve for a flake is shown in Figure 25. This low value of the expansion ratio, which remained constant during the entire test period was most likely caused by the surface restraint, which did not allow the surface of the specimen to deform in the lateral direction. Since the thickness is very low the whole cross-section is under the influence of the surface restraint and the resulting deformation is small.

Measurements of the thickness and width of the flakes immediately after opening of the compression apparatus indicate a value of the expansion ratio between 0.1-0.15. This shows that flakes recover more in the thickness direction. Similar results were obtained for 3 mm radial specimens, where the post-test expansion ratio was between 0.2 and 0.25, whereas values obtained during compression testing were below 0.1.

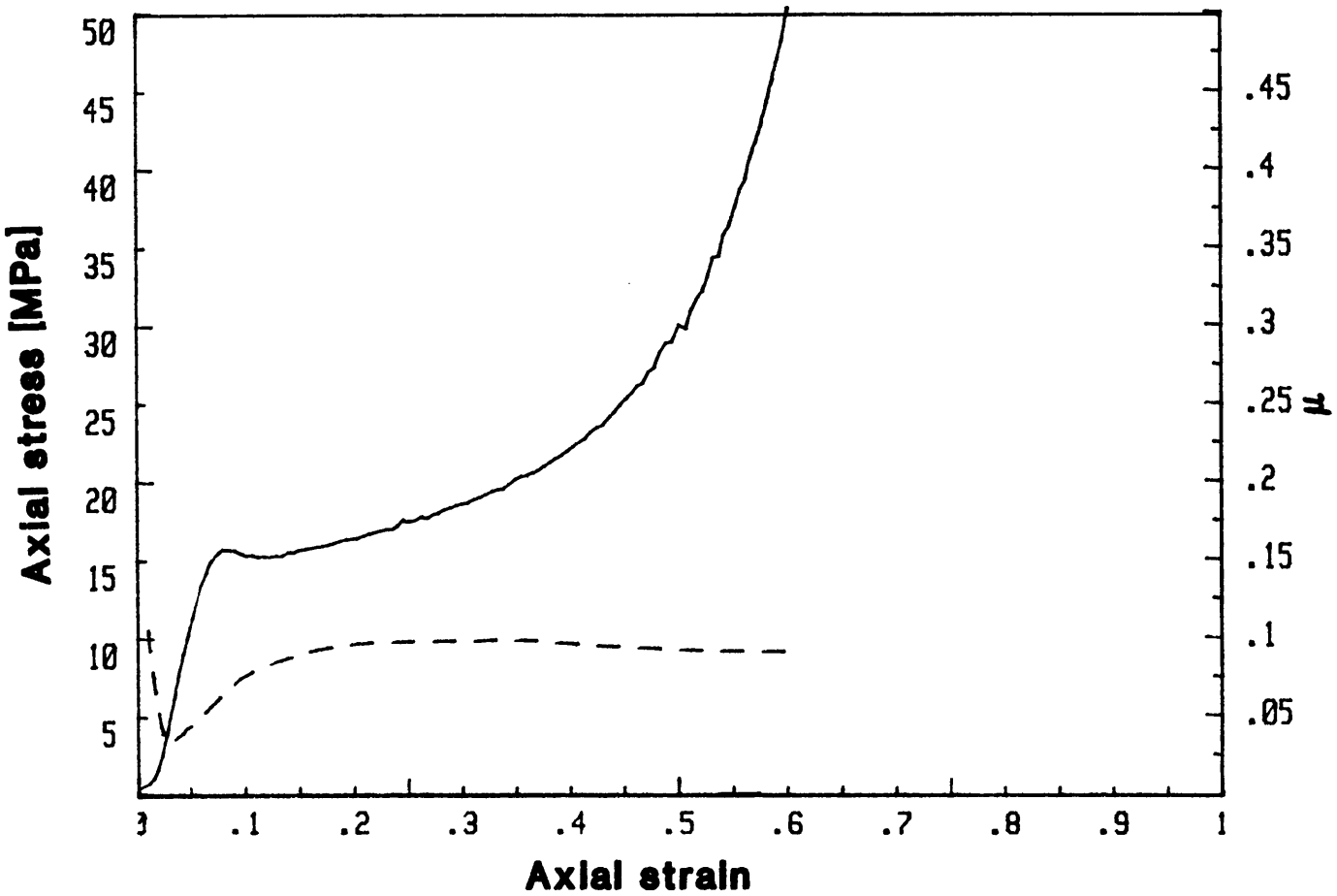

Figure 22. Strain-expansion ratio relationship for yellow poplar in radial direction for specimen measuring 20x20x20 mm.

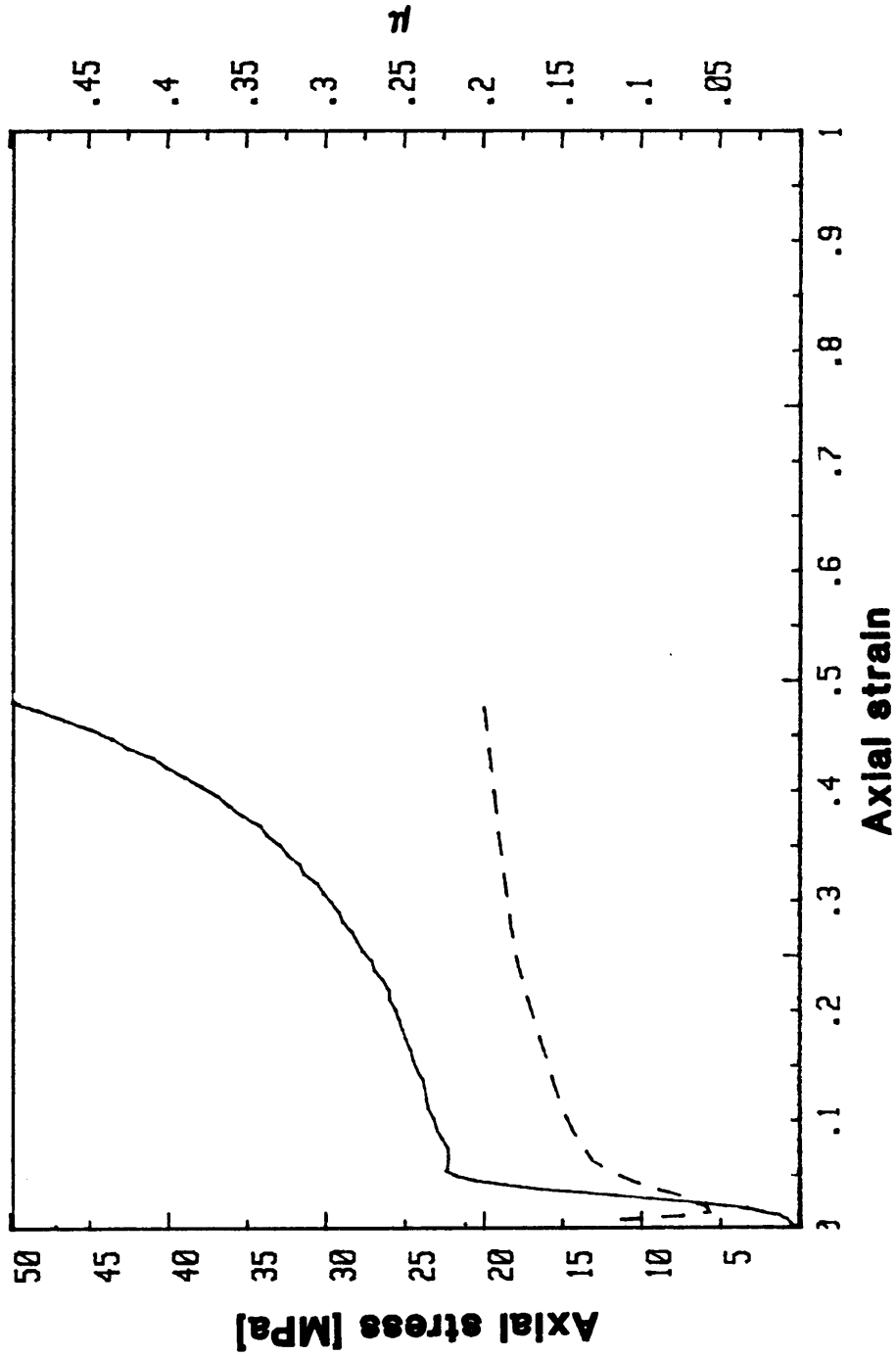

Figure 23. Strain-expansion ratio relationship for yellow poplar in radial direction for specimen measuring 20x20x5 mm.

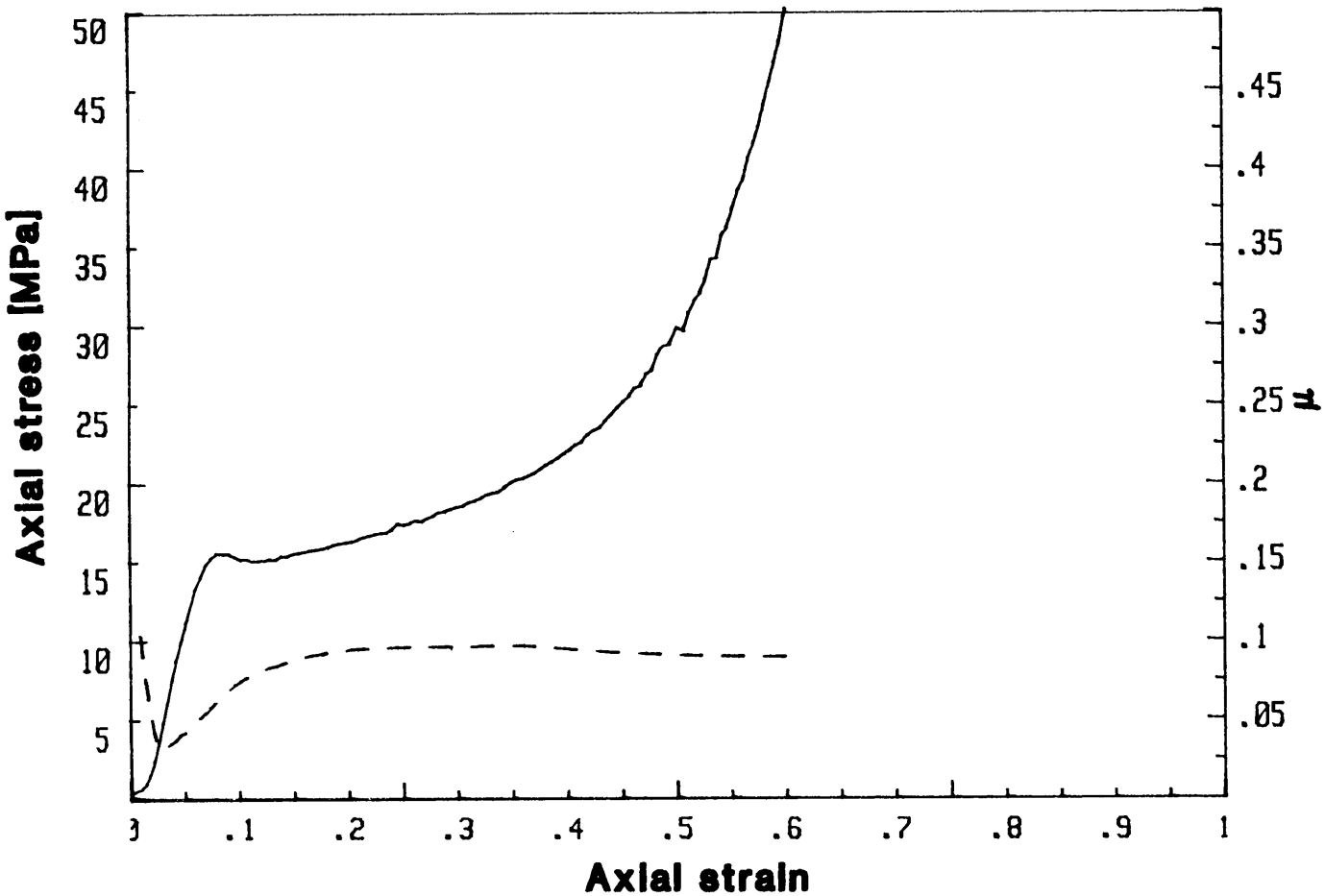

Figure 24. Strain-expansion ratio relationship for yellow poplar in radial direction for specimen measuring 20x20x3 mm.

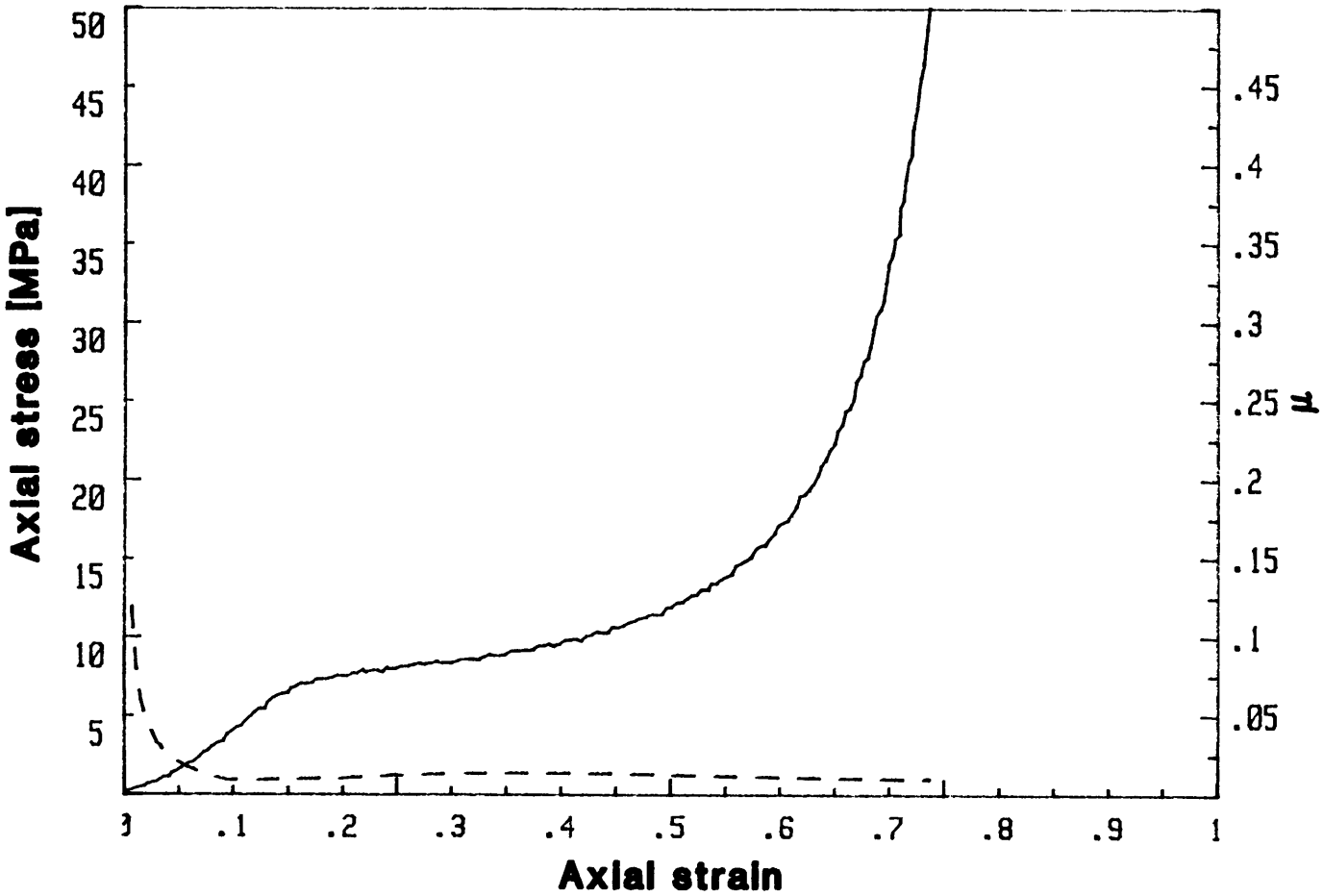

Figure 25. Strain-expansion ratio relationship for yellow poplar in radial direction for specimen measuring 20x20x1 mm.

The situation during the hot pressing of flakeboard, however, may be more complex. At the beginning of the pressing procedure the lateral expansion of a flake can be relatively high, because of low frictional forces caused by the normal stress. Also, the expansion ratio in the elastic region (Poisson's ratio) is high. When load increases, the friction increases and results in higher restraining forces. Thus, a decrease in the expansion ratio can be expected. As can be noticed from Figures 22-25, the load causing the yielding is high enough to suppress the specimen expansion. Therefore, if this load is achieved during a hot pressing process, a similar response can be expected, providing that friction between flakes will not be substantially different from friction of wood on steel.

Based on the observations above, Eq. [5] can be modified to incorporate the width change, which influences the volume and density change. The expansion change can be incorporated into the model using a simple approach of volume change. The model is in Figure 26. The lateral expansion in the fiber direction is neglected. Thus, volume change can be expressed as the area change. The relative density ρ'_{rel} after axial strain ε is:

$$\rho'_{rel} = \frac{\rho_{rel}}{1-\varepsilon}$$

The lateral expansion causes the increase of the area by the quantity $\mu\varepsilon$, which expresses the volume increase due to the expansion. Plates movement causes reduction of the area by $\varepsilon_1\varepsilon_2$ Since $\mu = \varepsilon_1/\varepsilon_2$, $\varepsilon_1\varepsilon_2 = \varepsilon^2\mu$ Then Eq. [5] becomes:

$$\sigma = \sigma_y \left[\frac{1-\rho_{rel}^{1/3}}{1-\left(\frac{\rho_{rel}}{1-\varepsilon+\mu\varepsilon-\mu\varepsilon^2}\right)^{1/3}} \right]^3 \qquad [6]$$

$$\sigma_y = E_s\rho_{rel}^3$$

Where

$\mu =$ expansion ratio

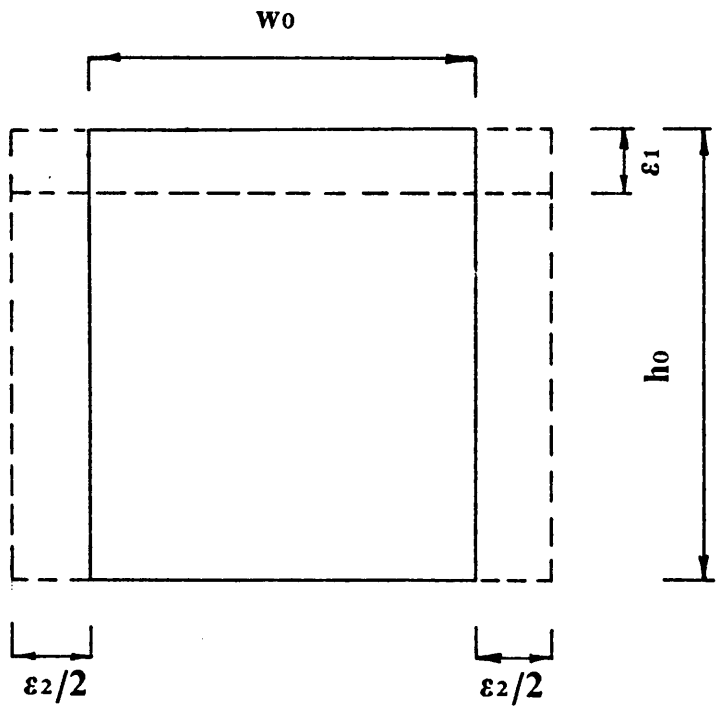

Figure 26. Influence of the non-zero expansion coefficient on the density without surface restraint: load in the direction of ε_1.

The model in Figure 26 can be improved by assuming that there is no lateral displacement at the boundary of the specimen which is in contact with the platens (see Figure 27). A parabolic shape of the displacement is assumed:

$$\sigma = \sigma_y \left[\frac{1 - \rho_{rel}^{1/3}}{1 - \left(\frac{\rho_{rel}}{1 - \varepsilon + 2/3\mu\varepsilon - \mu\varepsilon^2} \right)^{1/3}} \right]^3 \qquad [7]$$

The influence of different values of the expansion ratio on the relative density is shown in Figure 28. One can recognize that the non-zero expansion coefficient suppresses the rate of the change of the relative density. Based on the previous discussion we assume the expansion ratio is not negligible.

In Figure 29 Eq. [7] is used for prediction of the stress-strain relationship for treatments listed in Table 2. Average values were taken for the prediction. Differences in curve shapes demonstrate the influence of the moisture content and temperature. Curves are plotted for constant value of density for all treatments.

Testing of flakes

The results for flakes tested in the radial and tangential directions are in Table 6. Despite the random assignment to groups, there was a significant difference between densities in the tangential flakes for different treatments. Since the flake thickness was smaller than the annual ring thickness, there is a high variance in the flake density and a larger sample size is required to account for the differences in the density. Radial flakes, however, were consistent in the density because of ap-

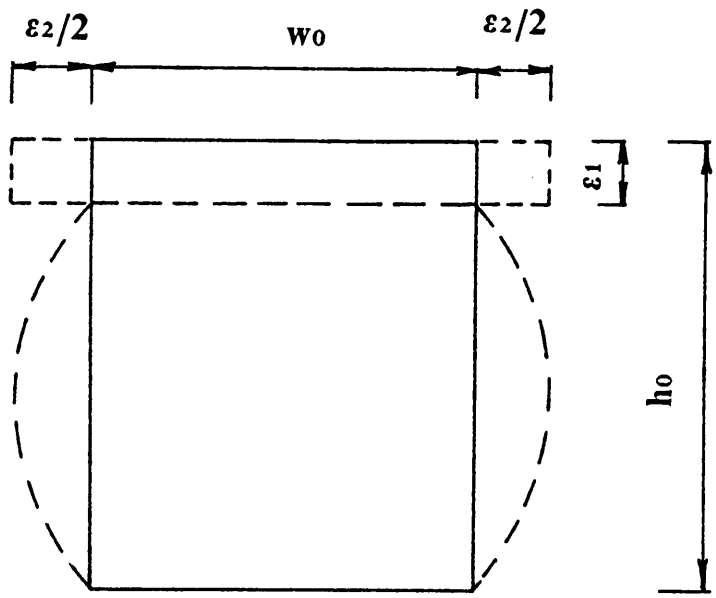

Figure 27. **Influence of the non-zero expansion coefficient on the density with surface restraint:** load in the direction of ε_1.

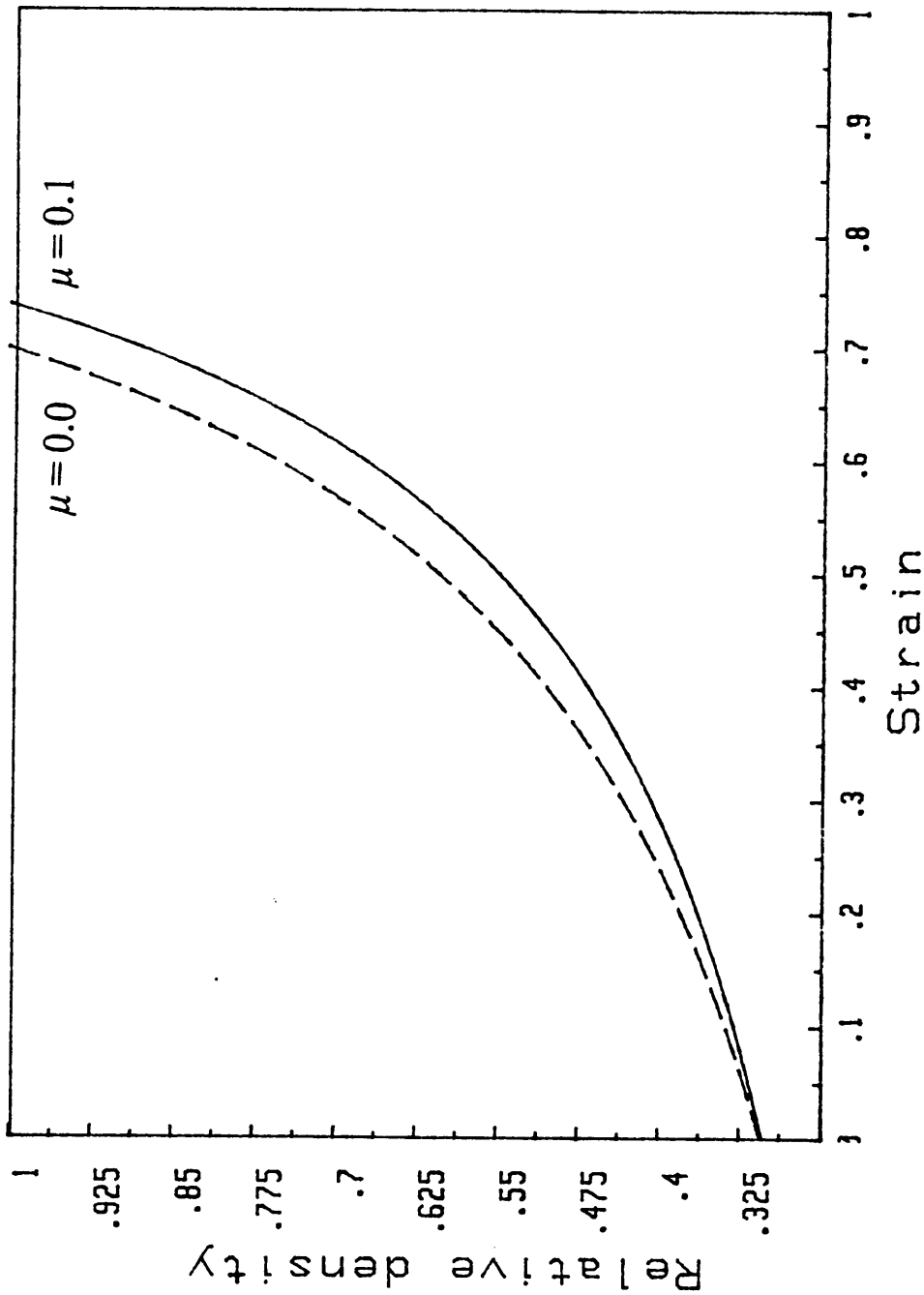

Figure 28. Relative density as a function of strain and expansion ratio.

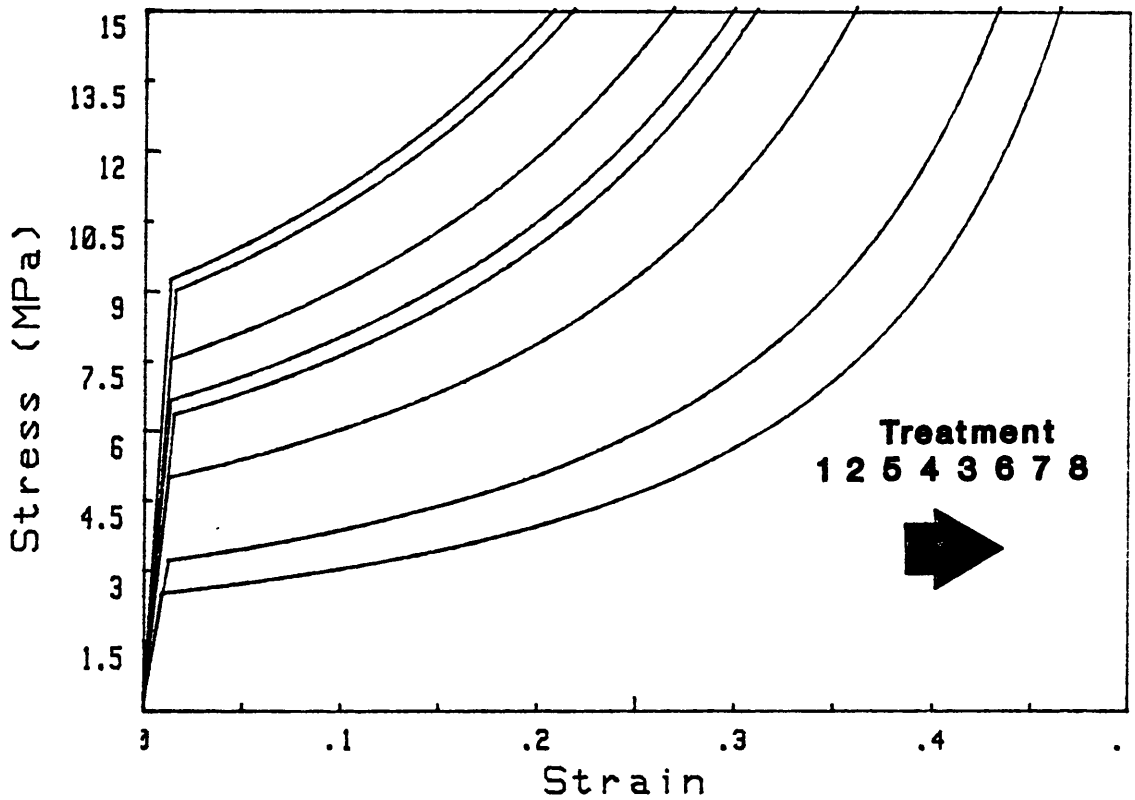

Figure 29. Prediction of compression behavior for yellow poplar for treatments listed in Table 2: density is constant for all curves.

proximately the same amount af earlywood and latewood present. To suppress the density influence, a statistical comparison of σ_y was carried out for the ratio σ_y/ρ^3 . Results for radial compression (tangential flakes) are presented in Table 7. One can recognize that as for cubes, there is no significant difference between several treatments, which implies the interaction between temperature and moisture content. The total average density was $\rho = 0.417$ g/cm^3 with the standard deviation s = 0.049 g/cm^3.

Since the value of E calculated from the tests of thin specimens has no meaning (because of surface effects), no evaluation was conducted on this quantity. A typical stress-strain curve for a flake is shown in Figure 25. The low slope in a linear region expresses the influence of the surface quality and other factors mentioned earlier.

Foam model applied to thin specimens

Sensitivity study

The sensitivity of the proposed model to different parameters was studied. As wood exhibits a high variability of properties, knowledge of the influence of different parameters on model behavior helps to determine which property should be studied closer. The influence of E, relative density (ρ_{rel}), σ_y, and μ on the model was investigated. One parameter was varied while the others remained constant. Based on the literature and previous results, the following constant values were chosen:

- $\rho_{rel} = 0.3$
- E = 680 MPa
- σ_y = 9.0 MPa

Table 6. Yield stress and density for yellow poplar flakes.

Trt.	n	MC	T	Dir	σ_y	s	ρ	s
-	-	%	°C	-	MPa	MPa	g/cm^3	g/cm^3
1	14	12	30	rd	6.65	1.86	0.393	0.047
2	5	10	30	rd	11.36	3.23	0.450	0.054
3	6	12	60	rd	7.75	2.45	0.483	0.055
3	6	12	60	tg	5.03	1.28	0.447	0.038
4	5	20	30	rd	5.05	0.97	0.382	0.048
4	5	20	30	tg	3.83	0.33	0.462	0.040
5	6	02	125	rd	7.47	3.13	0.383	0.055
6	5	0	225	rd	4.98	0.677	0.492	0.032
6	5	0	225	tg	3.11	1.19	0.458	0.010

Table 7. LSD test on differences between normalized yield stress in radial compression of yellow poplar flakes ($\alpha = 0.05$).

Radial direction						
Treatment	5	2	1	4	3	6
σ_y/ρ^3	129.0	124.1	110.6	92.5	90.4	41.8
	*	*	*			
			*	*	*	

Asterisks in the line mean that there is no statistical difference between treatments.

- $\mu = 0.1$

The influence of E is given in Figure 30. The range of the values tested was 100-800 MPa with 100 MPa steps. One can recognize that E does not have a significant influence on the non-linear part of the curve. This is a consequence of the model, because the σ_y (which is identical to the critical buckling stress) controls the high strain behavior. The linear region is obviously controlled by the E (see Figure 30).

The relative density was varied from 0.1 to 0.5 g/cm^3. The higher the density the shorter the plateau region. Since the value of the relative density in the model is to the third power, the influence is logically high (see Figure 31).

The σ_y (Figure 32) also significantly changes the length of the plateau. Lower σ_y causes a longer plateau and higher slope in the densification region, whereas higher σ_y acts in the opposite direction. If σ_y is high, there is a higher stress required to collapse the cell wall and the stress-strain curve becomes steeper in the plateau region. For a low σ_y value, most of the cell walls collapse at a lower stress and a greater portion of the densification takes place in the plateau region. Thus, the slope becomes steeper because the relative density approaches unity.

As mentioned earlier, the expansion ratio causes shifting of the stress-strain curve towards high strains, because the rate of the increase of the relative density decreases with increasing μ (Figure 33). There is no large difference between $\mu = 0.0$ and $\mu = 0.1$, however, neglecting this value can cause a difference in the prediction. It remains a question, what expansion ratio should be applied in a real situation (eg. flakeboard manufacturing). Based on our tests, we estimate μ to be less than 0.1.

When the high variability of wood properties is taken into account, as well as the fact that those properties are not independent random variables, a high scatter of the stress-strain curves can be obtained from experiments. As the density and σ_y are the most dominant controlling factors and

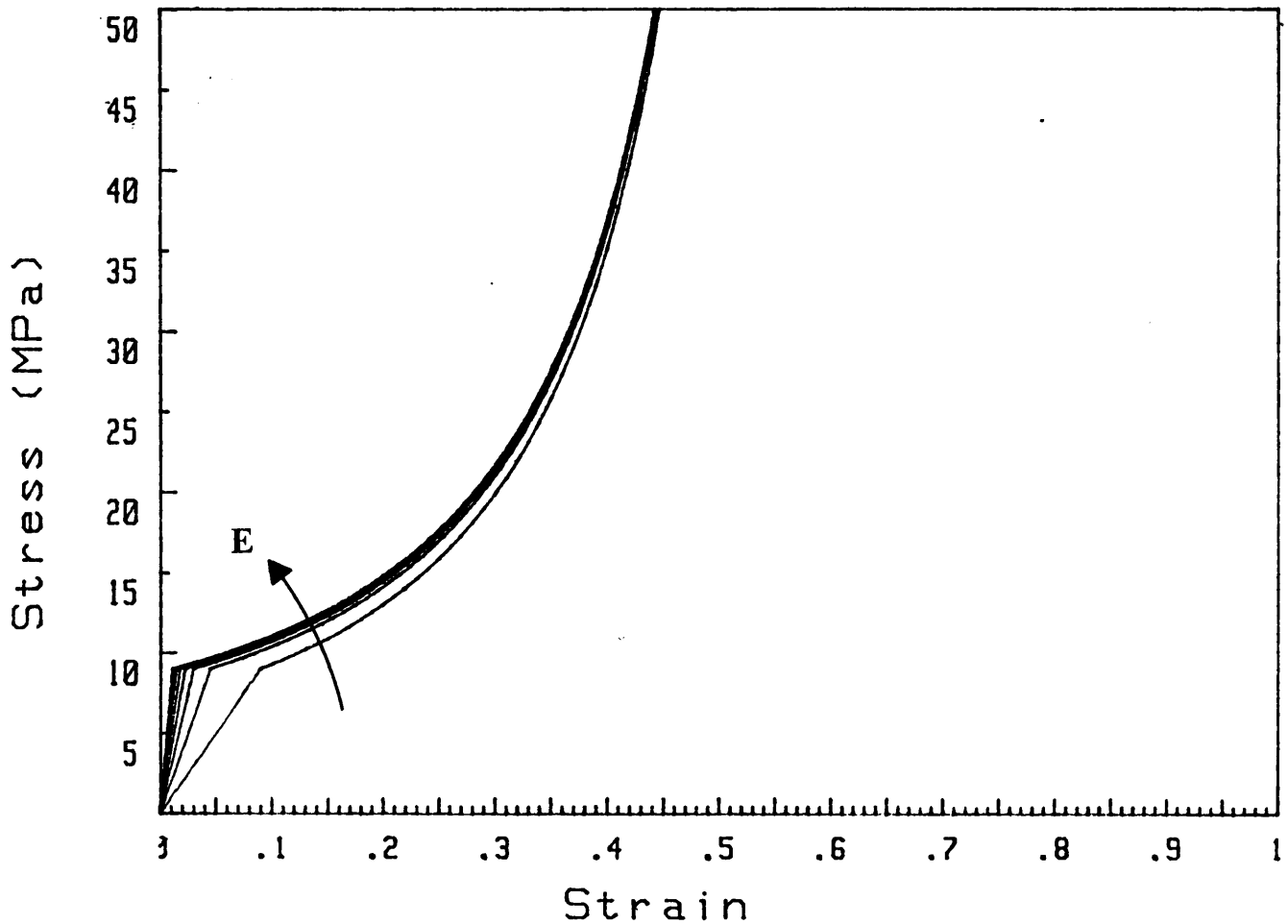

Figure 30. Influence of E on the proposed model: E varies between 100 and 800 MPa.

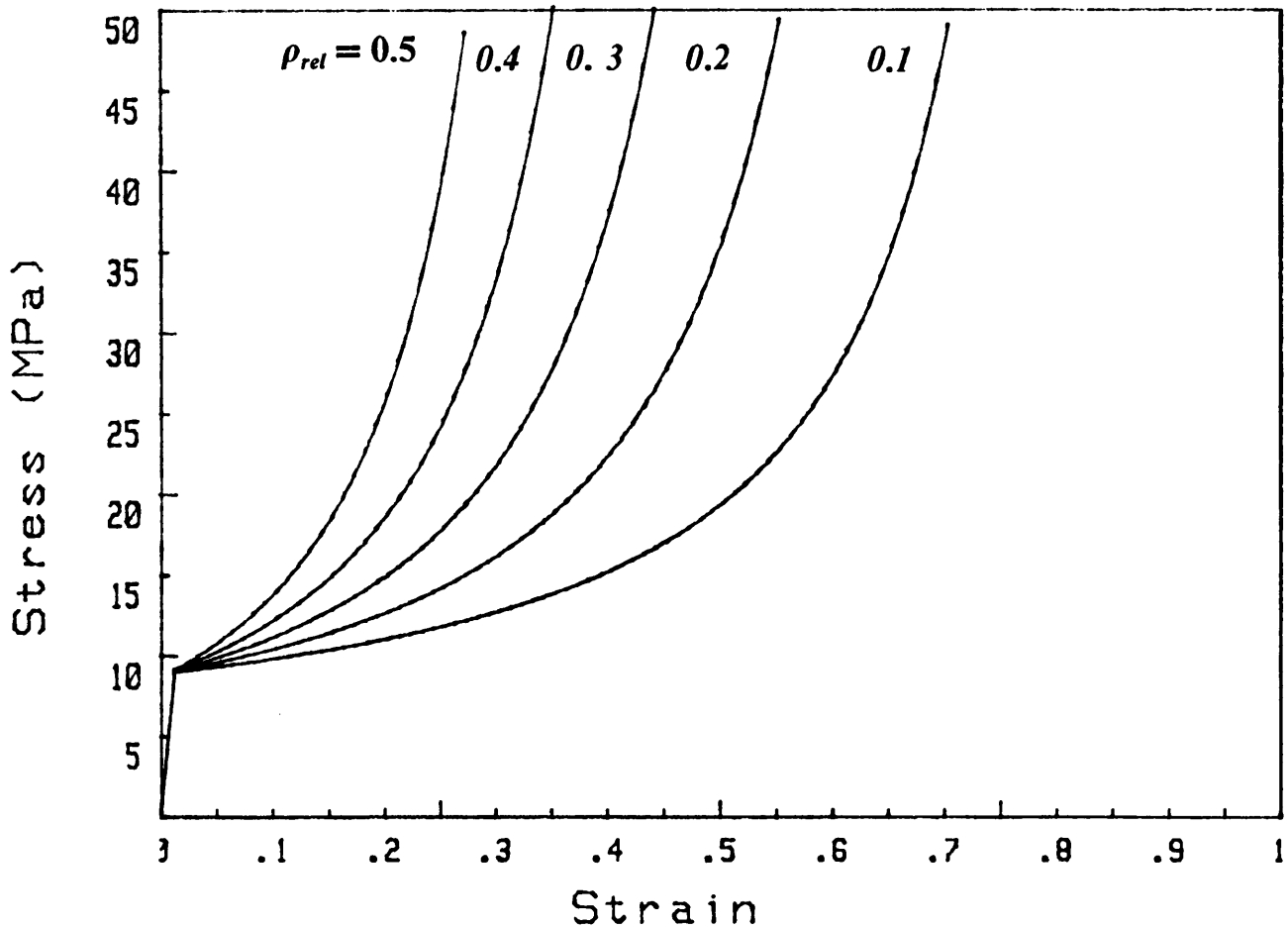

Figure 31. Influence of relative density on the proposed model: ρ_{rel} varies between 0.1 and 0.5 g/cm^3.

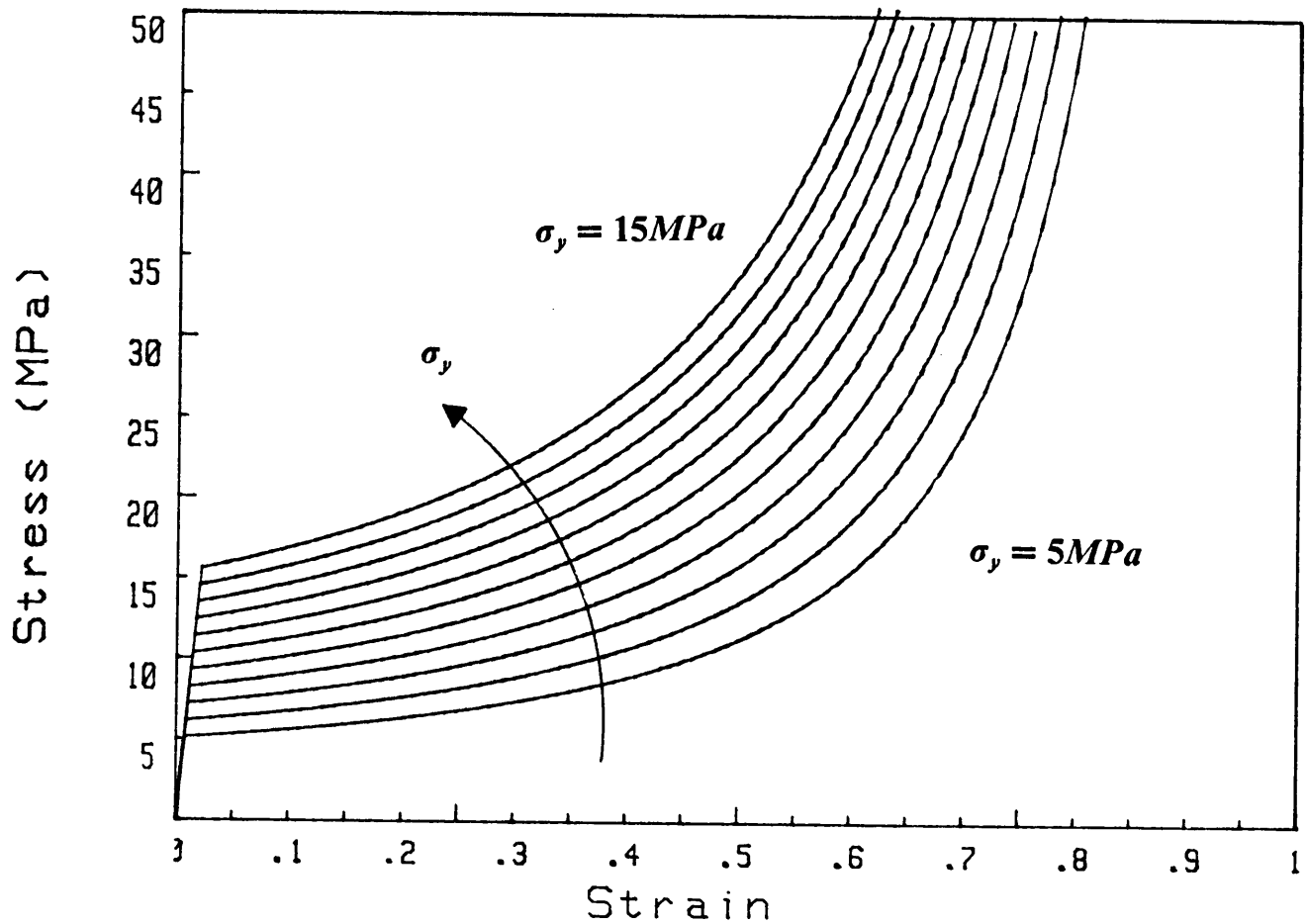

Figure 32. Influence of the yield stress on the proposed model: σ_y varies between 5 and 15 MPa.

as there is a strong correlation between them, the shape of the curves can be remarkably different even within a species. Also, if thin specimens are tested (flakes), the variability in the density and σ_y is higher because of different amounts of earlywood and latewood. The influence of these parameters on the predictive force of the model was studied as a stochastic process.

Quality of the model

To study the predictive quality of the model, theoretical stress-strain diagrams were compared with the results obtained from flake testing. Each measured point on the experimental curve was compared with the prediction based on Eq.[7]. Values of $\mu = 0.05$ and $\rho_s = 1.5$ g/cm^3 were taken as constant in Eq. [7]. The error of the prediction was calculated using the formulas:

$$Error1 = \sum_{i=1}^{N} \frac{|\sigma_{y,theor}(i) - \sigma_{y,exp}(i)|}{\sigma_{y,exp}(i)} 100 \qquad [8]$$

$$Error2 = \sum_{j=1}^{m} \frac{|\varepsilon_{y,theor}(j) - \varepsilon_{y,exp}(j)|}{\varepsilon_{y,exp}(j)} 100 \qquad [9]$$

Where:

$\sigma_{y,exp}(i)$ = experimental value of σ_y for i-th point

$\sigma_{y,theor}(i)$ = predicted value of σ_y for i-th point

$\varepsilon_{y,exp}(j)$ = experimental value of strain at yield stress for j-th point

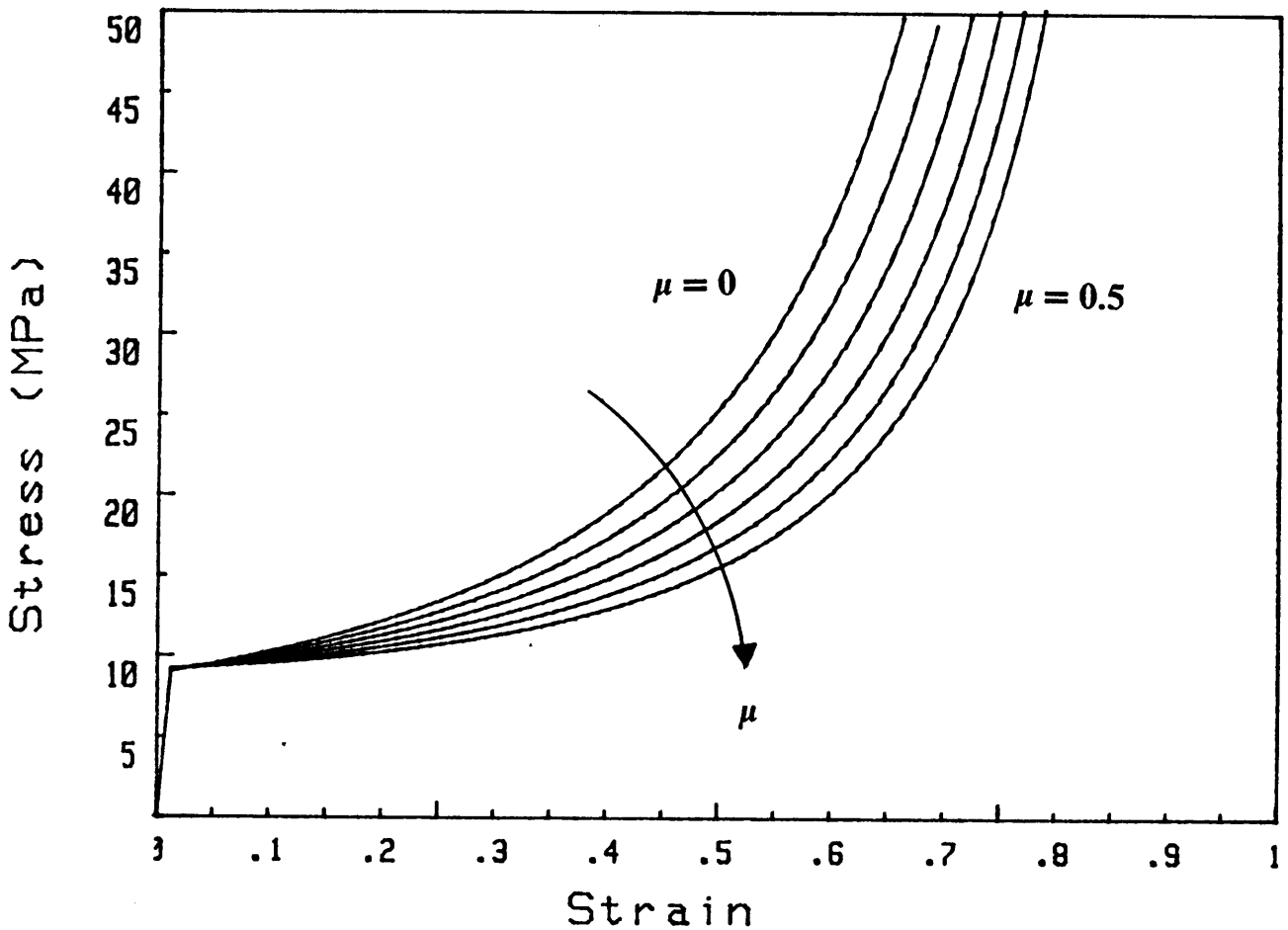

Figure 33. Influence of the expansion ratio on the proposed model: μ varies between 0.0 and 0.5 .

$\varepsilon_{y,theor}(j)$ = predicted value of strain at yield stress for j-th point

Eq. [8] was used when the slope of the stress-strain curve was less then 1.0, whereas Eq. [9] was used when the slope was greater then 1.0. Errors were calculated for each point on the experimental curve. A typical stress-strain diagram, with prediction, is shown in Figure 34. The portion predicting the elastic behavior is based on the results from testing the 20 mm cubes (see Table 2). The dashed line running parallel to the x-axis represents the amount of the strain associated with a thin specimen. The prediction begins at the yield stress. There Error1 and Error2 are equal to zero. Error1 represents the average vertical shifting and Error2 represents the horizontal shifting of the theoretical curve against the experimental stress-strain relationship.

The results for the 60 specimens tested under conditions described in Table 6 were used for the comparison. Error1 was 5.6% with a 62.0% coefficient of variation, Error2 was 11.7% with a 58.0% coefficient of variation. These results can be considered as very encouraging with respect to the initial assumptions made for the model. Except for the value of the density of the cell wall, all other values were determined by test and used for prediction. The average E value from Table 2 was used for the linear part. As was shown in the sensitivity study, E has negligible influence on the prediction beyond the yield stress. The possible variance in the density of the cell wall may have a significant effect on the difference between the experiment and prediction. The mean cell wall density ρ_s is reported to be from 1.44 to 1.56 g/cm^3 (Panshin and de Zeeuw 1980, Haygreen and Bowyer 1982). Since the ρ_{rel} is raised to the third power, a small change in ρ_s causes a relatively large change in the prediction (see chapter on sensitivity study). For example Error1 = 17.4% and Error2 = 11.8% for ρ_s = 1.54 was suppressed to 8.9% and 3.3% using ρ_s = 1.44. This shows the large influence of the ρ_s on prediction. As the values reported for the cell wall density are mean values, the individual measurements can vary even more. However, ρ_s is almost always an unknown quantity. Thus, the generally accepted value of 1.5 g/cm^3 is recommended. Another source of error can by the presence of cracks in the cell wall during high strain deformation, a phenomenon that is not treated by the model.

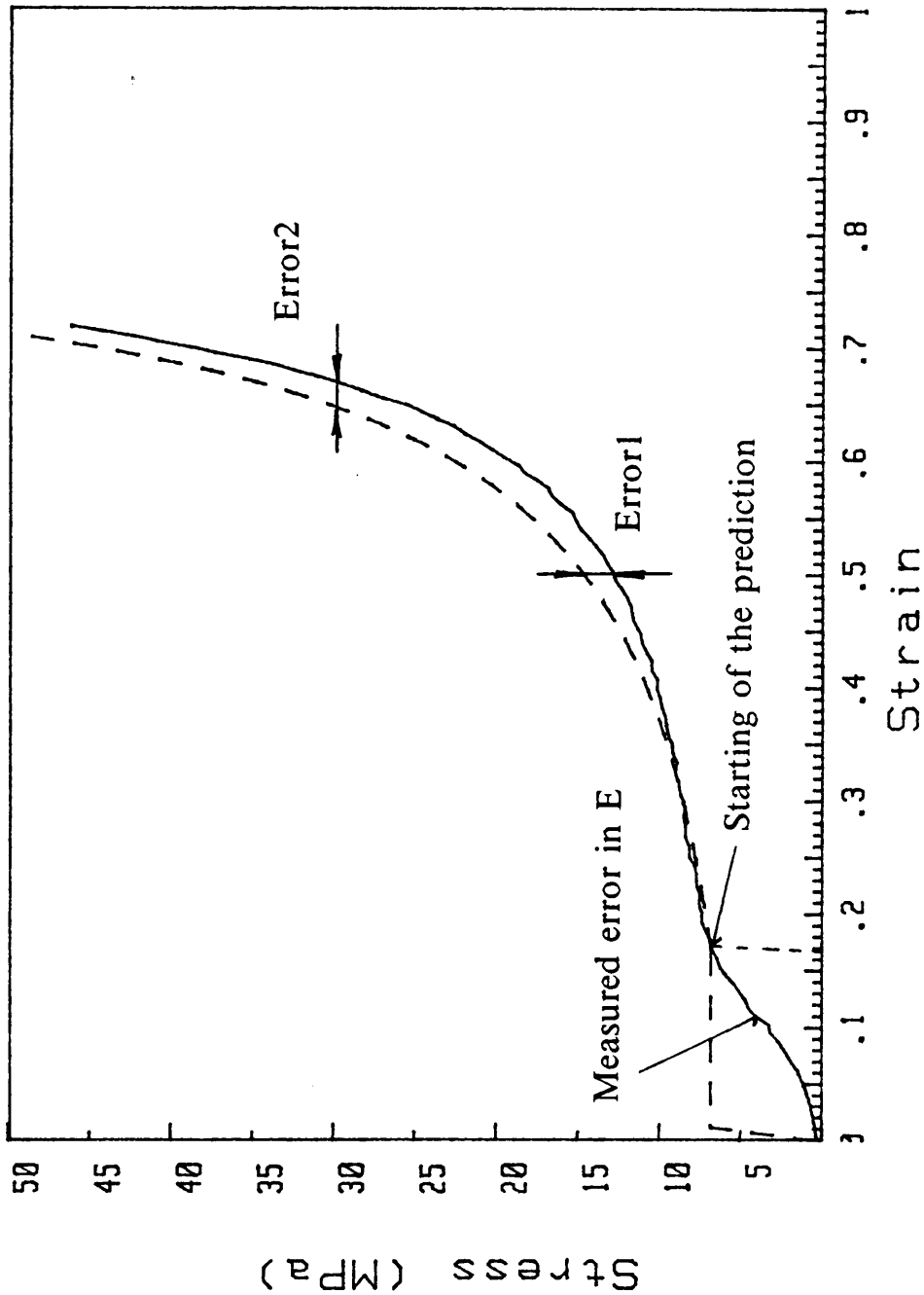

Figure 34. Calculation of the error of prediction.

As mentioned earlier, the coefficient in Eq. [1] is assumed to be equal to 1.0. Then the coefficient c_2 can be expressed from the known E and σ_y as the strain at the yield point. The calculated values of c_2, as well as E_s are given in Table 8. Since E is a function of the moisture content and temperature conditions, the same is true for E_s (see Eq. [1]). However, c_2 does not have to follow the same logic. A test of differences between c_2 for different treatments is shown in Table 9. One can recognize that a number of differences were detected. Duncan's multiple range test (Walpole 1985), however, did not detect any differences except for treatments 3 and 8 for the radial direction and 2 and 8 in the tangential and radial direction together. In the tangential direction Duncan's test gave the same result as Tukey's (LSD) test.

If c_2 is considered a constant independent of temperature, moisture content and direction, it has the value of 0.015 with a coefficient of variation 24%. The constant c_2 for the radial and tangential directions was 0.014 and 0.016 with a coefficient of variation 26% and 14%, respectively.

Table 8. Modulus of the cell wall and c_2 coefficient.

Trt.	n	MC	T	Dir	E_s	s	c_2	s
-	-	%	°C	-	MPa	MPa	-	-
1	6	8	30	rd	22 472	3 183	0.0133	0.0016
1	6	8	30	tg	12 746	1 510	0.0128	0.0010
2	6	8	60	rd	17 240	4 321	0.0162	0.0033
2	6	8	60	tg	7 754	1 652	0.0196	0.0024
3	6	8	100	rd	13 334	5 040	0.0191	0.0095
3	6	8	100	tg	8 846	1 528	0.0129	0.0019
4	6	12	30	rd	19 422	2 731	0.0135	0.0019
4	6	12	30	tg	9 692	1 717	0.0157	0.0013
5	6	12	60	rd	17 692	2 314	0.0137	0.0012
5	6	12	60	tg	7 336	1 395	0.0183	0.0032
6	6	20	30	rd	15 208	2 656	0.0129	0.0016
6	6	20	30	tg	6 116	1 281	0.0182	0.0026
7	6	20	60	rd	10 575	1 075	0.0127	0.0009
7	6	20	60	tg	4 268	1 100	0.0174	0.0015
8	6	0	225	rd	8 032	1 032	0.0092	0.0014
8	6	0	225	tg	4 424	1 012	0.0114	0.0026

Table 9. LSD test on differences between c_2 for radial and tangential direction ($\alpha = 0.05$).

Radial direction								
Treatment	3	2	5	4	1	6	7	8
c_2	0.0191	0.0162	0.0137	0.0135	0.0133	0.0129	0.0127	0.0092
	*	*						
		*	*	*	*	*	*	
					*	*	*	*
Tangential direction								
Treatment	2	5	6	7	4	3	1	8
c_2	0.0196	0.0183	0.0182	0.0174	0.0157	0.0129	0.0128	0.0114
	*	*	*	*				
		*	*	*	*			
						*	*	*
Tangential and radial direction								
Treatment	2	5	3	6	7	4	1	8
c_2	0.0175	0.0162	0.0160	0.0156	0.0150	0.0145	0.0131	0.0100
	*	*	*	*	*			
				*	*	*	*	
							*	*
		*	*	*	*	*	*	

Asterisks in the line means that there is no statistical difference between treatments.

Stochastic Model

Wood as a natural material exhibits high variability of properties. This variability is controlled by many factors starting from the variability between species to the variability within species, trees, position in the tree, etc. (Panshin and de Zeeuw, 1980). Whereas the variability between species can be eliminated by defining properties for each species, the lower sources of variability cannot be neglected. As has been shown by a number of researchers (Kollmann 1951, Panshin and de Zeeuw 1980, Bodig and Goodman 1972, Bodig nad Jayne 1982) there is a relationship between the mechanical properties and the density, or between the mechanical properties mutually. In other words, these properties are not statistically independent random variables. This means that any particular variable cannot take an arbitrary value, but must be correlated with others. Bodig and Goodmann (1972) related the elastic properties of different woods to the density. Bodig and Jayne (1982) report the relationship for strength properties in the following form:

$$Y = a\rho^{b} \qquad [10]$$

Where:

Y = property as a dependent variable

ρ = density at dry weight and wet volume

Whereas b is close to 1.0 for E in bending (linear relationship), b = 2.25 was found for σ_y. A correlation coefficient R^2 = 0.96 for σ_y and $R^2 = 0.965$ for E were reported. Bendtsen and Galligan(1979) studied the properties in transverse compression for different hardwood and softwood species. An $R^2 = 0.89$ for $\sigma_y$was reported. Although some skewness was found in the data, a normal model for the analysis was used.

Contrary to these results, Schniewind and Gammond (1978) found very low correlation between density and mechanical properties for diger pine (*Pinus spp.*) ($R^2 = 0.05$-0.38). However, experiments were performed on green wood and the coefficient of variation of moisture content was between 23 and 63%. This obviously overlapped the influence of the density despite the fact that most of the tests were conducted above the fiber saturation point.

In recent studies of mechanical properties of wood, a log-normal or Weibull (Weibull 1955) distribution were applied. However, the normal distribution approach still gives a good prediction for many applications. In fact, most of the data available are described by the first two moments (mean value and standard deviation) which fully defines only a normal distribution. Some studies also indicate no substantial differences between distributions applied to the data (O' Halloran et al 1988). It is understood that the normality assumption does not have to fully reflect the reality. However, it has been shown that a normal distribution gives satisfactory results for the properties discussed (Bodig and Jayne 1982).

To account for the natural variability, a stochastic model is introduced to simulate the scatter of the data. Thus, the expected reliability of the prediction can be studied. The simulation procedure can be used, not only to predict the single specimen behavior, but also to estimate the parameters for the population.

Theoretical basis

The Monte Carlo procedure described by Rubinstein (1981) was used to simulate the data and the stress-strain relationship. A polar method (Knuth 1969) was involved to generate random numbers. The algorithm is as follows:

1. Generate two sets of independent random numbers U_1, U_2, and V_1, V_2

$$V_1 = 2U_1 - 1 \qquad [11]$$

$$V_2 = 2U_2 - 1$$

V_1 and V_2 are uniformly distributed between -1 and + 1 (random points uniformly distributed inside the unit circle). U_1 and U_2 are distributed between 0 and 1.

2. Calculate a square of the magnitude of the random vector with components V_1 and V_2

$$S = V_1^2 + V_2^2 \qquad [12]$$

if $S \geq 1$ then repeat steps 1 to 2

3. Compute two normally distributed variables

$$X_1 = V_1 \sqrt{\frac{(-2 \ln S)}{S}} \qquad [13]$$

$$X_2 = V_2 \sqrt{\frac{(-2 \ln S)}{S}} \qquad [14]$$

4. To obtain the dependent normally distributed random variables the following formulae are used:

$$Y_1 = \bar{x}_1 + s_1 X_1$$

$$Y_2 = \bar{x}_2 + s_2 (R X_1 + \sqrt{1 - R^2}\ X_2) \qquad [15]$$

Where:

$\bar{x}$ = mean value (mean estimate)

s = standard deviation

R = correlation coefficient

This procedure can be used to generate any number of correlated normally distributed random variables (see Knuth 1969). Here we assume that E and σ_y are positively correlated with the specific gravity. Thus the procedure can be easily modified to generate the third statistically dependent variable. The listing of the simulation program is enclosed in Appendix B.

As a result of the simulation procedure, a set of values of E(I), σ_y (I) and ρ(I) is obtained (I is an I-th variable). For each set a theoretical stress-strain curve can be plotted and a statistical evaluation can be carried out. Thus, if statistical parameters for those three variables are known (mean value, standard deviation and coefficient of correlation) prediction characteristics can be studied. This enables an estimate of the statistical characteristics describing the response of wood to the applied strain. Therefore, the average densification stress and densification strain, as well as distribution characteristics and confidence intervals, can be predicted.

Monte Carlo simulation

For the Monte Carlo simulation the following parameters of random variables were taken as inputs:

Variable	Units	Mean	s
Density	g/cm^3	0.420	0.050
σ_y	MPa	9.0	1.2
μ		0.1	const.

These values represent the estimate of parameters for 30°C and 12% moisture content tests. The correlation coefficient between the density and σ_y was 0.9, and between density and E it was 0.7. A thousand values of ρ, σ_y and E were generated. Scattergrams for mutual relationships between variables are shown in Figures 35-37.

The resulting correlation coefficient for the E-σ_y relationship was 0.62. The probability density functions are plotted along with the histograms representing two random variables are in Figures 38-40. A statistical analysis of the means as well as a regression analysis, were performed.

The impact of the variability on the prediction of the transverse compression behavior is illustrated in Figure 41. The solid line represents the average expected response for 1000 measurements.

The two dashed lines nearest to the solid line represent the 99% confidence interval for the means. This indicates that if random samples of 1000 replications were drawn from the population, then 99% of the means would lie between these two lines. A single measurement, however, can fall into a much broader range, which is represented by the two dashed lines furthest from the solid line

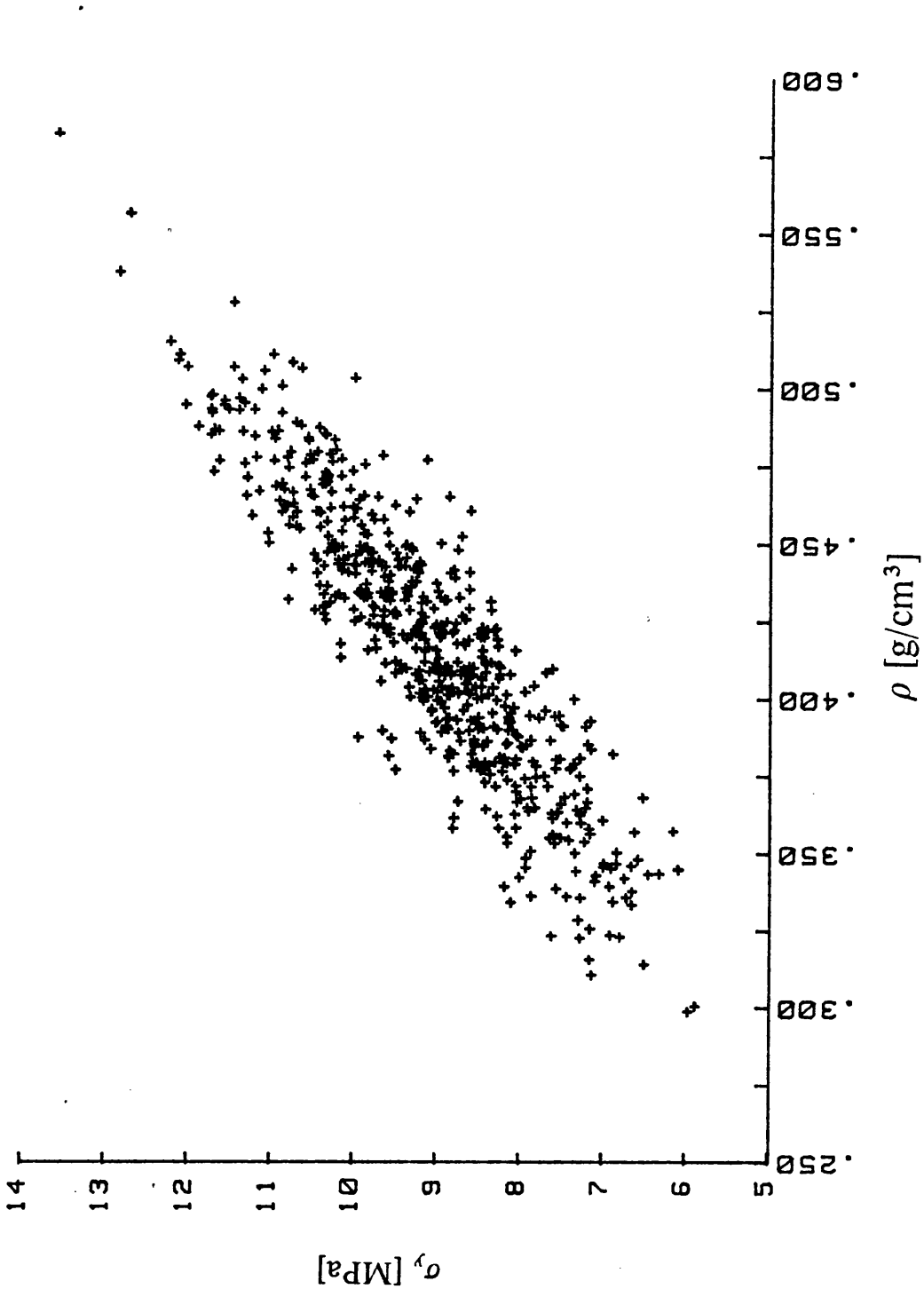

Figure 35. Density-yield stress relationship from the Monte Carlo simulation.

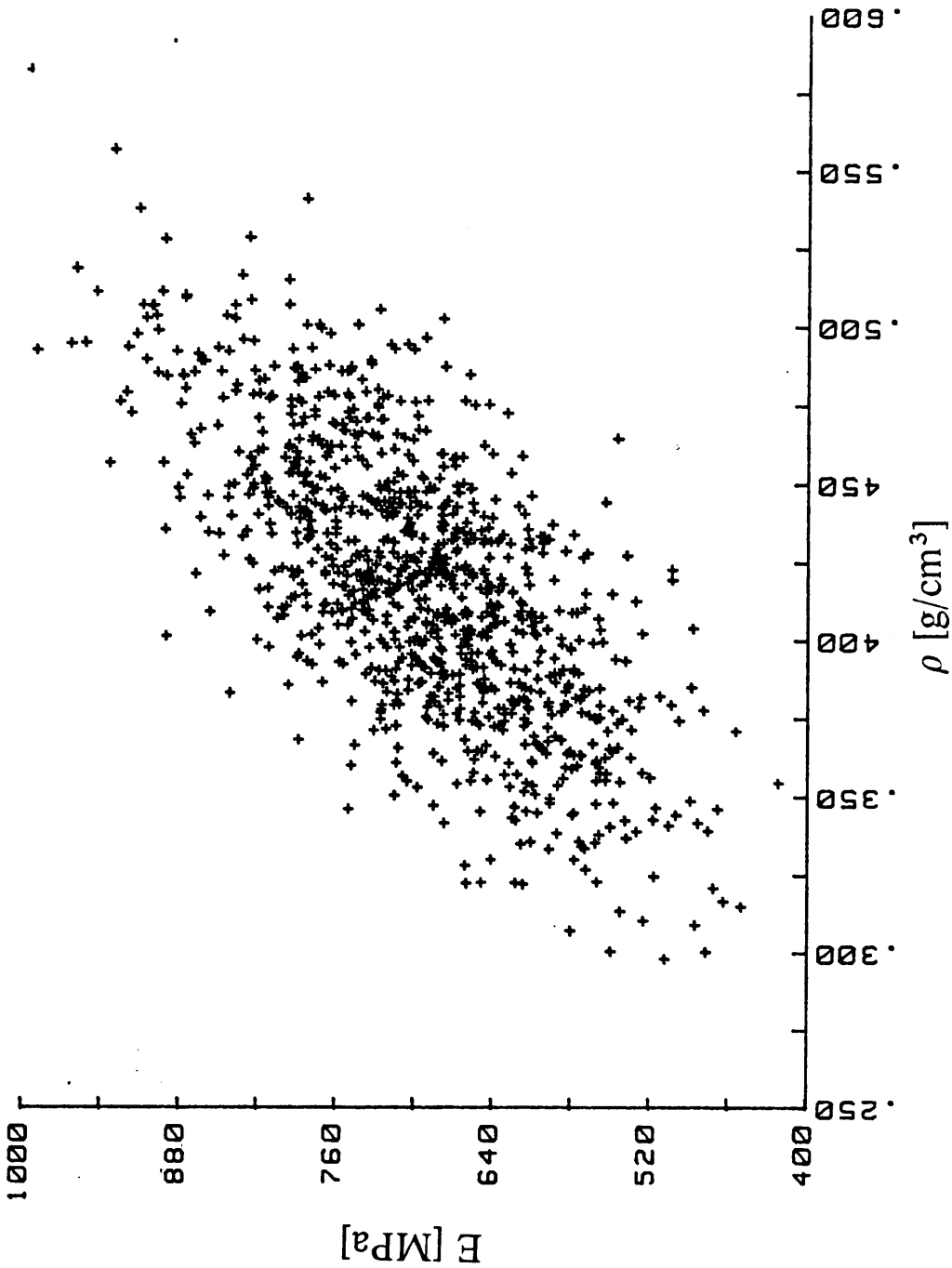

Figure 36. Density-E relationship from the Monte Carlo simulation.

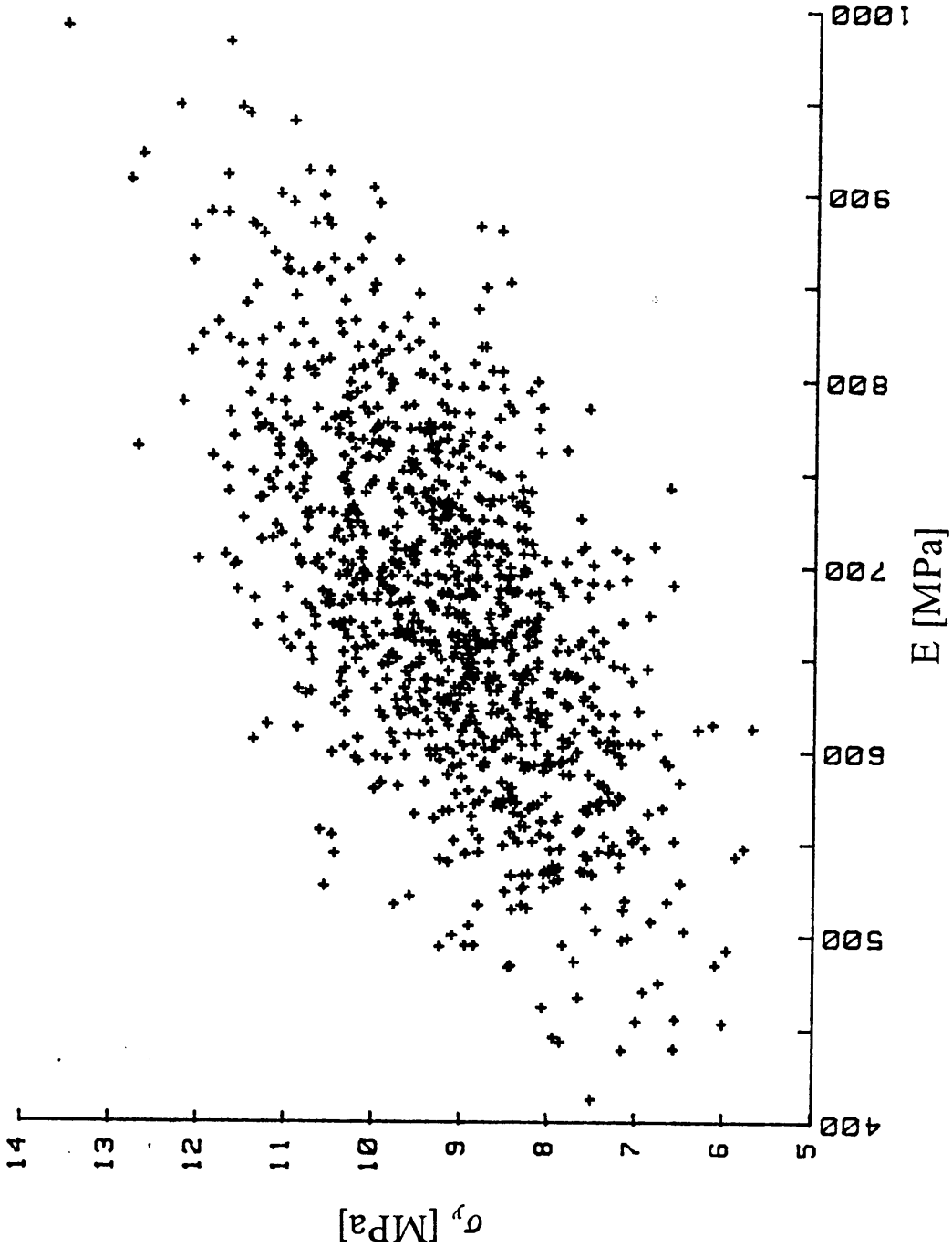

Figure 37. Modulus-yield stress relationship from the Monte Carlo simulation.

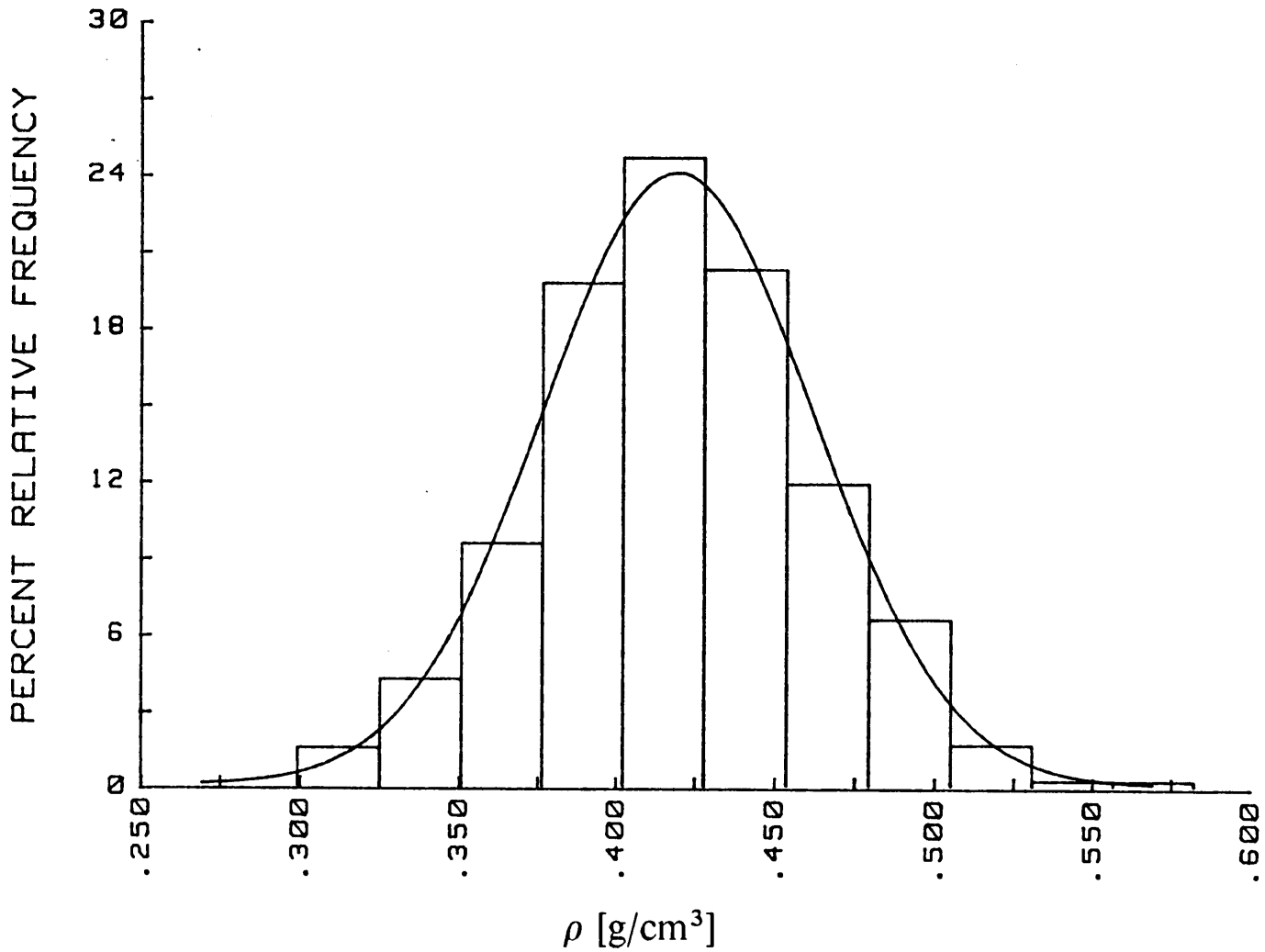

Figure 38. Histogram and probability density function for density: 1000 values.

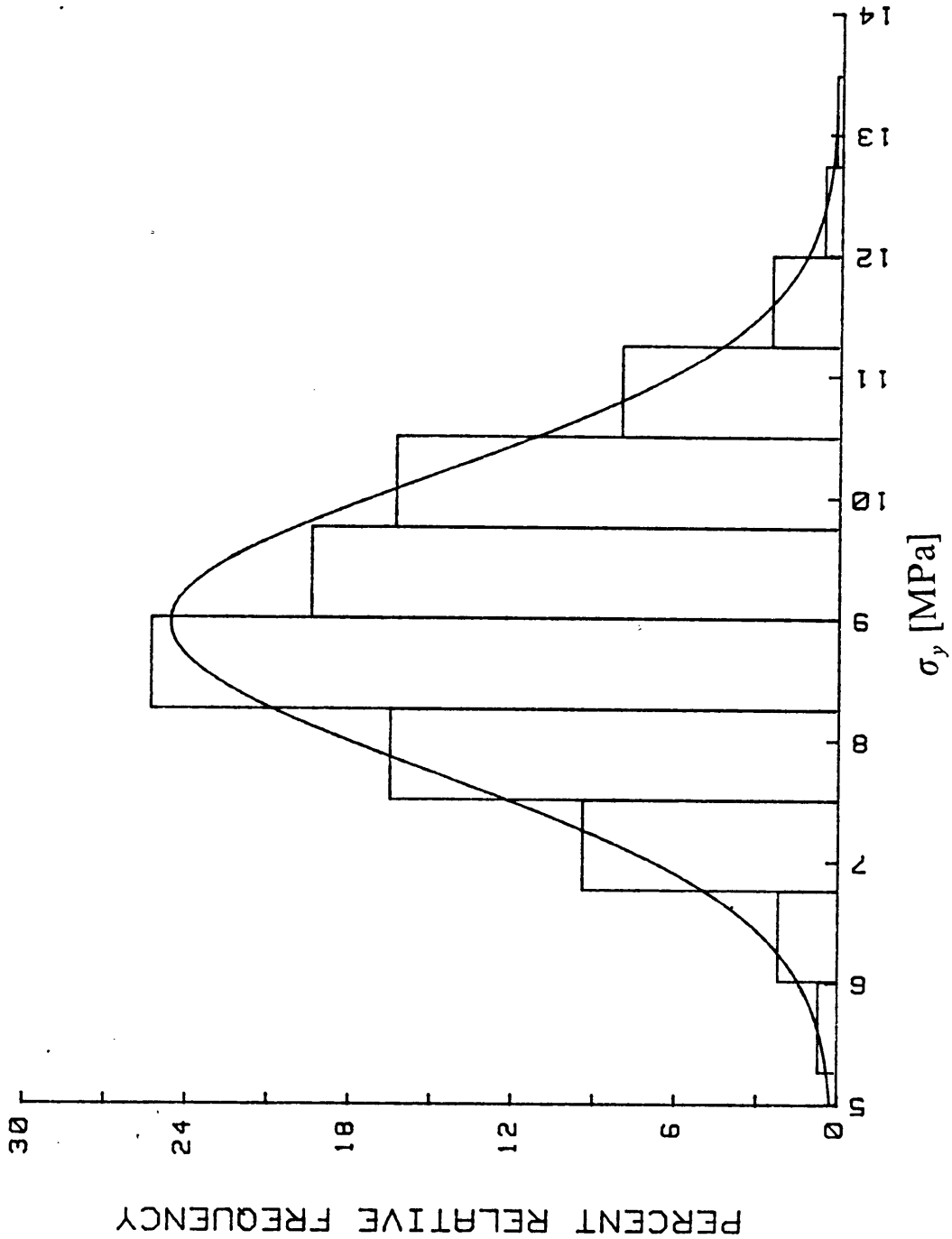

Figure 39. Histogram and probability density function for yield stress: 1000 values.

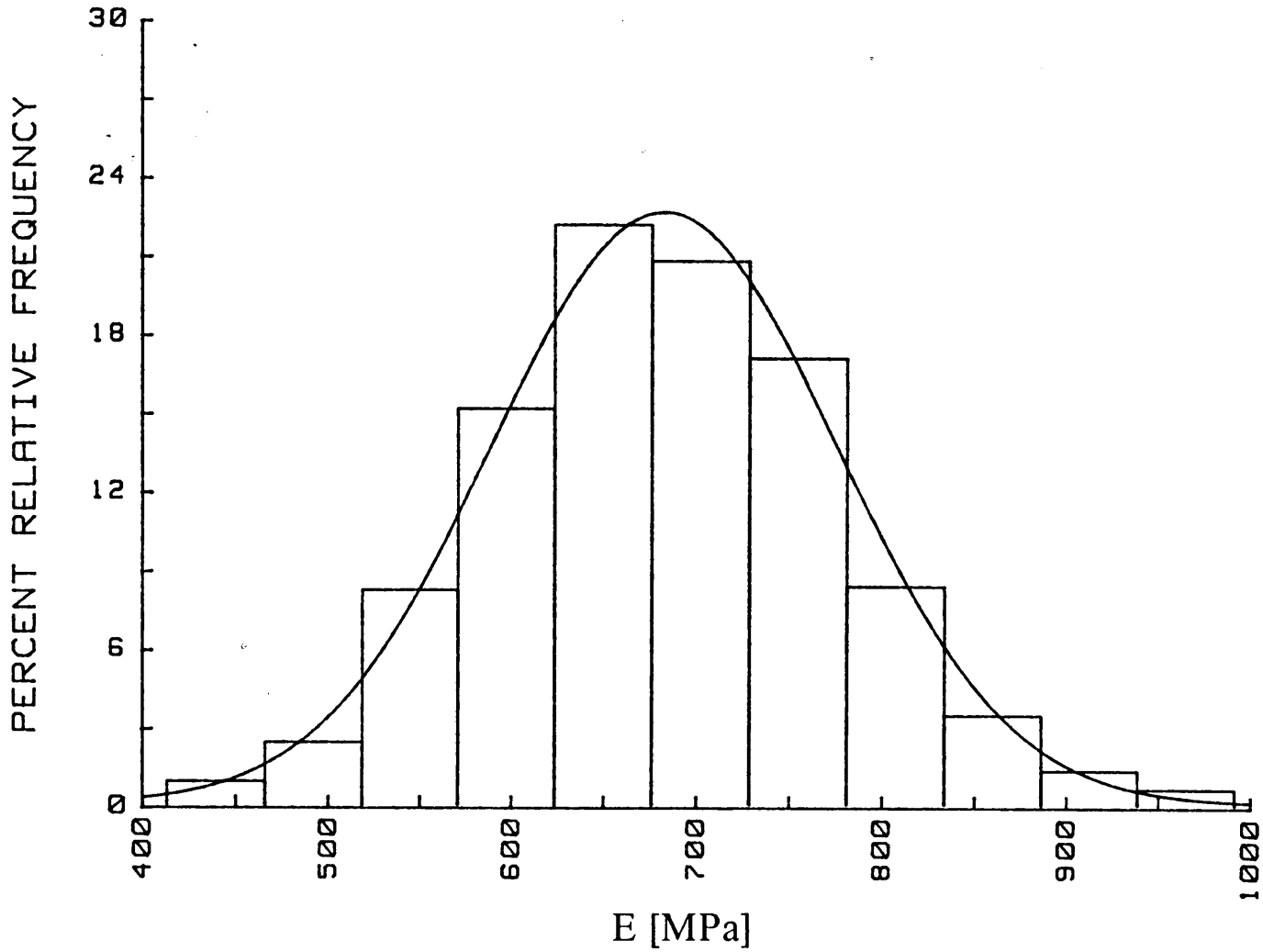

Figure 40. Histogram and probability density function for modulus: 1000 values.

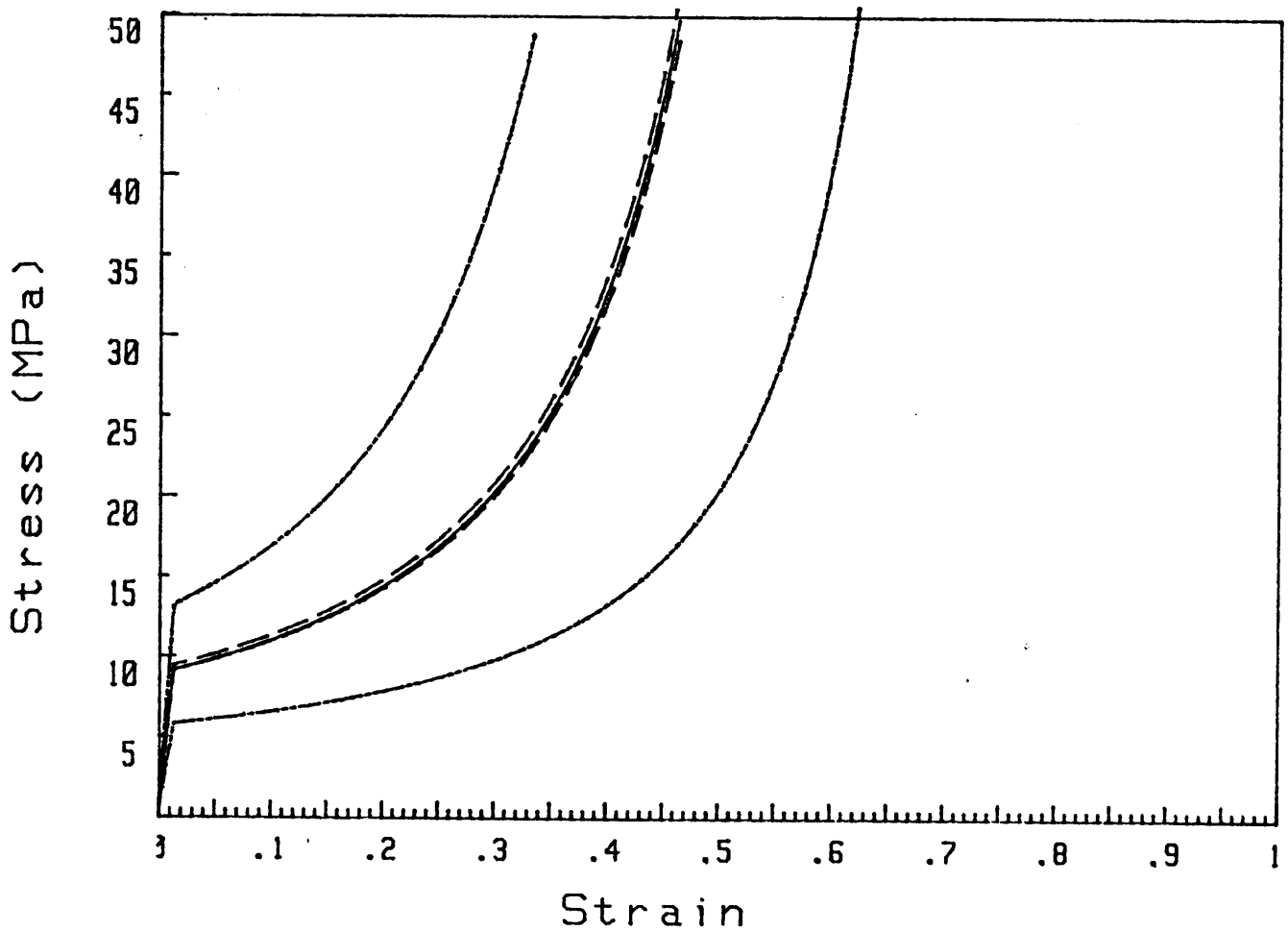

Figure 41. Expected stress-strain relationship for yellow poplar as a result of Monte Carlo simulation: 1000 values.

(99% confidence interval for a single measurement). The values for the 99% confidence intervals are in Table 10.

The Monte Carlo procedure can be used to simulate the uniformity of the densification across the density gradient in a flakeboard. One can recognize, that for a given level of stress some flakes will be highly densified, whereas some can still be elastically deformed. Thus this procedure offers, not only the qualitative image about the high strain deformation mechanism, but also the possibility of quantifying the expected density gradient. However, the vertical and horizontal flake distributions should be studied, which is beyond the scope of this work.

Table 10. Results from Monte Carlo simulation.

Single Value				
Variable	N	Min	Mean	Max
Density	1000	0.29	0.42	0.55
E	1000	403	682	961
σ_y	1000	5.33	8.96	12.59
Mean Value				
Variable	N	Min	Mean	Max
Density	1000	0.415	0.420	0.423
E	1000	675	682	690
σ_y	1000	8.86	8.96	9.06

Conclusions

Compression behavior of small yellow poplar specimens in the transverse direction was studied. A testing procedure for thin wood specimens was developed and the application of the theory developed for rigid plastic foams was studied. Based on the analysis of the experimental results, the following conclusions can be drawn:

1. The modulus of elasticity in transverse compression is dependent upon specimen height and increases with the specimen height. This is a geometrical phenomenon rather than material.

2. The yielding of wood under transverse compression is most likely caused by initial buckling of the cell wall and does not show any trend relating to the specimen height.

3. There is a lateral expansion during the high strain deformation. The expansion coefficient decreases rapidly at the yield point and remains approximately constant. The value of μ is slightly larger for thicker specimens, presumably because the constraint at the surfaces has an influence.

4. A modified foam theory gives good agreement with the experimental data for the temperature and moisture contents studied. Yield stress, density and E must be known as input parameters.

The model is quite robust against variation in E, but sensitive to ρ and σ_y variation. Both quantities are relatively easy to measure.

5. Yield stress and ρ are random statistically dependent variables. A Monte Carlo procedure can be used to simulate the transverse compression behavior.

Literature cited

Askhenazi, E.K. and E.V. Ganov. 1980. Anisotropy of structural materials. [in Russian]. Machinostroenie. Leningrad.256p.

Ashby, M.F., P.W.R. Beaumont, L.J. Gibson, D.G. Gilbert and S.K. Maiti. 1985. Deformation maps for cellular materials and solid polymers. Cambridge University Engn. Department.28p.

Babicki, R., T. Grzeczinski and H. Wroblenska. 1977. Effect of hydro-thermal treatment of green beech wood on its chemical and physico-mechanical properties. Wood Science and Technology. 11: 125-131.

Bendtsen A. and Galligan W. L. 1979. Mean and tolerance limit stresses and stress modelling for compression perpendicular to grain in hardwood and softwood species. USDA Forest Service. Res. Pap. FPL 337.14p.

Bodig, J. 1963. The peculiarity of compression of conifers in radial direction. For. Prod. Jour. 13 (10) :438.

Bodig, J. 1965. The effect of anatomy on the initial stress-strain relationship in transverse compression. For. Prod. Jour. 15 (5):197-202.

Bodig, J. 1966. Stress-strain relationship for wood in transverse compression. Jour. of Materials. 1 (3): 645-666.

Bodig, J. and B.A. Jayne. 1982. Mechanics of wood and wood composites. Van Nostrand Reinhold Company.New York.712p.

Casey , L.J. 1987. Changes in wood-flake properties in relation to heat, moisture, and pressure during flakeboard manufacture. MSC Thesis. VPI&SU.

Core H.A., W.W. Moschler and C. Chang. 1978. A note on prediction of wood properties in yellow-poplar. Wood and Fiber Science. 9(4): 258-261.

Easterling, K.E., R. Harrisson, L.J. Gibson and M.F. Ashby. 1982. On the mechanics of balsa and other woods. Proc. R. Soc. Lond. A 383:31-41.

Erinsch, P.P. and I.F. Kulevitsa. 1981. Investigation of the wood deformation at different types of plasticization. [in Russian]. Chimia Drevessiny (Wood Chemistry) (3):90-95.

Ganowicz, R., R. Guzenda and R. Plenzler. 1980. The influence of temperature on the modulus of elasticity of wood in the longitudinal direction. [in German]. Holztechnologie 21 (2):47-52.

Geimer, R.L. 1983. Method of pressing reconstituted lignocellulosic materials. US Patent 4 393 019.

Geimer, R.L. 1985. Steam injection pressing of isocyanate-bonded aspen flakeboards. Latitudes and limitations. USDA For. Prod. Lab. Res. Rep. #456.

Geimer, R.L., R.J. Mahoney, S.P. Laihnertz and R.W. Meyer. 1985. Influence of processing-induce damage on strength of flakes and flakeboards. FPL Res. Paper #463. US For. Prod. Lab., Madison, Wi.

Gibson L.J., M.F. Ashby, G.S. Schajer and C.I. Robertson. 1981. The mechanics of two-dimensional cellular materials. Proc. R. Soc. Lond. A 382:25-42.

Gruschetskii I. V. 1986. Failure of structures made of composite materials. [in Russian]. Riga Znanie.: 263p.

Guess, T.R. and R.H. Ericksen. 1983. Transverse compressive stress-strain behavior of thick kevlar/epoxy laminates. Compression testing of homogeneous materials and composites. ASTM STP 808:221-240.

Haygreen J.G. and J.L. Bowyer. 1982. Forest products and wood science. An introduction. The Iowa State Univ. Press. 495p.

Hillis, W.E. and A.N. Rosza. 1985. High temperature and chemical effect on wood stability. Part 2. The effect of heat on the softening of radiata pine. Wood Science and Technology 19: 57-66.

Hillis, W.E. and A.N. Rosza. 1985. High temperature and chemical effect on wood stability. Part 3. The effect of heat on the rigidity and the stability of radiata pine. Wood Science and Technology 19: 93-102.

Jones, R.M. 1975. Mechanics of composite materials. Hemisphere. New York. N.Y.355p.

Kellog R.M., C.B.R. Sastry and R.W. Wellwood. 1975. Relationships between cell-wall composition and cell-wall density. Wood and Fiber Science 7(3):170-177.

Khmelidze, T.P. 1986. Influence of temperature on strength and stiffness of wood of pine and larch [in Russian]. Derevoobrabativaja Promyshlennost (Wood Industry). (10):15-16.

Knuth, D.E. 1969. The art of computer programming. Vol.2. Seminumerical algorithms. Adison-Wesley Publishing Company. Reading. Mass.624p.

Kollmann, F. and W. A. Cote 1968. Principles of Wood Science and Technology. Volume I. Solid Wood. Berlin - Göttingen - Heidelberg.592p.

Kunesh, R.H. 1968. Strength and elastic properties of wood in transverse compression. For. Prod. Jour. 18(1):65-72.

Kurjatko, S. 1974. Effect of temperature and structural orientation on water diffusion throuh spruce wood. [in Slovac]. Drevarsky vyskum. 19:93-102.

Ladomersky, J. and Pajtik, J. 1987. Effect of the selected chemical-treatments on the stress-strain characteristics of wood [in Slovac]. Drevarsky vyskum. 112:55-67.

Malmeister, A.K., V.P. Tamuzh and G.A. Teters. 1980. Strength of polymers and composites. [in Russian]. Zinathe. Riga.572p.

Meinecke, E.A. and R.C. Clark. 1973. Mechanical properties of polymeric foams. Technomic poblishing Co. Inc. 105p.

Melcer, I. 1985. Plastification from the standpoint of the wood structure and properties as a polycomponent biopolymer composition. [in Slovac]. Drevo 40:91-93.

Menges, G. and F. Knipschild. 1982. Stiffness and strength: Rigid plastic foams. Pages 27-72 in Hilyard, N.C., ed. Mechanics of cellular plastics. MacMilian Publishing Co., New York, NY.

Neuhaus, H. 1983. Elastic behavior of spruce wood as a function of moisture content. [in German]. Holz als Roh-und Werkstoff. 41 (1): 21-25.

O' Halloran M.R., J.A. Johnson, E.G. Elias and T.P. Cunningham, Jr. 1988. Consideration of reliability-based design for structural composite products. Forest Products Journal. 38 (4): 35-43.

Östman, B.A.-L. 1985. Wood tensile strength at temperatures and moisture contents simulating fire conditions. Wood Science and Technology 19: 103-116.

Papirno, R., J.F. Mescall and A.M. Hansen. 1983. Fracture in axial compression tests of cylinders. Compression testing of homogeneous materials and composites. ASTM STP 808:40-63.

Rektorys, K. 1981. Used mathematics [in Czech]. SNTL Prague. 1139p.

Scharr, g. 1986. On the torsional elasticity of wood depending on wood temperature and load period. [in German]. Holz als Roh- und Werkstoff. 44 (2): 57 - 60.

Schneider, A. 1971. Investigations on the influence of heat treatments within a range of temperature from 100 to 200°C on the modulus of elasticity, maximum crushing strength, and impact work of pine sapwood and beechwood. [in German]. Holz als Roh- und Werkstoff. 29 (11):431-433.

Skhirando, T.P., T.V. Cukhayia and V.M. Reznikhov. 1983. The influence of the moisture content on chemical changes of wood during fiberboard manufacturing. [in Russian]. Chemia Drevessiny. (6):90-93.

Schneeweiss, G. 1963. The size effect in transverse compression. [in German]. Holzforschung und Holzverwertung 15 (6):125-130.

Schniewind, A.P. and B. Gammon. 1978. Some strength properties of diger pine. Wood and Fiber Science. 9 (4):289-294.

Sumi, H. 1978. High temperature drying of wood. II. Effect of heating conditions on some mechanical properties and color of Western Hemlock. Journal of Jap. Wood Res. Soc. 24 (6):391-399.

Taylor, S.E and D.A. Bender. 1987. Simulating correlated lumber properties using a modified multivariate normal approach. Journal of Paper No. 87-4005. Texas A&M University.

Thomas, B.J. and R.G. Pearson. 1976. Properties of steam-pressed particleboards. Forest Products Journal. 26 (11): 46-50.

Timoshenko, S. P. and J. M. Gere. 1961. Theory of elastic stability. McGraw-Hill Book Company.New York.541p.

Walpole, R.E. and R.H. Myers. 1985. Probability and statistics for engineers and scientists. MacMillian Publishing Company. New York. NY.639p.

Wingate-Hill, R. and R.B. Cunningham. 1986. Moisture removal from green sapwood during plateau pressing. New Zealand Journal of Forestry Science 16 (1): 109-117.

Wingate-Hill, R. and K.W. Growes. 1988. Compression dewaterinng of green wood. Appita 41 (2):129-134.

Weibull W. 1955. New methods for computing parameters of complete or truncated distributions. The Aeronautical Research Institute of Sweden.: 21.

Woeste, F.E., S.K. Suddarth and W.L. Galligan. 1979. Simulation of correlated lumber properties data.-A regresion approach. Wood Science 12 (2):73-79.

Wolcott, M.P. 1987. The micromechanics of thin wood specimens in transverse compression. VPI&SU. Dept. of Wood Science and For. Prod. Unpublished.

Wolcott, M.P., B. Kasal, F.A. Kamke and D.A. Dillard. 1988. Testing small wood specimens in transverse compression. Submitted to Wood and Fiber Science.

Zadorina, E.S. and N.N. Tschernova. 1965. Influence of temperature and moisture on some mechanical properties of larch [in Russian]. Derevoobrabativayia Promyshlennost. (10):7-8.

Appendix A. Two dimensional model of cellular material

Here a theory developed by Gibson et al (1982) is presented in abbreviated form. A regular hexagon is assumed.

The two dimensional model is based on the assumption that a foam can be modelled using an average cell representing the overall foam response to loading. The derivation is based on the geometry in Figure 42. The relative density of the hexagon can be expressed as the ratio of the area of the cell wall and the total area of the hexagon:

$$\frac{\rho}{\rho_s} = \frac{(2 + h/l)\, t/l}{2 \cos\theta\, (h/l + \sin\theta)} \qquad [A1]$$

where: h = height of the hexagon side

l = length of the hexagon side

t = thickness of the cell wall

θ = angle between the hexagon wall and the horizontal

ρ = foam density

ρ_s = wall density

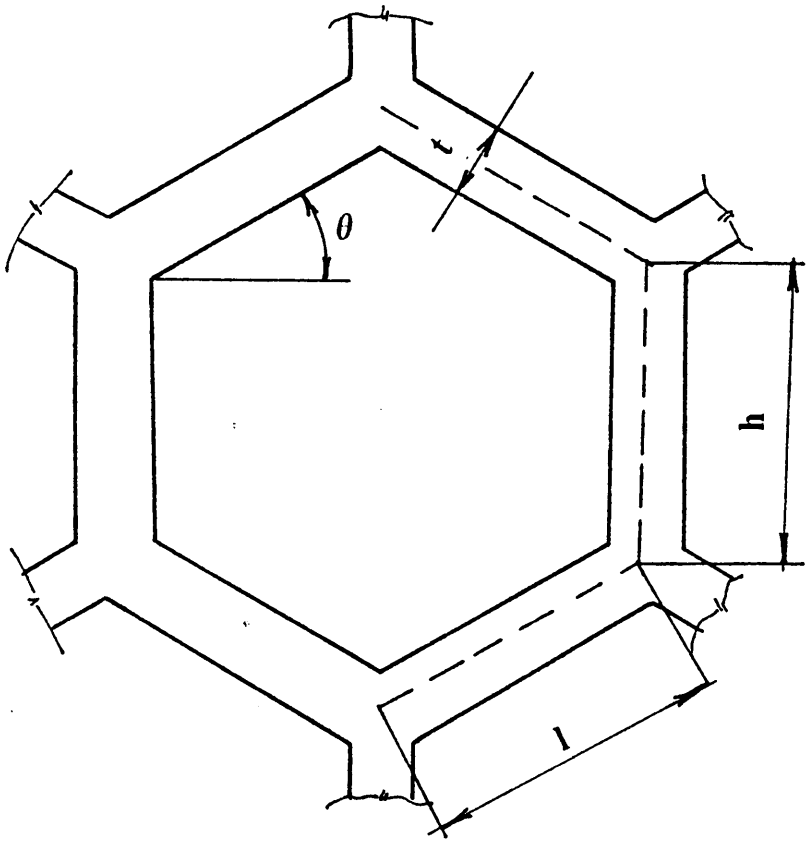

Figure 42. Schematic model of a regular hexagon.

For a regular hexagon with $\theta = 30°$ and h = 1 Eq. [A1] becomes:

$$\rho_{rel} = \frac{\rho}{\rho_s} = \frac{2}{\sqrt{3}} \frac{t}{l} \qquad [A2]$$

Where: ρ_{rel} = relative density

The linear elastic response is modelled as the elastic bending of the cell wall. Shear deformations and axial extension or compression is neglected and small deformations are assumed.

If a stress σ_1 is applied., then from the equilibrium condition the vertical reaction C = 0 (see Figure 43) and the bending moment is:

$$M = \frac{1}{2} P\, l\, \sin\theta \qquad [A3]$$

Where:

$$P = \sigma_1 (h + l\, \sin\theta)\, b \qquad [A4]$$

The cell wall deflects by:

$$\delta = \frac{P l^3\, \sin\theta}{12 E_s I} \qquad [A5]$$

Strain from the component $\delta \sin\theta$ parallel to the direction 1 is:

$$\varepsilon_1 = \frac{\delta\, \sin\theta}{l\, \cos\theta} = \frac{\sigma_1 (h + l\, \sin\theta)\, b\, l^2\, \sin\theta^2}{12 E_s I \cos\theta} \qquad [A6]$$

Then the Young's modulus is:

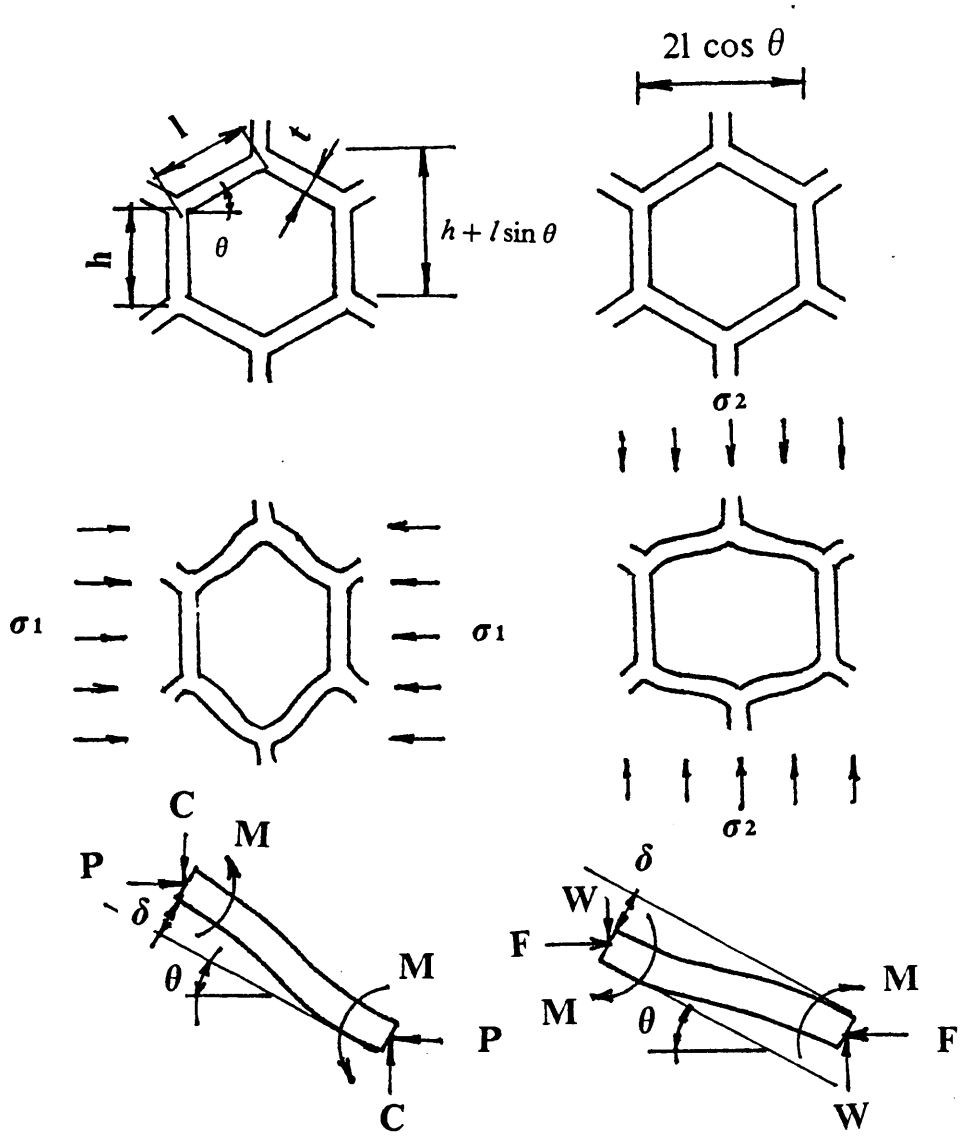

Figure 43. Elastic bending

$$E_1 = \frac{\sigma_1}{\varepsilon_1} \qquad [A7]$$

For a regular hexagon with $\theta = 30°$, moduli for directions 1 and 2 are the same. Then from Eq. [A7] we get:

$$E_1 = E_2 = E = \frac{4}{\sqrt{3}} E_s \frac{t^3}{l^3} = \frac{3}{2} \rho_{rel}^3 \qquad [A8]$$

The elastic buckling of the cell wall allows further large deformations at almost constant load. It has been observed that the buckling mode is similar to that illustrated in Figure 44 (Gibson et al 1982). Beam BE acts as an Euler column constrained by rotational springs at both ends. For the critical buckling load we get:

$$P_{cr} = \frac{n^2 \pi^2 E_s}{l^2} \qquad [A9]$$

Where: n^2 = the end constraint factor, which is a function of the stiffness of the rotational spring

The buckling stress can be then expressed:

$$\sigma_{el} = \frac{P_{cr}}{2\, l\, b\, \cos\theta} = \frac{E_s t^3 n^2 \pi^2}{6\, l\, h^2\, \cos\theta} \qquad [A10]$$

For a regular hexagon with h = 1 and n = .343 Eq. [A10] becomes:

$$\sigma_{el} = c_2 E_s \rho_{rel}^3 \qquad [A11]$$

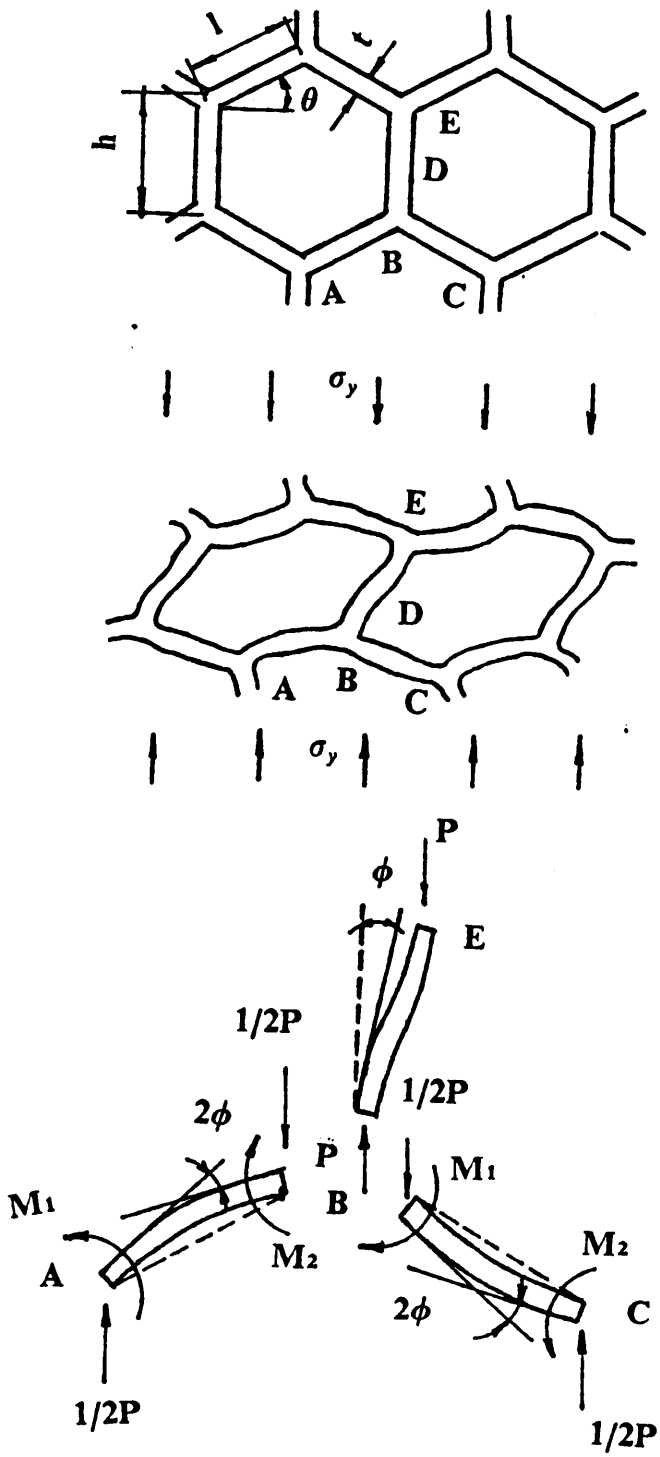

Figure 44. Elastic buckling

If the material of the cell wall exhibits a plastic yield point, the structure will collapse plastically if a plastic moment is reached. Since we assume a regular hexagon, we can take any of the two directions for the derivation. If the loading in the direction 1 is taken (see Figure 45) then the work done by the force is:

$$P = \sigma_1 (h + l \sin\theta) b \qquad [A12]$$

Plastic work done at hinges A,B,C,D equals:

$$4M_p \phi \geq 2\sigma_1 b (h + l \sin\theta)\phi l \sin\theta \qquad [A13]$$

Where :

θ = plastic rotation

M_p = fully plastic moment of the cell wall in bending

$$M_p = \frac{1}{4} \sigma_y b t^2$$

σ_y = yield stress of the cell wall material

$$(\sigma_1)_{pl} \leq \frac{\sigma_y t^2}{2 l(h + l \sin\theta) \sin\theta} \qquad [A14]$$

Calculating the maximum moment in the beam and equating it to M_p we get:

$$M_{\max} = \frac{1}{2} \sigma_1 (h + l \sin\theta) b l \sin\theta \qquad [A15]$$

from which:

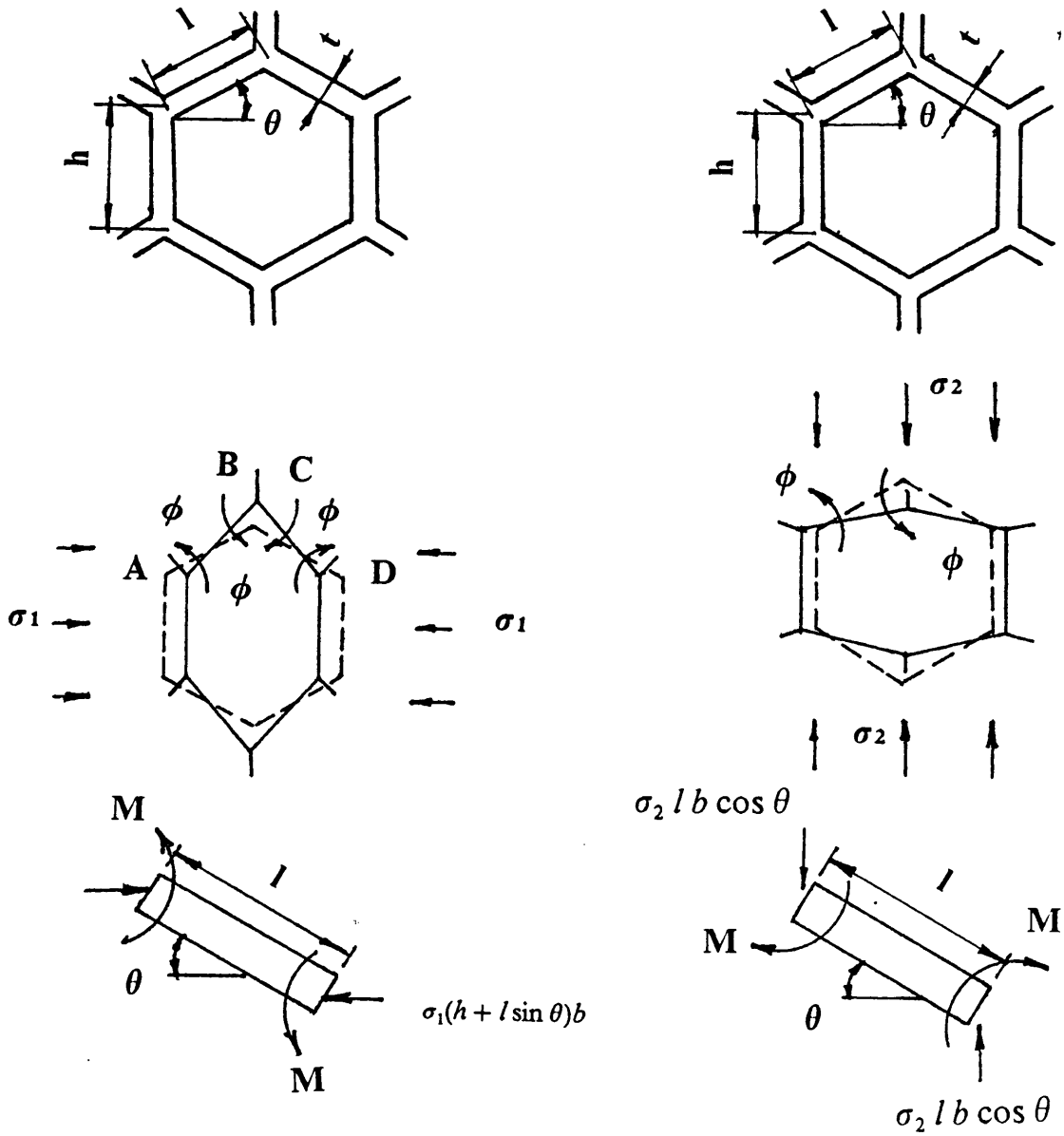

Figure 45. Plastic collapse

$$(\sigma_1)_{pl} \geq \frac{\sigma_y t^2}{2\, l(h + l \sin\theta) \sin\theta} \qquad [A16]$$

Then from Eq. [A14] and [A16] we obtain:

$$(\sigma_2)_{pl} = \frac{\sigma_y t^2}{2\, l^2 \cos\theta^2} \qquad [A17]$$

Again, for regular hexagon:

$$(\sigma_1)_{pl} = \frac{2}{3} \frac{t^2}{l^2} \sigma_y \qquad [A18]$$

$$\sigma_{pl} = c_3\, \sigma_{rel}^{3/2}$$

Ashby et al (1985) postulated that the elastic buckling was controlling phenomenon in foam non-linear behavior. The relative density after a nominal compressive strain ε is expressed as:

$$\frac{\rho(\varepsilon)}{\rho_s} = \frac{\rho}{\rho_s} \left(\frac{1}{1-\varepsilon} \right) \qquad [A19]$$

Where: $\frac{\rho}{\rho_s} =$ initial relative density

Densification is complete, when $\rho(\varepsilon)/\rho_s = 1$ and when the strain is:

$$\varepsilon_f = 1 - \frac{\rho}{\rho_s}$$

Length of the edges which are about to buckle is given by:

$$l(\varepsilon) = l_0 \frac{1 - \left(\frac{\rho(\varepsilon)}{\rho_s}\right)^{1/3}}{1 - (\rho/\rho_s)^{1/3}} \qquad [A20]$$

Eq. [A20] is based on a distribution of cell edge-lengths and angles and no closer explanation is given by the authors. Using Eq.[A19], Eq.[A20] can be expressed:

$$l(\varepsilon) = l_0 \frac{1 - (\frac{\rho_{rel}}{(1-\varepsilon)})^{1/3}}{1 - \rho_{rel}^{1/3}} \qquad [A21]$$

Combining Eqns. [A9], [A10], A[11] and [A21], Eq.[5] at page 9 can be derived.

Appendix B. Geometrical approach to the derivation of the expansion ratio for cellular material

Here a simple geometrical approach is used to derive the expansion ratio as a function of the axial strain. Geometry of the regular hexagon is shown in Figure 46. To keep the derivation simple, plastic hinges are assumed. When the hexagon is loaded in the direction 1, the axial displacement can be expressed as:

$$\delta_1 = l(\frac{1}{2} - \sin\alpha) \qquad [A22]$$

Lateral displacement as:

$$\delta_2 = l(\cos\alpha - \frac{\sqrt{3}}{2}) \qquad [A23]$$

and strains ε_1 and ε_2 as:

$$\varepsilon_1 = \frac{-\delta_1}{l} \qquad [A24]$$

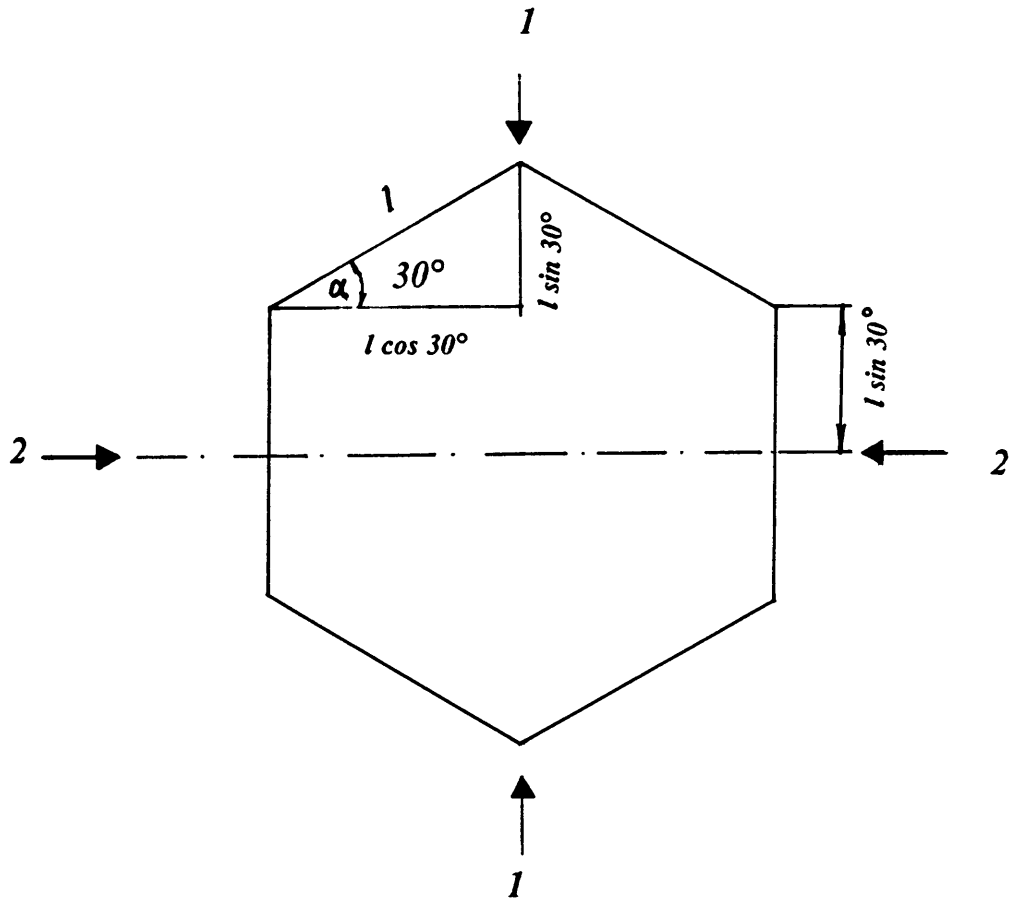

Figure 46. Schematic model of lateral expansion of the hexagon.

$$\varepsilon_2 = \frac{\delta_2}{\frac{\sqrt{3}}{2}\, l}$$

From which the expansion ratio μ can be obtained:

$$\mu = \frac{2(\cos\alpha - \frac{\sqrt{3}}{2})}{\sqrt{3}\,(\frac{1}{2} - \sin\alpha)} \qquad [A25]$$

This approach defines μ up to $\varepsilon_1 = 0.5$. At this strain the hexagon becomes a quadrilateral and further assumptions should be made.

If the hexagon is loaded in the direction 2, following derivation can be carried out:

$$\varepsilon_1 = -\frac{\delta_1}{l\sqrt{3}/2} \qquad [A26]$$

$$\alpha = arcsin(h/l) = arcsin\,(\frac{\sqrt{3}}{2}(1 - \varepsilon_1)) \qquad [A27]$$

Lateral strain ε_2 is:

$$\varepsilon_2 = \frac{2(l\cos\alpha - l/2)}{2\frac{l}{2} + 2} = \cos\alpha - \frac{1}{2} \qquad [A27]$$

and expansion coefficient is:

$$\mu = -\frac{\varepsilon_2}{\varepsilon_1} \qquad [A28]$$

For a cylindrical cell we assume no cell wall elongation during the deformation (no change in circumference). An elliptical shape after deformation is assumed. The circumference of the ellipse can be expressed by approximate formula (Rektorys 1981):

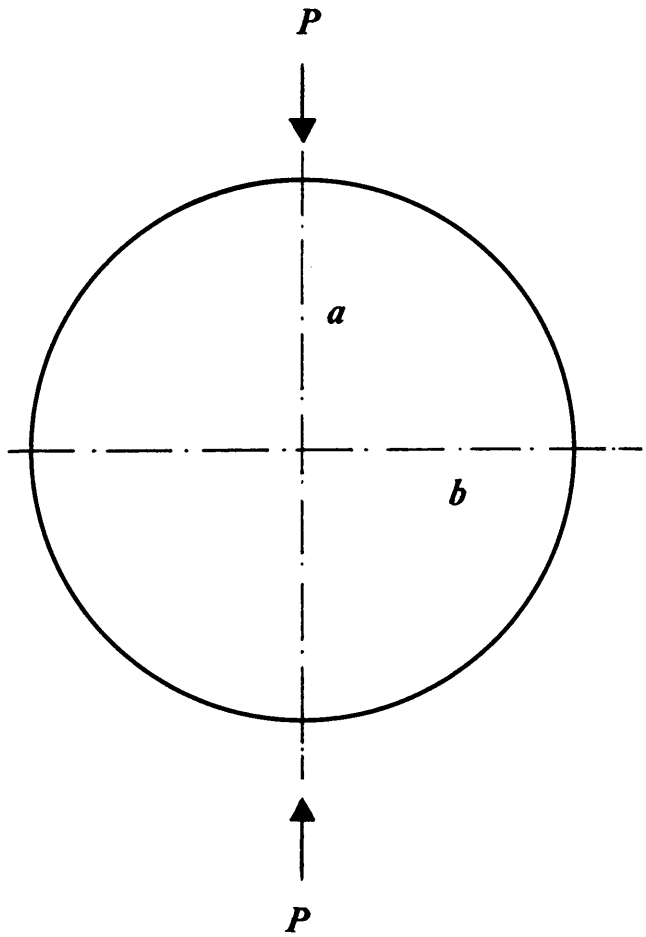

Figure 47. Model of cylindrical cell

$$o \simeq \pi[1.5(a+b) - \sqrt{ab}\,] \qquad [A29]$$

Where:

a - semi-major axis

b - semi-minor axis

Let a = b = 1.0 before deformation and apply strain ε_1 in the direction of b-axes. The new axis length is:

$$b' = 1 - \varepsilon_1 \qquad [A30]$$

and circumference after straining is:

$$o' \simeq \pi[1.5(a' + 1 - \varepsilon_1) + \sqrt{a'(1-\varepsilon_1)}\,] \qquad [A31]$$

Eq. [A31] is solved numerically for a′ under the condition o′ = o. Results for different models are shown in Figure 49. If a buckling of the ring is assumed first, the axial and radial deflections can be expressed (Timoshenko, Gere 1961) as:

$$\Delta b = P\frac{b^3}{4EI}(\pi - \frac{8}{\pi}) \qquad [A32]$$

$$\Delta a = P\frac{a^3}{2EI}(\frac{4}{\pi} - 1)$$

which for a = b = 1.0 leads to μ = 0.918.

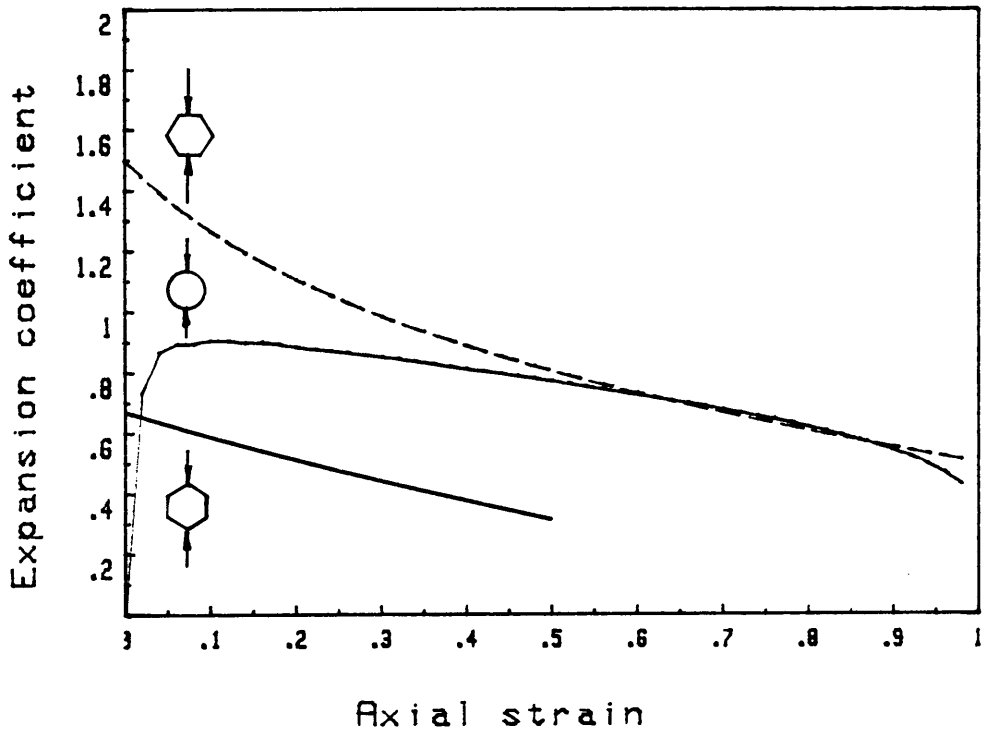

Figure 48. Expansion ratio as a function of the axial strain for different cell models

Appendix C. Computer program for Monte Carlo simulation

```
1     !_____________________________________________________________________
2     !                                                                    |
4     !     SIMULATION OF TRANSVERSE COMPRESSION BEHAVIOR OF WOOD          |
5     !____________________________________________________________________
6     !
7     ! Bohumil Kasal      |       November 1988   |   VPI&SU        |
8     !____________________________________________________________________
9     !                                                                    |
10    ! This program uses Monte Carlo procedure to simulate the compression |
11    ! behavior of wood.                                                  |
12    ! Density, yield stress and MOE are dependent random variables.      |
13    ! To use this program following quantities must be known:            |
14    !      1. Mean values for all three variables                        |
15    !      2. Standard deviations for all three variables                |
16    !      3. Correlation coefficient between density and yield stress   |
17    !         and density and MOE.                                       |
18    ! Normal distribution of the variables is assumed.                   |
19    ! Program is based on:
20    !                    1.Knuth, Donald E. (1969) The art of the        |
21    !                       computer programing. Volume 2. Seminumerical |
22    !                       algorithms. Reading. Mass. Addison-Wesley.   |
23    !                                                                    |
24    !                    2.Statistical library for the HP Series 200     |
25    !                      computers. Manual Part No. 98820-13111.       |
26    !                      Hewlett-Packhard Co. 1982. Fort Collins       |
27    !                      Colorado.                                     |
29    !*********************************************************************
30    RANDOMIZE
180   DIM C$[3],N$[60]
435   !____________________________________________________________________
436   !        READING DATA FOR THE SIMULATION
437   !--------------------------------------------------------------------
438   !
439   Seed=RND*10000^(10*RND)
440   RANDOMIZE Seed
442   DATA 10,.7          ! N=number   of runs     Rho=correlation coeff.
443   READ N,Rho           !                        between the density and MOE
444   DATA .42,.042       ! Mean1=density          Sd1=standard deviation
445   READ Mean1,Sd1
446   DATA 680,90         ! Mean2=MOE              Sd2=standard deviation
447   READ Mean2,Sd2
448   DATA 9,1.2,.90      ! Mean3=Yield stress     Sd3=standard deviation
449   READ Mean3,Sd3,Rho3 ! Rho3=correlation coeff. between the density
450   GOTO 458            !      and yield stress
451   !____________________________________________________________________
```

```
452  !
454  IF (N<1) OR (Rho<=0) OR (Rho>=1) THEN 434
458  CALL Set_up1(N,Seed,Mean1,Sd1,Mean2,Sd2,Rho,Mean3,Sd3,Rho3)
460  DISP "PROGRAM COMPLETE."
465 End:  END
470  SUB Set_up(N,Mean1,S1,Mean2,S2,Rho)
480    RAD
485    !
490    ALLOCATE Y1(1:N),Y2(1:N)
495 Repeat:  Repeat=3
500  FOR I=1 TO Repeat
502        Seed=RND*2^31-1
505        RANDOMIZE Seed
515        CALL Random_norm2(N,Mean1,Mean2,S1,S2,Rho,Y1(*),Y2(*))
520        CALL Mean(N,Y1(*),Mean)
525        CALL Standard_dev(N,Y1(*),Sd)
530        PRINT USING 535;Seed,Mean,Sd
535        IMAGE /,"Seed:",12D,"  Mean1:",3D.3D,"  Std.Dev1:",3D.3D
540        CALL Mean(N,Y2(*),Mean)
545        CALL Standard_dev(N,Y2(*),Sd)
550        PRINT USING 555;Mean,Sd
555        IMAGE 14X,"     Mean2:",3D.3D,"  Std,Dev2:",3D.3D
560        CALL Correlation(N,Y1(*),Y2(*),Ccoeff)
565        PRINT USING 570;Ccoeff
570        IMAGE  7X,"Correlation Coefficient:",3D.3D
575     NEXT I
580  SUBEND
585  SUB Mean(N,X(*),Mean)
595    RAD
600  Mean=0
605  FOR I=1 TO N
610     Mean=Mean+X(I)
615  NEXT I
620  Mean=Mean/N
625  SUBEND
630  SUB Variance(N,Mean,X(*),Variance)
640    RAD
645  Variance=0
650  FOR I=1 TO N
655     Variance=Variance+(X(I)-Mean)^2
660  NEXT I
665  Variance=Variance/(N-1)
670  SUBEND
675  SUB Standard_dev(N,X(*),Sd)
685    RAD
```

```
690  IF N<2 THEN SUBEXIT
695  Temp_=0
700  Sumx=Temp_
705  Sumxx=Temp_
710  FOR I=1 TO N
715     Xi=X(I)
720     Sumx=Sumx+Xi
725     Sumxx=Sumxx+Xi*Xi
730  NEXT I
735 Sd=SQR((Sumxx-Sumx*Sumx/N)/(N-1))
740 SUBEND
745 SUB Random_normal(N,X(*))
755   RAD
765 Baddata=N MOD 2 OR (N<1)
770 IF NOT Baddata THEN Begin
775 Error: PRINT FNLin$(2);"ERROR IN SUB Random_normal."
785 IF N MOD 2 THEN PRINT "N MUST BE EVEN."
790 PRINT "N: ";N
791 CONTROL 2,2;0
795 PAUSE
796 CONTROL 2,2;1
800 GOTO 765
805 Begin: FOR I=1 TO N/2
806        RANDOMIZE
810 P1:       U1=RND
815           U2=RND
820           V1=2*U1-1
825           V2=2*U2-1
830 P2:       S=V1*V1+V2*V2
835 P3:       IF S>=1 THEN P1
840 P4:       Temp=SQR(-2*LOG(S)/S)
845           X(I*2-1)=V1*Temp
850           X(I*2)=V2*Temp
855        NEXT I
860 SUBEND
865 SUB Random_norm2(N,Mu1,Mu2,Mu3,Sigma1,Sigma2,Sigma3,Rho,Rho3,Y1(*),Y2(*),Y3(
*))
875   RAD
880 DIM Temp_(1:2)
885 IF (Sigma1>0) AND (Sigma2>0) THEN 910
890 PRINT FNLin$(2);"ERROR IN Random_norm2.  SD<=0.";FNLin$(2)
891 CONTROL 2,2;0
895 PAUSE
896 CONTROL 2,2;1
900 GOTO 885
```

```
910 IF NOT (N MOD 2) THEN 945
915 IF N<>1 THEN CALL Random_normal(N-1,Y1(*))
920 IF N<>1 THEN CALL Random_normal(N-1,Y2(*))
921 IF N<>1 THEN CALL Random_normal(N-1,Y3(*))
925 CALL Random_normal(3,Temp_(*))
930 Y1(N)=Temp_(1)
935 Y2(N)=Temp_(2)
936 Y3(N)=Temp_(3)
940 GOTO 960
945 CALL Random_normal(N,Y1(*))
950 CALL Random_normal(N,Y2(*))
951 CALL Random_normal(N,Y3(*))
953 Temp=SQR(1-Rho*Rho)
954 Temp1=SQR(1-Rho3*Rho3)
956  FOR I=1 TO N
957    Y2(I)=Mu2+Sigma2*(Rho*Y1(I)+Temp*Y2(I))
958    Y3(I)=Mu3+Sigma3*(Rho3*Y1(I)+Temp1*Y3(I))
965 NEXT I
975 FOR I=1 TO N
980 Y1(I)=Sigma1*Y1(I)+Mu1
985 NEXT I
990 SUBEND
995 SUB Correlation(N,X(*),Y(*),Coeff)
1005   RAD
1010 Temp_=0
1015 Sumx=Temp_
1020 Sumy=Temp_
1025 FOR I=1 TO N
1030    Sumx=Sumx+X(I)
1035    Sumy=Sumy+Y(I)
1040 NEXT I
1045 Xmean=Sumx/N
1050 Ymean=Sumy/N
1055 Temp_=0
1060 Sumx=Temp_
1065 Sumy=Temp_
1070 Sum=Temp_
1075 FOR I=1 TO N
1080    Sumx=Sumx+(X(I)-Xmean)^2
1085    Sumy=Sumy+(Y(I)-Ymean)^2
1090    Sum=Sum+(X(I)-Xmean)*(Y(I)-Ymean)
1095 NEXT I
1100 Coeff=Sum/(SQR(Sumx)*SQR(Sumy))
1105 SUBEND
1110 SUB Set_up1(N,Seed,Mean1,Sd1,Mean2,Sd2,Rho,Mean3,Sd3,Rho3)
```

```
1120   RAD
1125    !
1130   ALLOCATE X(1:N),Y(1:N),Z(1:N)
1131   Seed=(RND*1000)^(RND*10)
1135   RANDOMIZE Seed
1145 PRINTER IS 1
1150 CALL Random_norm2(N,Mean1,Mean2,Mean3,Sd1,Sd2,Sd3,Rho,Rho3,X(*),Y(*),Z(*))
1151  CALL Foamplot(N,Mean1,Mean2,Mean3,Sd1,Sd2,Sd3,Rho,Rho3,X(*),Y(*),Z(*))
1165 PRINTER IS 1
1170    CALL Print_file(N,X(*),Y(*),Z(*))
1175 SUBEND
1415 SUB Print_file(N,X(*),Y(*),Z(*))
1425   RAD
1430 DIM C$[3],File$[20]
1435 LINPUT "WOULD YOU LIKE TO SAVE THE DATA SET? (Y/N)",C$
1440  CALL Yesno(C$,Ynflag)
1445 IF Ynflag=2 THEN SUBEXIT
1450 IF Ynflag=3 THEN 1435
1455 LINPUT "ENTER FILE NAME.  E.G.: File:INTERNAL ?",File$
1465 ON ERROR GOTO Recovery
1470  ASSIGN @File1 TO File$
1475  OFF ERROR
1480  GOTO 1515
1485 Recovery: IF ERRN<>56 THEN Error
1495  CREATE BDAT File$,3*N*10/256+1
1505  ASSIGN @File1 TO File$
1506  OFF ERROR
1510 GOTO 1555
1515 LINPUT "FILE ALREADY EXISTS. OK TO WRITE ON IT? (Y/N)",C$
1520  CALL Yesno(C$,Ynflag)
1525 IF Ynflag=2 THEN 1435
1530 IF Ynflag=3 THEN 1515
1535 ON ERROR GOTO Error1
1555     OUTPUT @File1;X(*)
1570     OUTPUT @File1;Y(*)
1571     OUTPUT @File1;Z(*)
1580  ASSIGN @File1 TO *
1585 OFF ERROR
1590 DISP "DATA HAS BEEN STORED SUCCESSFULLY.  ";
1595 SUBEXIT
1600 Error: PRINT FNLin$(2);"ERROR";ERRN;"IN SUB Print_file."
1610  OFF ERROR
1615 GOTO 1435
1625 Error1: IF ERRN<>59 THEN Error
1630 PRINT FNLin$(2);"SORRY, FILE IS NOT LARGE ENOUGH."
```

```
1635 PRINT "I SUGGEST THAT YOU CHOOSE A NEW NAME AND I WILL CREATE THE FILE FOR
YOU.";FNLin$(2)
1640 GOTO 1435
1645 SUBEND
1650  DEF FNLin$(INTEGER X)
1655    INTEGER I
1660    IF X=0 THEN RETURN CHR$(13)
1665    Eol$=CHR$(13)&CHR$(10)
1670    IF X<0 THEN Eol$=CHR$(10)
1675    ALLOCATE R$[X*LEN(Eol$)]
1680    R$=""
1685    FOR I=1 TO X
1690      R$=R$&Eol$
1695    NEXT I
1700    RETURN R$
1705    FNEND !
1710  DEF FNSpa$(INTEGER X)
1715    INTEGER I
1720    ALLOCATE R$[X+(NOT X)]
1725    R$=""
1730    FOR I=1 TO X
1735      R$=R$&CHR$(32)
1740    NEXT I
1745    RETURN R$
1750    FNEND !
1760  SUB Yesno(C$,Ynflag)
1770    IF (C$[1,1]="Y") OR (C$[1,1]="y") THEN
1780       Ynflag=1
1790       ELSE
1800         IF (C$[1,1]="N") OR (C$[1,1]="n") THEN
1810         Ynflag=2
1820         ELSE
1830           Ynflag=3
1840    END IF
1841    END IF
1850    SUBEND
1860    SUB Foamplot(N,Mean1,Mean2,Mean3,Sd1,Sd2,Sd3,Rho,Rho3,X(*),Y(*),Z(*))
1870    !
1880    !
2000  !*****************************************************************!
2001  !*****                    FOAMPLOT                        *********!
2002  !*****************************************************************!
2005  !_________________________________________________________________
2006  ! A foam theory developed by Gibson and Ashby is used to predict the!
2007  ! wood behavior under the perpendicular to the fibers direction.    !
```

```
2008  ! Stress-strain curve is derived as a function of the density.      |
2009  ! Modulus of elasticity and yield stress can be also predicted, but |
2010  ! it is more accurate to use these parameters as an input.          |
2011  ! Unlike the original theory, this model consider the Poisson's     |
2012  ! Ratio non-zero value. Poisson's Ratio is expressed as a function  |
2013  ! of the strain (curve 1 and 2), constant (curve 3) and zero (4).   |
2014  ! This is a significant differnce from the original theory where    |
2015  ! this ratio was considered to be zero.                             |
2016  !_____________________________________________________________________
2022  DEG
2025  GINIT
2029  !
2058      !
2060 Begin:GRAPHICS OFF
2062      GRAPHICS ON
2063  FOR Z1=1 TO 2   !Second time through for hardcopy
2064    Stress_max=50
2066    Strain_max=1
2067    Device=3
2068    Device$="INTERNAL"
2069    GOSUB Plot
2076    IF Z1=2 THEN
2077      Ans$="Y"
2078      END IF
2081 Quest:INPUT "Do you want a hard copy?",Ans$
2082      IF Ans$="n" OR Ans$="N" THEN Quit
2083      Device=705
2087      Device$="HPGL"
2088      GOSUB Plot
2563   NEXT Z1
2564 Quit:!
2565      PEN 0
2566      GRAPHICS OFF
2569      STOP
2570!=====================================================================
2579   !
2871 !=====================================================
2872 !         Plotting subroutine
2873 !oooooooooooooooooooooooooooooooooooooooooooooooooooooooo
2874 Plot: OUTPUT KBD;"■K"
2875      GINIT
2876      GCLEAR
2877      LINE TYPE 1
2878      PLOTTER IS Device,Device$
2879  PEN 1
```

```
2882  LORG 6
2883  MOVE 0,50
2884  LDIR 90
2885  LORG 6
2886  LABEL "Stress (MPa)"
2887  LDIR 0
2888  MOVE 65,5
2889  LORG 4
2890  LABEL "Strain"
2891  CSIZE 4,.5
2892  MOVE 65,95
2893  LORG 6
2894  VIEWPORT 15,120,15,90
2895  FRAME
2896  WINDOW 0,Strain_max,0,Stress_max
2897  AXES .01,Stress_max/10,0,0,5,2,3
2898  CSIZE 4,.4
2899  LORG 9
2900  VIEWPORT 3,120,15,90
2901  FOR I=0 TO Stress_max STEP Stress_max/10
2902      MOVE .10,I
2903      LABEL I
2904  NEXT I
2905  VIEWPORT 15,120,10,90
2906  LORG 4
2907  CSIZE 3.5,.5
2908  FOR I=0 TO Strain_max STEP .10
2909      MOVE I,0
2910      LABEL I
2911  NEXT I
2912  VIEWPORT 15,120,15,90
2913      !
2923 !*****************************************************************
2933 !*                        PLOTTING                              ***
2943 !*****************************************************************
2945          Mu=.2
2953      FOR I=1 TO N
2954          St=.01
2956  !       PRINT "DENS=";X(I),"Y.S.=";Z(I),"MOE=";Y(I)
2963          MOVE 0,0
2973          DRAW Z(I)/Y(I),Z(I)
2976          X(I)=X(I)/1.5
2977          Eps1=(Z(I)/Y(I))
2978          K=0
2983          FOR Eps=(Z(I)/Y(I)) TO 1 STEP St
```

```
2984              K=K+1
3023              Sigma=Z(I)*((1-X(I)^(1/3))/(1-X(I)^(1/3)/(1-Eps+(2/3)*Eps*Mu-
Mu*Eps^2)^(1/3)))^3
3024              IF Sigma>=35 THEN St=.001
3026              IF K=1 THEN Delta=Z(I)-Sigma
3027              Sigma=Sigma+Delta
3028              IF Sigma>=50 OR Sigma<0 THEN Next
3033              DRAW Eps,Sigma
3043           NEXT Eps
3053 Next: NEXT I
3075  !oooooooooooooooooooooooooooooooooooooooooooooooooooo
3076  RETURN
3078  SUBEND
```

The vita has been removed from the scanned document